Probabilistic Mapping of Tsunami Hazard and Risk for Gisborne City and Wainui Beach

W.L. Power
X. Wang
N. Horspool
C. Mueller

GNS Science Consultancy Report 2015/219
March 2016

GNS SCIENCE
TE PŪ AO

DISCLAIMER

This report has been prepared by the Institute of Geological and Nuclear Sciences Limited (GNS Science) exclusively for and under contract to the Gisborne District Council (GDC). GNS Science accepts no responsibility for any use of or reliance on any contents of this report by any person other than GDC and shall not be liable to any person other than GDC, on any ground, for any loss, damage or expense arising from such use or reliance. However, in the event that, notwithstanding this statement of disclaimer, GNS Science is at law held to have a duty of care to a third party, liability to that third party shall be limited and excluded on the same terms as liability to GDC is excluded and limited under the contract with GDC. Any party using or relying on this report will be regarded as having accepted the terms of this disclaimer.

Use of Data:

Date that GNS Science can use associated data: March 2016

BIBLIOGRAPHIC REFERENCE

Power, W.L.; Horspool, N.; Wang, X.; Mueller, C. 2016. Probabilistic Mapping of Tsunami Hazard and Risk for Gisborne City and Wainui Beach, *GNS Science Consultancy Report* 2015/219. 79 p.

CONTENTS

FIGURES

TABLES

APPENDICES

EXECUTIVE SUMMARY

Gisborne District Council (GDC) is interested in taking a risk-based approach to managing its natural hazards. In order to gain a better understanding of and manage the tsunami hazard affecting the region GDC has plans to undertake probabilistic tsunami hazard mapping for all its major communities along the coast. GDC has begun this effort by contracting GNS Science to conduct a pilot study, focussing on conducting probabilistic tsunami hazard mapping for Gisborne City and Wainui Beach.

GNS Science previously undertook two tsunami inundation studies commissioned by GDC for the coastal communities of: Gisborne and Wainui in 2009 (Wang et al., 2009), and Tokomaru Bay, Hicks Bay, and Te Araroa in 2012 (Barberopoulou, et al., 2012). These studies were intended to inform evacuation planning and model inundation from a set of source scenarios. Since then, GNS Science has produced results from its national probabilistic tsunami hazard model (Power, 2013), which estimates the size of the tsunami at the coast for specified probabilities. This information has been used here as the basis for developing a probabilistic understanding of the tsunami hazard inland in Gisborne City and Wainui.

The Tsunami Land-Use & Evacuation Planning Workshop was held in Gisborne in October, 2014 to consider the implications of the GNS Science Review of Tsunami Hazard in New Zealand and to determine best practice to address inconsistencies in the application of tsunami science for evacuation and land use planning. One of the issues identified in this workshop was the modelling level requirements for different purposes (e.g., evacuation, land use planning) and circumstances (e.g., remote coastlines or high-density urban populations). The subsequently revised Director's Guidelines for Tsunami Evacuation Zones recommended the use of "Level 3 or 4" probabilistic mapping to provide results with sufficient accuracy for land use planning purposes.

In this report GNS Science presents results from a "Level 3" tsunami inundation study conducted for Gisborne City and Wainui Beach. The "Level 3" approach consists of identifying tsunami scenarios consistent with the tsunami hazard on specified timeframes, modelling of these scenarios, and combining the results into a map of tsunami hazard. From this maps of expected inundation flow depths were produced at Average Recurrence Intervals (ARIs) of 100, 500, 1000, and 2500 years.

A further analysis was conducted, using only the scenarios arising from local tsunami sources. These were combined with models of population fragility to assess the level of tsunami risk in terms of annual fatality probability assuming no mitigation.

This report documents the outcomes of these investigations.

1.0 INTRODUCTION

Gisborne District Council (GDC) is interested in taking a risk-based approach to managing its natural hazards. In order to gain a better understanding of and manage the tsunami hazard affecting the region GDC has plans to undertake probabilistic tsunami hazard mapping for all its major communities along the coast. GDC has begun this effort by contracting GNS Science to conduct a pilot study, focussing on conducting probabilistic tsunami hazard mapping for Gisborne City and Wainui Beach.

In this report GNS Science presents results from a “Level 3” tsunami inundation study conducted for Gisborne City and Wainui Beach. The “Level 3” approach consists of identifying tsunami scenarios consistent with the tsunami hazard on specified timeframes, modelling of these scenarios, and combining the results into a map of tsunami hazard. From this, maps of expected inundation flow depths were produced at Average Recurrence Intervals (ARIs) of 100, 500, 1000, and 2500 years.

In addition, an estimation of annualised fatality rate was made, considering only Local source events, i.e. those with travel times to Poverty Bay of less than one hour, and therefore assuming that evacuation was successfully made for Regional and Distant source tsunamis.

This page is intentionally left blank.

2.0 BACKGROUND

GNS Science previously undertook two tsunami inundation studies commissioned by GDC for the coastal communities of: Gisborne and Wainui in 2009 (Wang et al., 2009), and Tokomaru Bay, Hicks Bay, and Te Araroa in 2012 (Barberopoulou, et al., 2012). These studies were intended to inform evacuation planning and model inundation from a set of source scenarios. Since then, GNS Science has produced results from its national probabilistic tsunami hazard model (Power, 2013), which estimates the size of the tsunami at the coast for specified probabilities. This information has been used here as the basis to develop a probabilistic understanding of the tsunami hazard inland in Gisborne City and Wainui.

The Tsunami Land-Use & Evacuation Planning Workshop was held in Gisborne in October, 2014 to consider the implications of the GNS Science Review of Tsunami Hazard in New Zealand and to determine best practice to address inconsistencies in the application of tsunami science for evacuation and land use planning. One of the issues identified in this workshop was the modelling level requirements for different purposes (e.g., evacuation, land use planning) and circumstances (e.g., remote coastlines or high-density urban populations). The subsequently revised Director's Guidelines for Tsunami Evacuation Zones recommended the use of "Level 3 or 4" probabilistic mapping to provide results with sufficient accuracy for land use planning purposes.

This page is intentionally left blank.

3.0 OBJECTIVE

This project is to develop a set of probabilistic tsunami hazard maps for Gisborne City and Wainui Beach. It is intended that the mapping will assist GDC in taking a risk-based approach to managing its tsunami risk. This involves developing an understanding of the risk so that the Council may progress to considering different possible approaches (e.g., land use planning, evacuation structures) to avoiding and/or mitigating it. It is also intended to allow the Council to act in alignment with the most current Ministry of Civil Defence and Emergency Management (MCDEM) guidelines addressing tsunami risk, thereby contributing to the safety of the community. Two main objectives were identified:

a. *Use the COMCOT (Cornell Multi-grid Coupled Tsunami model) tsunami model (Wang and Power, 2011) to create probabilistic tsunami hazard maps for Gisborne City and Wainui Beach based on inundation depths for the 500-year, 1,000-year, and 2,500-year annual recurrence intervals (ARIs). These ARIs were suggested by GDC since they are the same as those addressed in the Building Code's ultimate limit state earthquake design standards (AS/NZS 1170). Consideration of the same ARIs in this assessment will allow the Council to begin comparing earthquake design standards to tsunami risk. The COMCOT tsunami model is routinely used and constantly improved for tsunami research at GNS Science. It has been used previously for tsunami inundation modelling for several New Zealand cities exposed to tsunami hazard. The choice of scenarios used for each ARI will be determined from the New Zealand Probabilistic Tsunami Hazard model (Power, 2013).*

b. *To put the hazard maps into context, Gisborne District Council also wishes to define what could be considered an "intolerable" tsunami risk, and suggest the extent of the area occupied by permanent habitation that falls into this category (assuming no mitigation measures are put in place).*

This project is intended as a pilot study, the methods of which may be extended to all of the major coastal communities within Gisborne District, in future.

This page is intentionally left blank.

4.0 METHODS AND ASSUMPTIONS

The methodology of this project consists of the following steps:

General steps

Grid Development: Existing bathymetric and topographic grids (see Wang, 2009) were updated for this project.

Selection and definition of scenarios: Based on the findings of the Review of Tsunami Hazard in New Zealand (2013 update), earthquake sources were selected as significant contributors to the hazard at the 100, 500, 1000 and 2500 year ARIs.

Model runs: Six models as defined by the scenarios selected in the previous step were run through to full inundation in a single grid covering Poverty Bay, Gisborne City and Wainui Beach for each of the four annual recurrence intervals (24 model runs in total).

Objective A specific

Processing: The results from the model runs were combined and analysed using a weighted median approach. From these maps of inundation occurrence and maximum flow depth were created for the ARIs under consideration.

Objective B specific

Calculation of local-source-only ARIs: Results from the Review of Tsunami Hazard in New Zealand (2013 update) were modified to generate hazard curves based only on sources local to Gisborne. From these the local-source-only ARIs were estimated for the modelled local-source scenarios.

Fragility function derivation: Review and adopt fatality functions that model fatality rate against tsunami height were reviewed and adopted.

Processing: A weighted median flow depth distribution was estimated for each of the local-source-only ARIs. Fatality probability as a function of location was estimated. The fatality probability at each ARI was integrated to approximate the annualised individual fatality risk (AIFR) at each location.

Interpretation: The modelled AIFRs were compared with guidelines for risk tolerance defined by T. Taig (2012) and used in Berryman (2005) and Horspool et al. (2015).

4.1 ASSUMPTIONS

All tsunamis were assumed to occur at mid-tide (see Discussion in Section 10).

At the request of Gisborne District Council, a sea-level rise of 0.5m (estimated rise over the next 50 years) was assumed.

Results from the 'Review of Tsunami Hazard in New Zealand (2013 Update)' (Power, 2013) are used as the basis for this study. The assumptions, approximations and limitations of that study (and in particular those noted on p.169) are therefore applicable to this work.

This study aims at an 'unbiased' evaluation of hazard and risk. This is different from the development of tsunami evacuation maps, where it is conventional to 'err on the side of caution' in regard to the many uncertainties regarding potential tsunamis (see Discussion in Section 10).

In the model scenarios a crustal rigidity of 50 GPa is assumed for consistency with the results in Power (2013).

5.0 NUMERICAL MODEL

The tsunami model, COMCOT (Cornell Multi-grid Coupled Tsunami model) was used to simulate the tsunami generation, propagation and coastal flooding in the coastal areas of Gisborne. The model was originally developed at Cornell University, USA in 1990's (Liu et al., 1995) and since 2009 it has been continuously under development at GNS Science, New Zealand (Wang & Power, 2011). Using a modified staggered finite difference scheme to solve linear/nonlinear shallow water equations, COMCOT was developed to investigate the evolution of long waves in the ocean, particularly tsunami, including its generation, propagation, run-up and inundation. To account for the shallowness of water depth and ensure enough spatial resolution in near-shore regions, nested grid configuration is implemented in COMCOT, through which the model can use a relatively larger grid resolution to efficiently simulate the propagation of tsunamis in the deep ocean and then switch to apply finer grid resolutions in coastal regions. In this approach, the computational efficiency and the numerical accuracy will also be well balanced.

This model has become publicly available and has been widely used by researchers to study different aspects of tsunami impacts. It has been systematically validated against analytical solutions (Cho, 1995), experimental studies (Liu et al., 1994a, Liu et al., 1995, Cho, 1995) and benchmark problems (Wang et al., 2008) and has consistently shown its satisfactory accuracy and efficiency. Some of its applications include the study of the 1960 Chilean Tsunami (Liu et al., 1994b), the 1986 Taiwan Hualien Tsunami (Liu et al., 1998), the 2003 Algerian Tsunami (Wang & Liu, 2005), the 2004 Indian Ocean Tsunami (Wang and Liu, 2006, 2007), and the 2009 Samoa tsunami (Beaven et al., 2010). It has also been widely applied to evaluate the tsunami hazards in New Zealand, such as the national wide Probabilistic Tsunami Hazard Analysis by Power et al. (2013) and the tsunami inundation studies in Gisborne (Wang et al., 2009), Tauranga (Prasetya and Wang, 2011), Napier (Fraser et al., 2014), and Wellington (Mueller et al., 2014) among others.

Multiple source mechanisms have been integrated in this tsunami simulation package, including subaerial/submarine landslides and earthquakes with transient rupture and/or variable slip distributions. In this study, a variety of source scenarios were simulated and instantaneous rupture is assumed for all the source scenarios. The ground and seafloor displacement is calculated using the displacement theory documented in Okada (1985). The effect of ground subsidence or uplift due to fault rupture, especially those from local faults, was included in the numerical simulations.

5.1 MODEL GRIDS

In numerical simulations, we need a digital representation of bathymetry and topography, i.e., Digital Elevation Model (DEM) which combines bathymetric and topographical data into a single gridded dataset containing the information of land elevation and water depth at a specified spatial resolution. To account for the spatial scale variations of a tsunami travelling in different regions from its source to coastal regions of interest, the tsunami modelling software - COMCOT (Wang and Power, 2011) uses a series of nested DEM 'grids' of cascading resolutions to solve the motion and transformation of a tsunami.

In this study, four levels of DEM grids at a cascade of refining spatial resolutions were used to simulate tsunami generation, propagation, and coastal flooding.

- The data for the first level DEM grids, grid layer 01, came from the NGDC ETOPO topographic and bathymetric database which covers the whole Pacific to simulate tsunami generations and propagations from distant sources at a spatial resolution of 2 arc-minutes (~1.8km on the Equator, Figure 5.1).
- The data for the second level grids, grid layer 02, was derived from LINZ Charts, the Seabed Mapping CMAP and GEBCO 08 datasets which covers the whole New Zealand and its offshore regions at 20 arc-seconds (~470m in Gisborne region, Figure 5.2).
- The third level grids, i.e., grid layer 03, derived from the same sources as the second level grids, covers the southern end of North Island at a spatial resolution of 4.0 arc-seconds (~94m in Gisborne region, Figure 5.3).
- The fourth level grids, grid layer 04, cover the Poverty Bay and its surrounding suburbs, including Muriwai, Manutuke, Gisborne City center and Wainui, at a spatial resolution of about 18 meters (Figure 5.4). This high resolution DEM data was derived from a combination of LiDAR (Light Detection and Ranging) topographical data provided by Gisborne District Council and bathymetric data derived from nautical charts for detailed tsunami inundation simulations in the coastal areas of Gisborne. Additional editing of this grid was made to remove bridge decks from the LiDAR data, where these would otherwise artificially restrict tsunami flow along rivers.
- The model resolution of 18m in grid layer 04 represents a compromise between running time and the ability to resolve details on a finer scale. Sensitivity testing of tsunami models of Napier recommended the use of inner grids in the 15-20m range, as further reduction in grid size produced minimal changes in results but greatly increased running time (Fraser, pers. comm.).

The conventional COMCOT arrangement in which the tsunami propagation in the innermost grid is modelled using the non-linear shallow water equations and the other grids use the linear shallow water equations, was used for all scenarios except those of the Outer Rise faults.

It was found that the tsunamis produced by earthquakes on the Outer Rise faults had a strong interaction with the Penguin and Ariel Rocks, and consequently the non-linear shallow water equations were employed in both grids 3 and 4 for these scenarios.

To the south of the airport there is a small area of marshland that is below current Mean Sea Level (MSL). In the modelling presented here there is an additional 0.5m of sea level rise assumed. Under these assumptions there is a wider area that is below the new MSL. Within the COMCOT model these areas are assumed to be filled with water to the level of the new MSL (Figure 5.5), which may or may not be the case in reality depending on how these areas are managed. The tsunami hazard and risk estimates in this area are affected by this assumption (see Discussion). There are also coastal areas near Muriwai that become below MSL, but as these areas are generally connected to the sea this represents a plausible assumption of ingress by the sea.

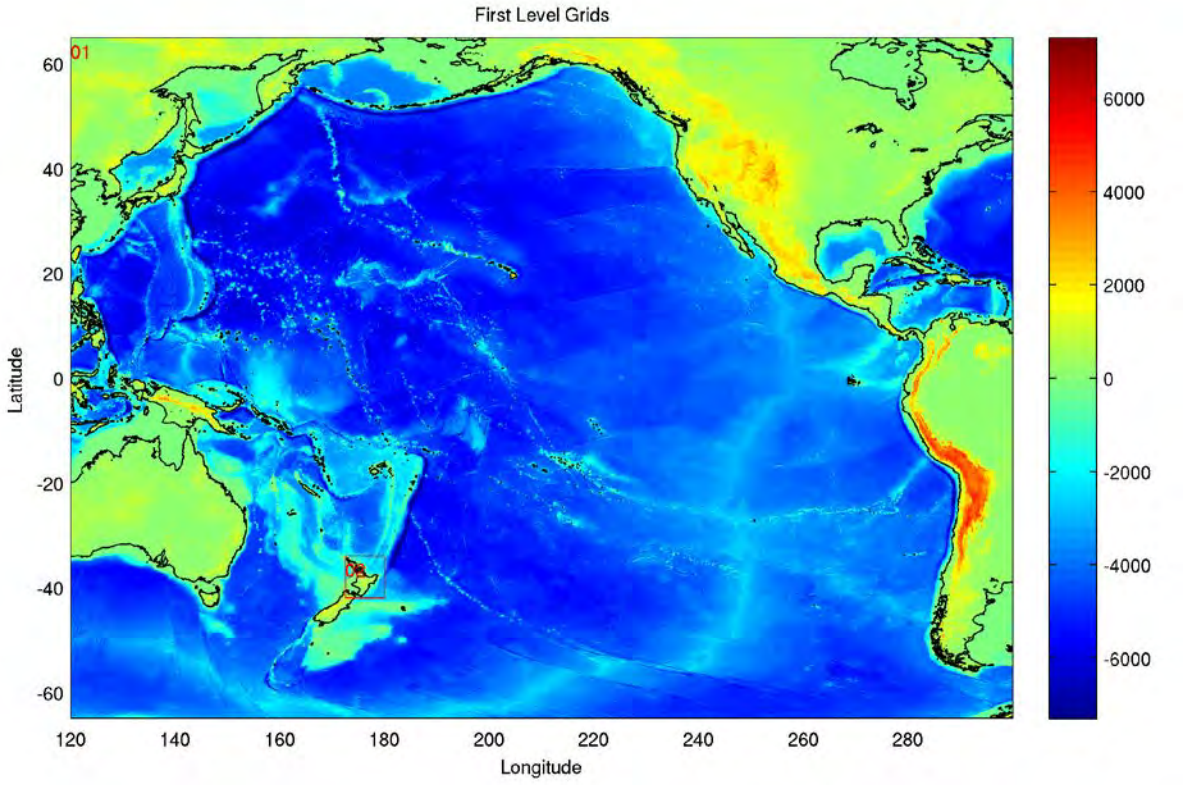

Figure 5.1 Nested grid setup for tsunami generation and propagation modelling. The first level grids - layer 01 spans the whole Pacific for tsunamis from local, regional and distant sources. The red rectangular box outlines the range of the second level grids – layer 02. See Figure 5.2, Figure 5.3 and Figure 5.4 for closer detail of grid layers 02, 03, 04. The topographic colour scale is in meters.

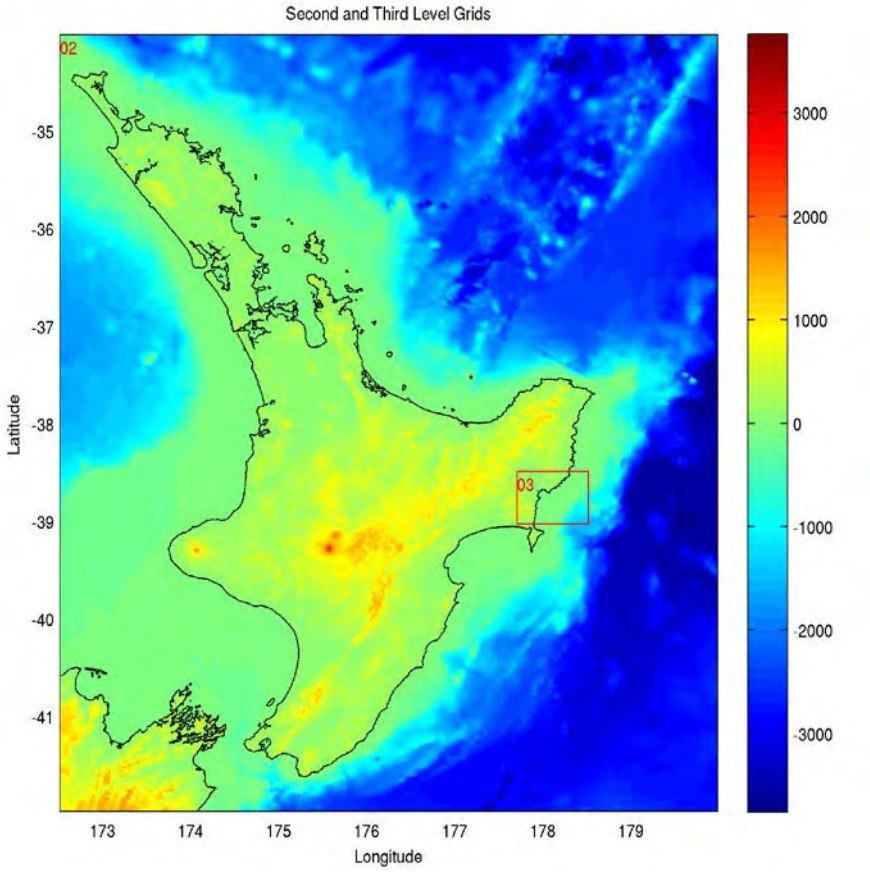

Figure 5.2 Nested grid setup for tsunami generation and propagation modelling. This figure shows the nested grid layer 02 which focus on the North Island of New Zealand and the offshore region at increasing levels of detail. The red rectangular box outlines the range of the third level grids – layer 03. See Figure 5.3 and Figure 5.4 for closer detail of grid layers 03, 04. The topographic colour scale is in meters.

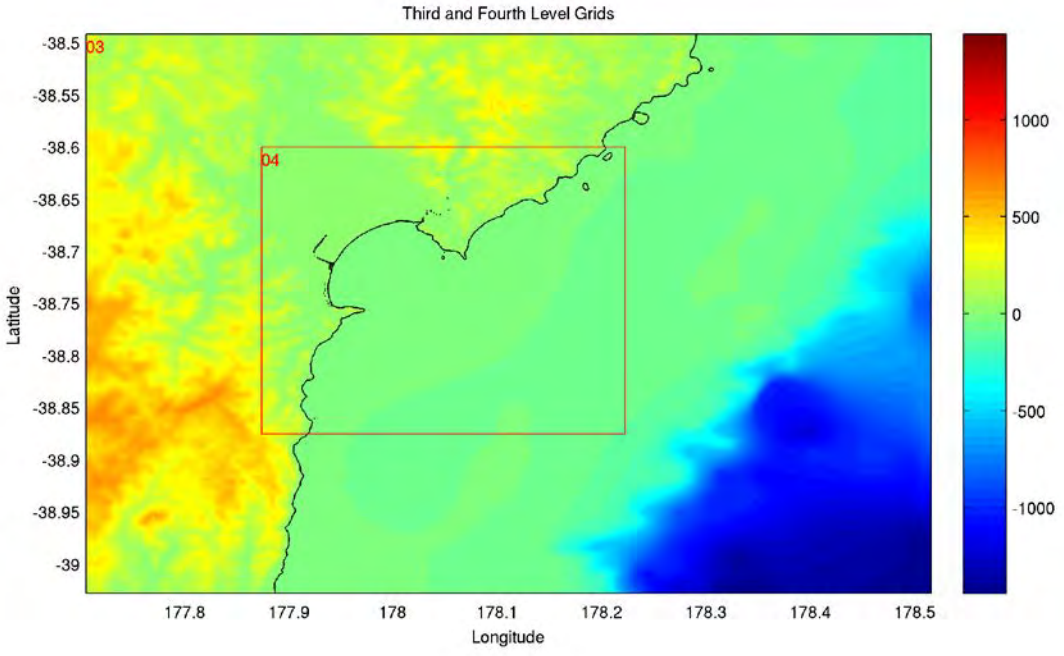

Figure 5.3 Nested grid setup for tsunami propagation modelling. This figure shows nested grid layer 03 which focus on Gisborne and its offshore region at increasing levels of detail. The red rectangular box outlines the range of the fourth level grids – layer 04. See Figure 5.4 for closer detail of grid layer 04. The topographic colour scale is in meters.

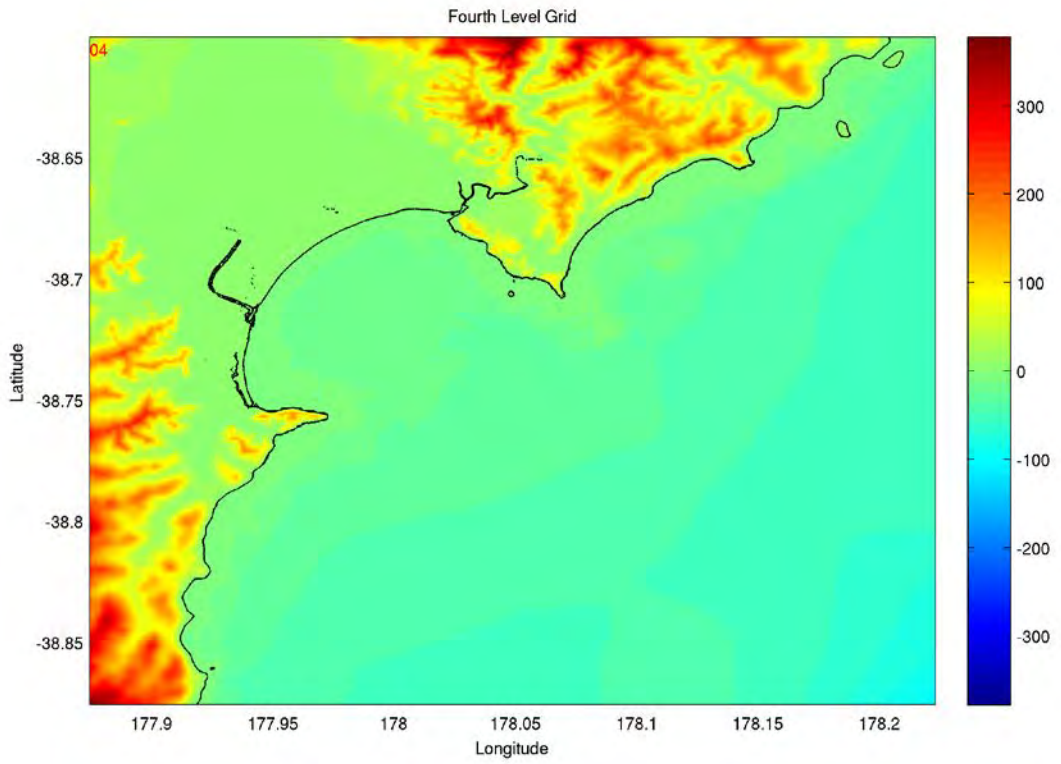

Figure 5.4 Nested grid setup for tsunami propagation and inundation modelling in Gisborne. This figure shows nested grid layer 04 which has the highest level of detail at about 18 m spatial resolution. The topographic colour scale is in meters.

Figure 5.5 Areas identified as being below Mean Sea Level, located south of the Airport (runway seen running N-S in top half of image), under the assumption of 0.5m sea level rise.

5.2 ROUGHNESS COEFFICIENT

In tsunami inundation modelling, one widely adopted approach is to use ground surface roughness coefficients (e.g., Manning's n) in a bottom friction model in place of ground features such as buildings, vegetation and other land cover types, in order to approximate the retarding and energy dissipation effects of such features on tsunami flows. However, the selection of roughness coefficients for different land covers is relatively subjective. For a given type of land cover, its corresponding roughness value presents a large range of variations in existing literatures of tsunami inundation studies.

By reviewing roughness values used for different land covers in the published literatures as well as considering specific patterns of land covers in New Zealand, a set of land cover roughness groups has been developed and each land cover group has been assigned a preferred roughness value for tsunami simulations (Table 5.1). The roughness value here refers to Manning's n in Manning's formula for modelling bottom friction during flooding (Wang and Power, 2011).

Table 5.1 Roughness values (Manning's n) for land-cover roughness groups.

Roughness group of land cover	Roughness value (n)
Water (e.g., rivers, lakes, offshore)	0.011
Tall vegetation (e.g., trees, forest)	0.040
Scrub (e.g., scrubland, bush)	0.040
Low vegetation (e.g., cropland, pasture, grassland)	0.030
Bare land (e.g., beach, exposed field)	0.025
Urban open area (e.g., parks, fields, parking areas)	0.025
Built-up area (e.g., residential/commercial/industrial areas)	0.060

This development of land cover groups and roughness values has been used in this tsunami modelling study in Gisborne. Figure 5.6 shows the spatial variation of landslide cover groups and roughness values in Gisborne.

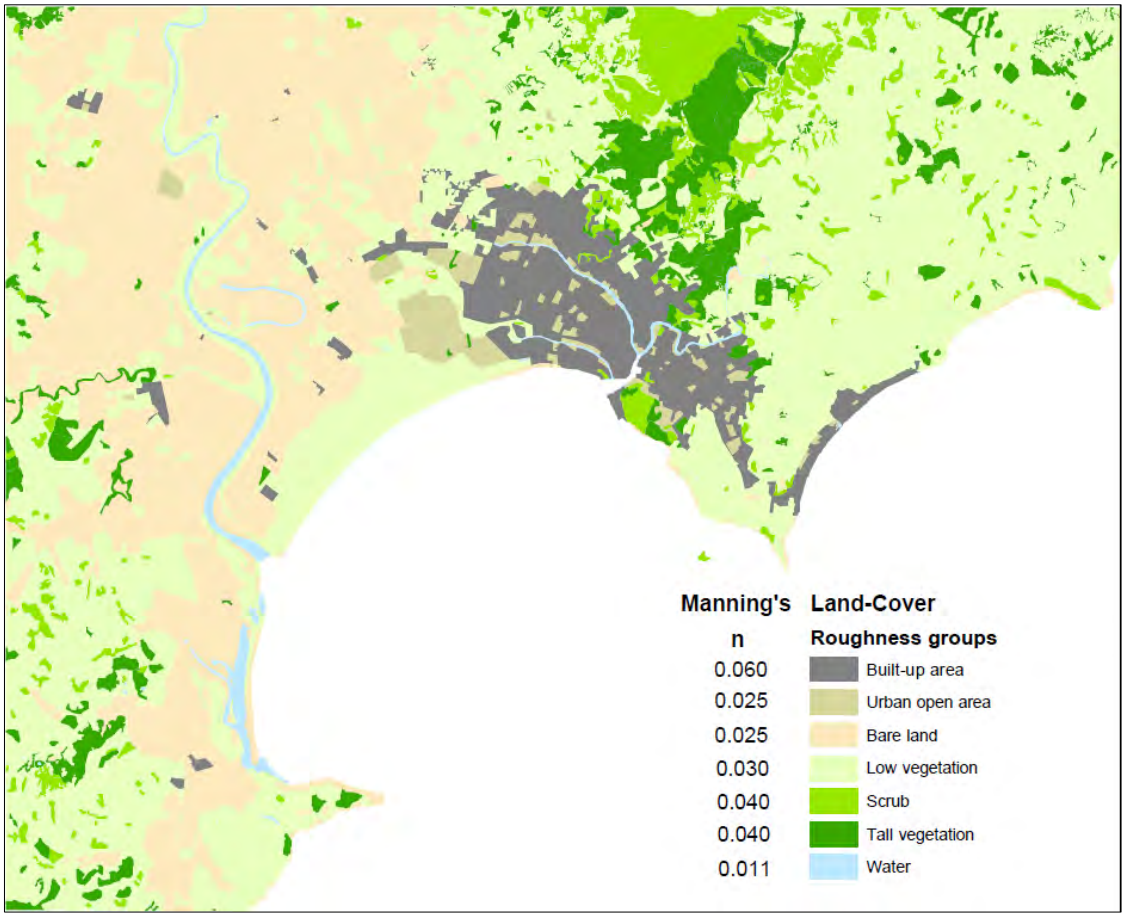

Figure 5.6 This figure shows the land cover groups and their corresponding roughness values in Gisborne. Colour-coded areas indicate different roughness groups of land cover.

This page is intentionally left blank.

6.0 HAZARD RESULTS

The 'Review of Tsunami Hazard in New Zealand (2013 Update)' (Power, 2013) produced the tsunami hazard curve for Gisborne (including Wainui Beach) shown in Figure 6.1

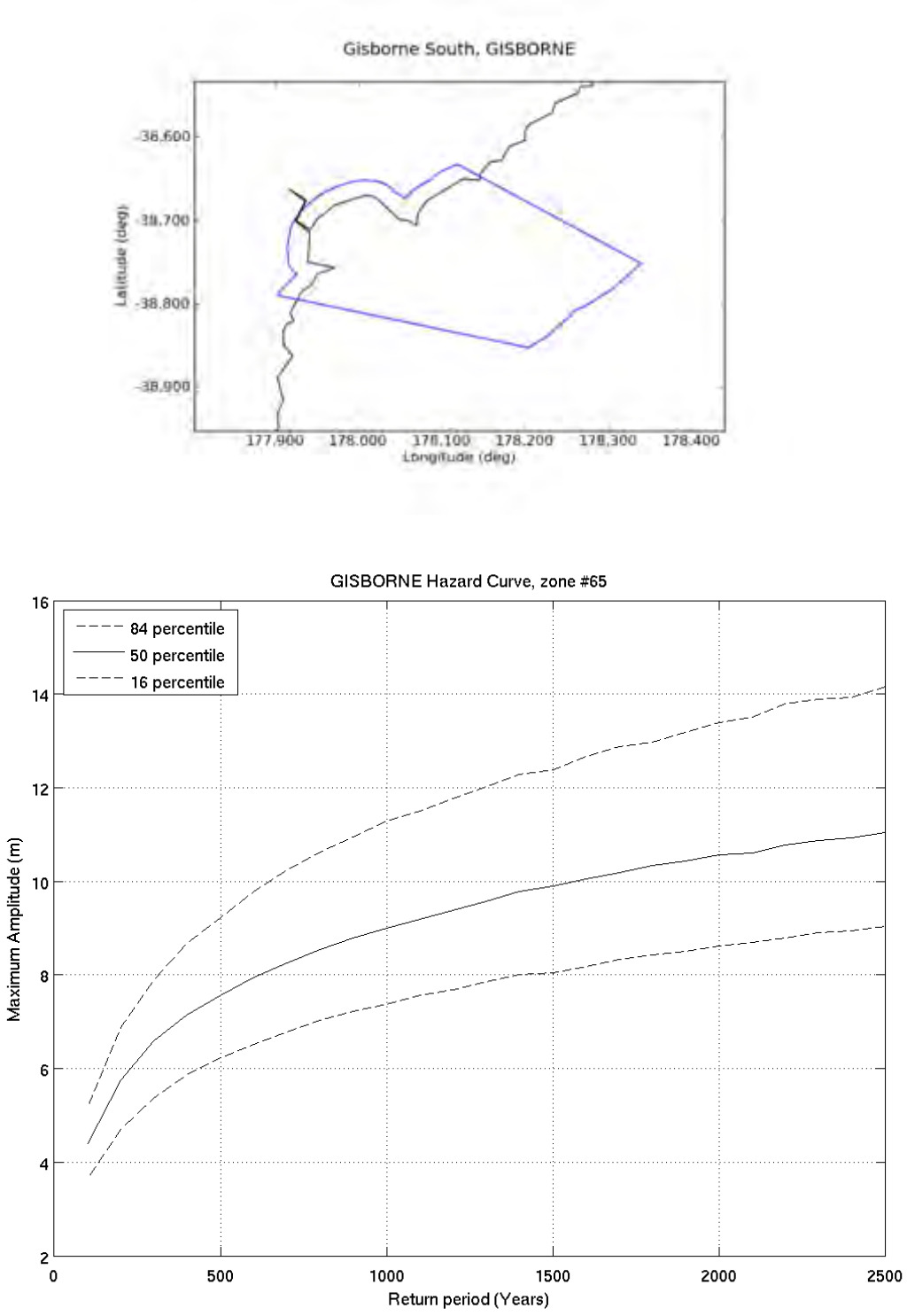

Figure 6.1 Area map and tsunami hazard curve for Gisborne.

The X axis shows the return period in years, this indicates the average interval between events exceeding the maximum tsunami wave amplitude shown on the Y-axis. It should be noted that maximum amplitude describes that maximum increase in water elevation that occurs within the domain – as the maximum amplitude varies along the coast, most locations in the domain are expected to receive a lower amplitude (see Discussion).

The solid line in Figure 6.1 represents the best estimate of the tsunami hazard curve. Yet there are many uncertainties in regard to the sources of potential tsunamis and in regard to how they are modelled. For this reason the effect of these uncertainties have also been modelled, and these are represented by the dashed-lines which are in effect 'error-bars' around the hazard curve.

This report is focussed on an unbiased assessment of tsunami hazard for the purposes of land-use planning. Therefore analysis of the results focuses on the solid line 'best estimate'. This is in contrast to the development of evacuation zones, for which the 'upper error-bar' is generally used, reflecting a conservative approach to uncertainty.

The 'Review of Tsunami Hazard in New Zealand (2013 Update)' also included dea-aggregations[1] of the 500 year and 2500 year tsunamis in Gisborne in the form of Pie charts (Figure 6.2).

[1] Deaggregations show the relative frequency with which different tsunami sources produce tsunami of the specified maximum height.

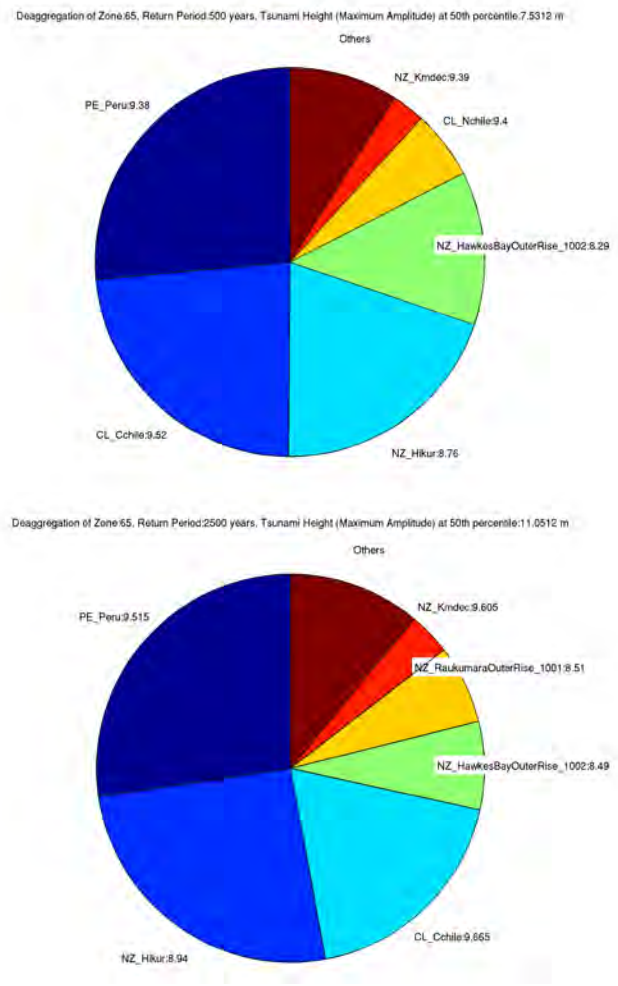

Figure 6.2 Deaggregation of tsunami sources for Gisborne at 500 yr (top) and 2500 yr (bottom) return periods.

For the purposes of the current study we also consider the 100 year and 1000 year deaggregations, and these are collectively better expressed in table form (Table 6.1).

Table 6.1 Deaggregation of tsunami hazard for Gisborne.

Gisborne Probabilistic study scenario spreadsheet				
Return times studied (yrs)	100	500	1000	2500
Rigidity assumed (Gpa)	50			
100 Years scenarios				
Target wave amplitude from 2013 report (m)	4.4			
Source name	**Effective Magnitude**	**Percentage of deagg**	**Percentage of top six**	**Percentage of local only**
Peru	9.16	27.1	32.15	
Central Chile	9.3	20.6	24.44	
Hikurangi	8.535	12.7	15.07	47.74
Northern Chile	9.2	10	11.86	
Raukumara Outer Rise	8.11	9.2	10.91	34.59
Kermadec Trench	9.075	4.7	5.58	17.67
500 Years scenarios				
Target wave amplitude from 2013 report (m)	7.53			
Source name	**Effective Magnitude**	**Percentage of deagg**	**Percentage of top six**	**Percentage of local only**
Peru	9.38	26.4	29.01	
Central Chile	9.52	23.4	25.71	
Hikurangi	8.76	19.9	21.87	56.06
Hawkes Bay Outer Rise	8.29	12.8	14.07	36.06
Northern Chile	9.4	5.7	6.26	
Kermadec Trench	9.39	2.8	3.08	7.89
1000 Years scenarios				
Target wave amplitude from 2013 report (m)	8.99			
Source name	**Effective Magnitude**	**Percentage of deagg**	**Percentage of top six**	**Percentage of local only**
Peru	9.46	26.4	30.24	
Hikurangi	8.84	25.3	28.98	69.13
Central Chile	9.58	20.9	23.94	
Raukumara Outer Rise	8.42	8.1	9.28	22.13
Northern Chile	9.48	3.4	3.89	
Kermadec Trench	9.48	3.2	3.67	8.74
2500 Years scenarios				
Target wave amplitude from 2013 report (m)	11.05			
Source name	**Effective Magnitude**	**Percentage of deagg**	**Percentage of top six**	**Percentage of local only**
Peru	9.515	27.3	30.64	
Hikurangi	8.94	25.6	28.73	59.40
Central Chile	9.665	18.7	20.99	
Hawkes Bay Outer Rise	8.49	7.3	8.19	16.94
Raukumara Outer Rise	8.51	6.6	7.41	15.31
Kermadec Trench	9.605	3.6	4.04	8.35

For each of the 4 return periods (100, 500, 1000, 2500 years) Table 6.1 shows the six largest contributors to the corresponding tsunami hazard.

The ‘Effective Magnitude’ is a concept explained in detail on page 129 of Power (2013). There are many factors, besides the earthquake magnitude, that influence how strongly a tsunami affects a particular piece of coast, some of these are uncertain and some vary naturally from event to event. In Power (2013) the effect of these uncertainties and variabilities are approximated by treating them as if they had the effect of shifting the earthquake magnitude up or down. This leads to the ‘effective magnitude’ tabulated here.

In some situations the ‘effective magnitude’ may be larger than the largest actual magnitude currently believed plausible for a particular source.

The ‘Percentage of deagg’ describes how large a proportion that source represents in the ‘pie charts’ Figure 6.2. The ‘Percentage of top six’ describes these proportions if the ‘Others’ category is excluded – these six percentages then add up to 100%.

The ‘Percentage of local only’ describes the proportion that each local tsunami source represents as a percentage of the total weighting attributed to the tabulated local sources.

For the purposes of Objective B the hazard model data was re-processed, excluding those tsunami sources that were not local to Gisborne (specifically those sources where the travel time was greater than 1 hour). The selection of sources within one hour travel time was made using WinITDB (ref; Figure 6.3); only sources wholly or partially within the 1 hour travel time contour were included. After making this exclusion, the resulting hazard curve is shown in Figure 6.4.

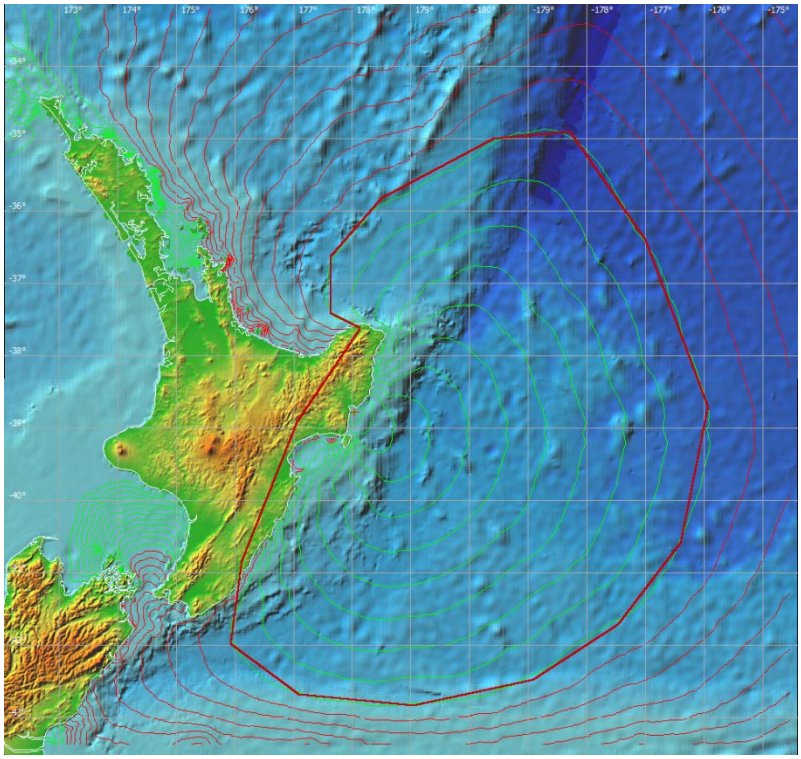

Figure 6.3 One hour tsunami travel time contour from Poverty Bay (thick red line) as derived from WinITDB and used for selection of local tsunami sources.

In order to re-use the local source models in Table 6.1 for the purposes of Objective B it is necessary to evaluate which return period those sources correspond to on the local-source only hazard curve.

Superimposed on the local-source only hazard curve (Figure 6.4) are red lines corresponding to the 100, 500, 1000 and 2500 year all-source tsunami heights. From this the return periods for encountering local-source tsunamis of these same heights were found. The results are tabulated in Table 6.2.

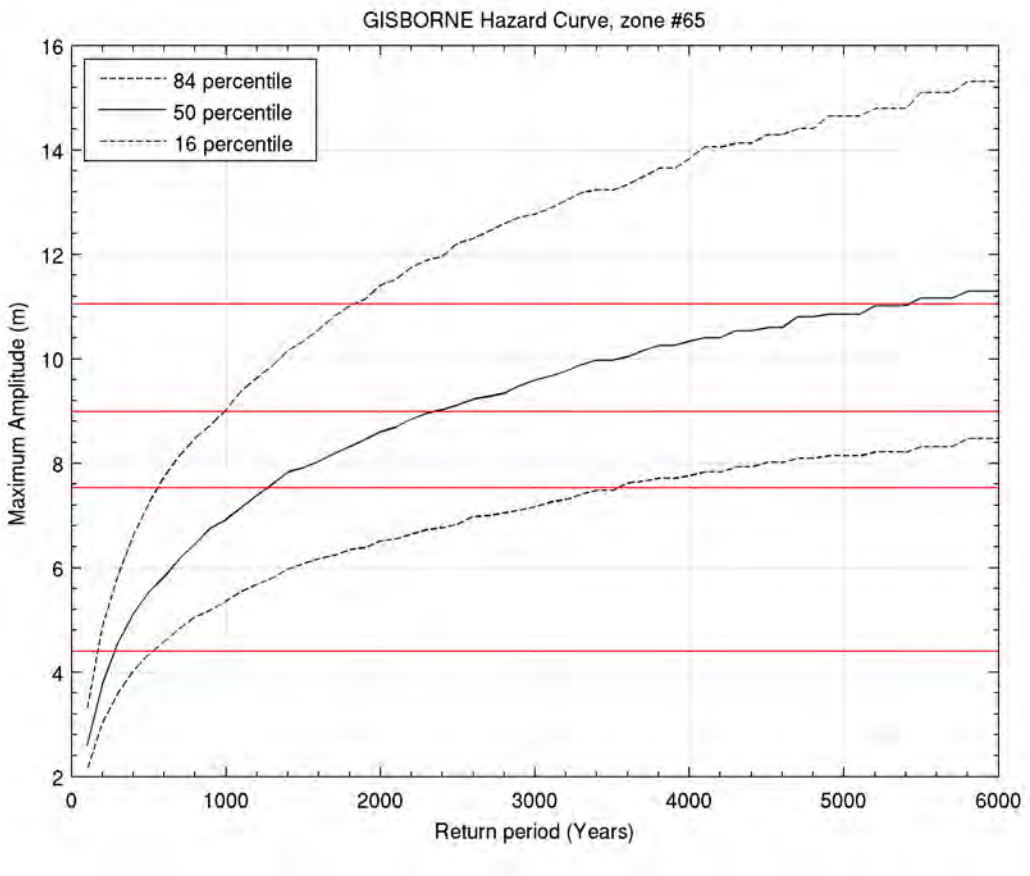

Figure 6.4 Local source only hazard curve for Gisborne (Poverty Bay). The red horizontal lines correspond to the 100, 500, 1000 and 2500 year all-sources tsunami heights.

Table 6.2 Return periods for specified tsunami heights, considering all sources, and local sources only.

Tsunami height (m)	All source return period (yr)	Local only return period (yr)
4.4	100	280
7.53	500	1270
8.99	1000	2350
11.05	2500	5420

7.0 SCENARIOS

A total of 24 tsunami scenarios were created and run, 6 for each of the 4 return periods. The scenarios can be divided into 3 categories:

1. Distant earthquakes on subduction interfaces: Peru, Northern Chile, Central Chile
2. Local or Regional earthquakes on subduction interfaces: Hikurangi, Kermadec Trench
3. Local earthquakes on Outer Rise faults: Raukumara Outer Rise, Hawkes Bay Outer Rise

Modelling of the scenarios was performed using the COMCOT-API (Mueller et al, 2014), a set of software routines that allows for consistent modelling of a varied sets of scenarios.

The scenarios based on Distant earthquakes (1) were composed by composing the earthquake rupture surface from sets of individual 'unit sources' representing 100 x 50 km patches of the corresponding plate interface. The set of 'patches used here was developed by NOAA (Éble and NCTR staff, 2014). The total number of patches to be used was estimated from scaling relationships (Abe, 1975; Power et al., 2007), the choice of which patches to use was made manually, and a slip corresponding to the magnitude was estimated by the COMCOT-API. For some very large magnitude events the rupture areas extended onto adjacent subduction zones.

The scenarios of Local or Regional earthquakes on subduction interfaces (2) were handled differently for the Kermadec Trench and for Hikurangi. For the Kermadec Trench the scenarios were created in a similar fashion to the Distant earthquakes, except that the 100 x 50 km unit source 'patches' were taken from Power et al (2012). For the most important local source, the Hikurangi plate interface, a very detailed geometrical model of the plate boundary was used (Williams et al., 2013), a central location for each rupture was manually chosen, and the COMCOT-API was used to select the appropriate area and slip to form the simulated earthquake.

The scenarios based on Outer Rise earthquakes were adapted from the table on page 208 in Power (2013). Although the plausibility of Outer Rise faults on the Hikurangi margin is demonstrated by historical earthquakes of the appropriate mechanism, such as the Mw 6.7 Gisborne earthquake in 2007, the location and geometry of the faults have not been mapped using geophysical measurements and the faults have not been directly observed. The tabulated data in Power (2013) is based on expert opinion. The minimum depth for ruptures on these faults has been set at 5km, and a maximum fault plane width of 60km has been assumed, fault plane length was adjusted according to scaling relations (Abe, 1975; Power et al., 2007).

Estimated flow depths from the modelling of these scenarios is shown in Figure 7.1 - Figure 7.24. Onshore these figures show the maximum depth of water reached, offshore they show the maximum water level.

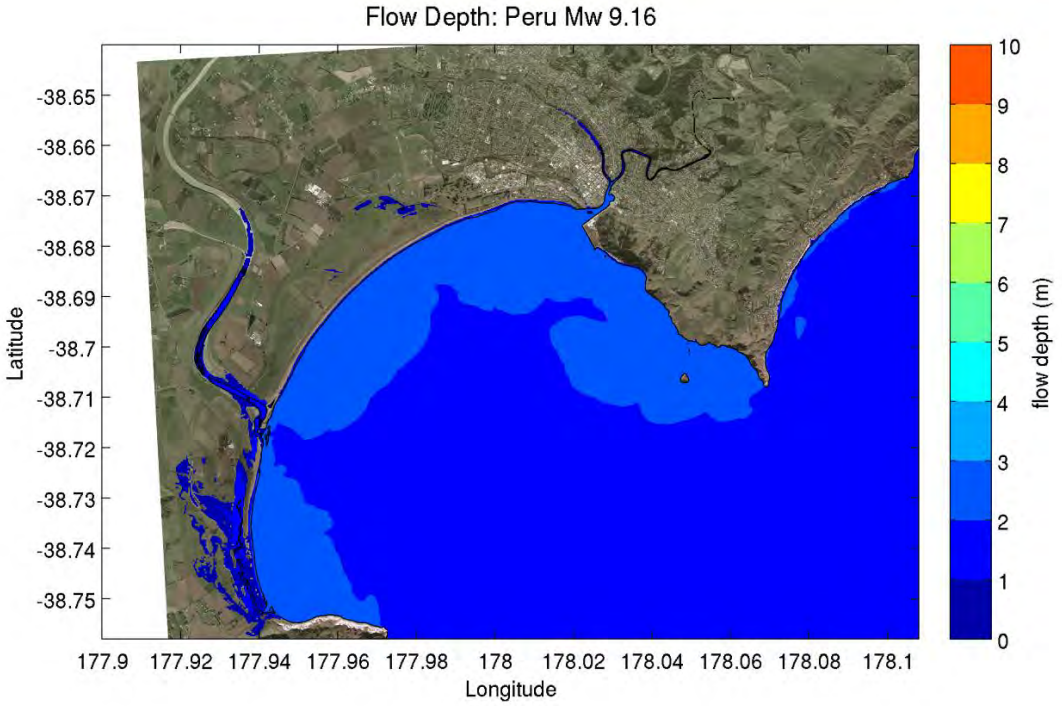

Figure 7.1 Maximum onshore flow depth in metres for the Peru Mw 9.16 scenario (from the deaggregation of the 100 year tsunami). Offshore the colour scale shows the maximum water level.

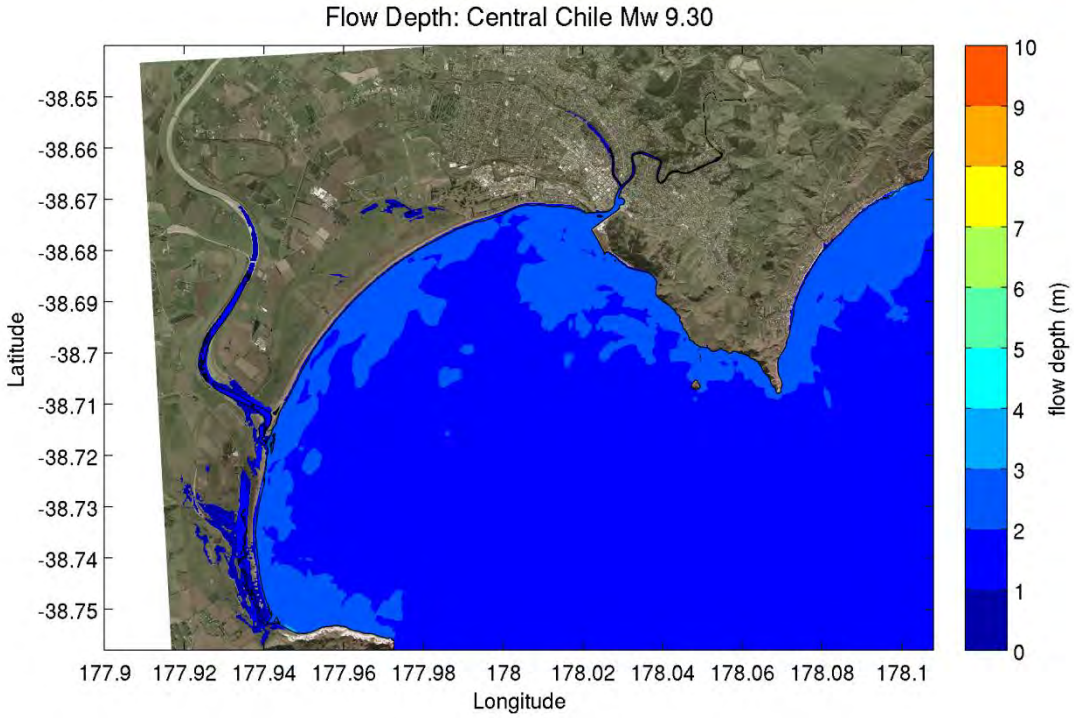

Figure 7.2 Maximum onshore flow depth in metres for the Central Chile Mw 9.30 scenario (from the deaggregation of the 100 year tsunami). Offshore the colour scale shows the maximum water level.

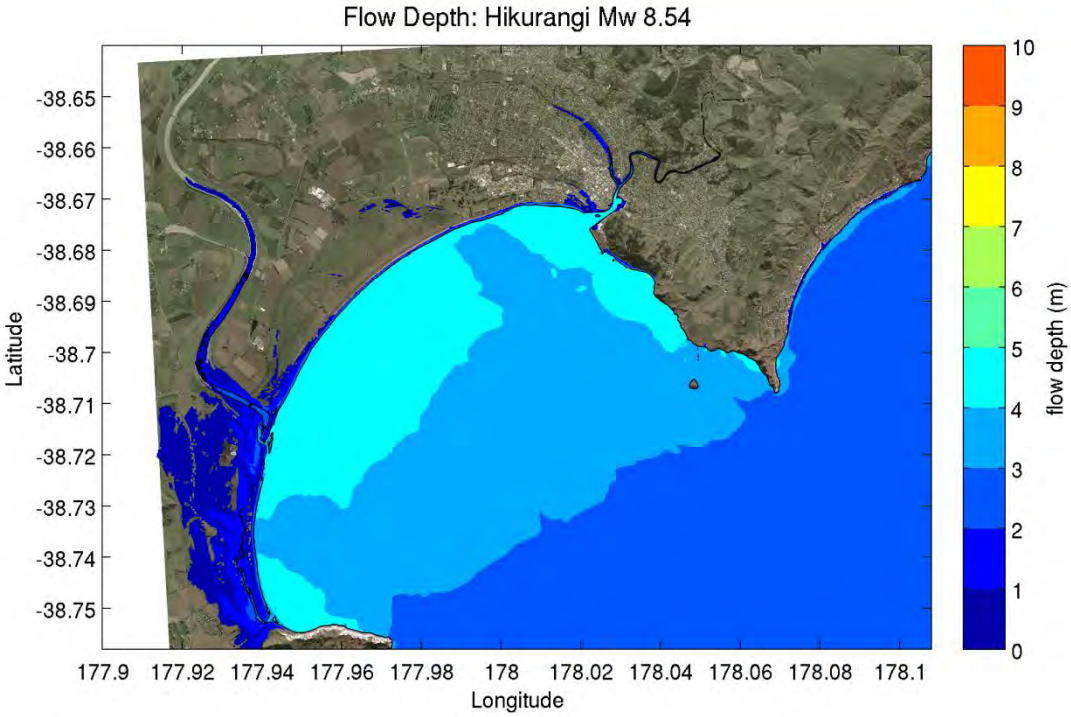

Figure 7.3 Maximum onshore flow depth in metres for the Hikurangi Mw 8.54 scenario (from the deaggregation of the 100 year tsunami). Offshore the colour scale shows the maximum water level.

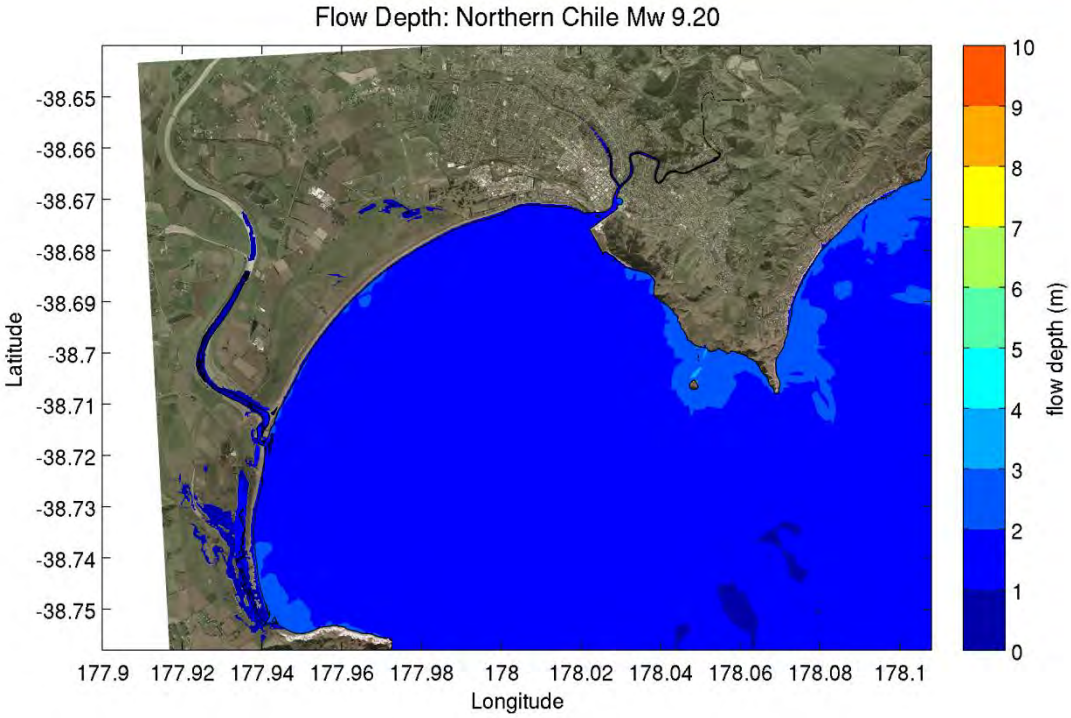

Figure 7.4 Maximum onshore flow depth in metres for the Northern Chile Mw 9.20 scenario (from the deaggregation of the 100 year tsunami). Offshore the colour scale shows the maximum water level.

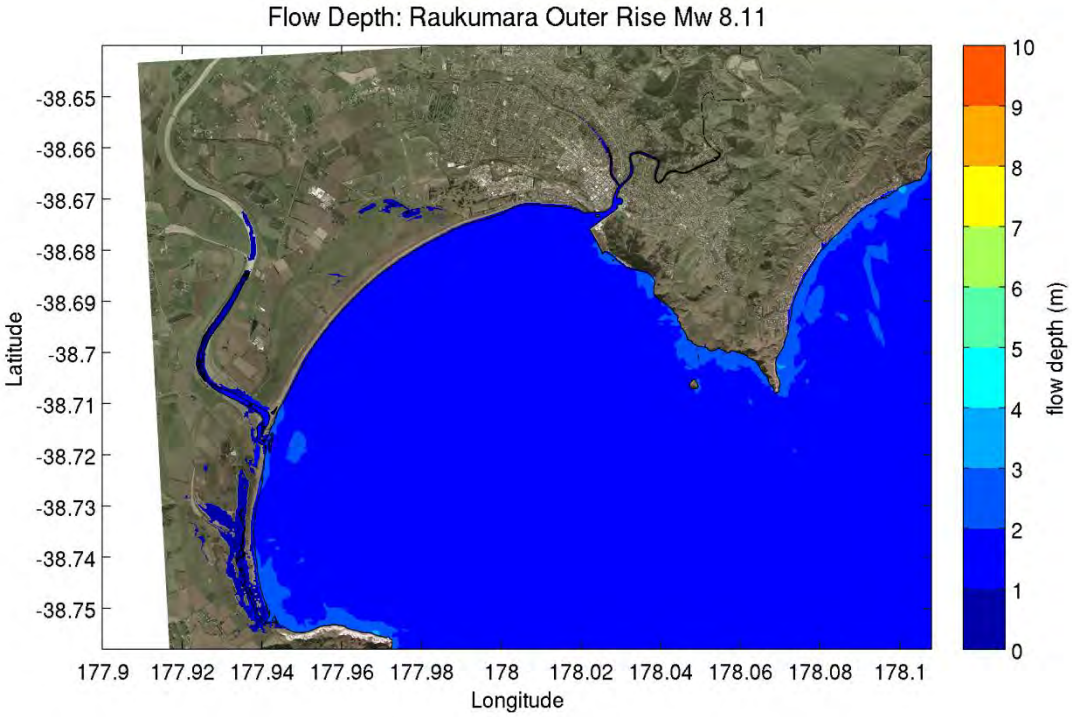

Figure 7.5 Maximum onshore flow depth in metres for the Raukumara Outer Rise Mw 8.11 scenario (from the deaggregation of the 100 year tsunami). Offshore the colour scale shows the maximum water level.

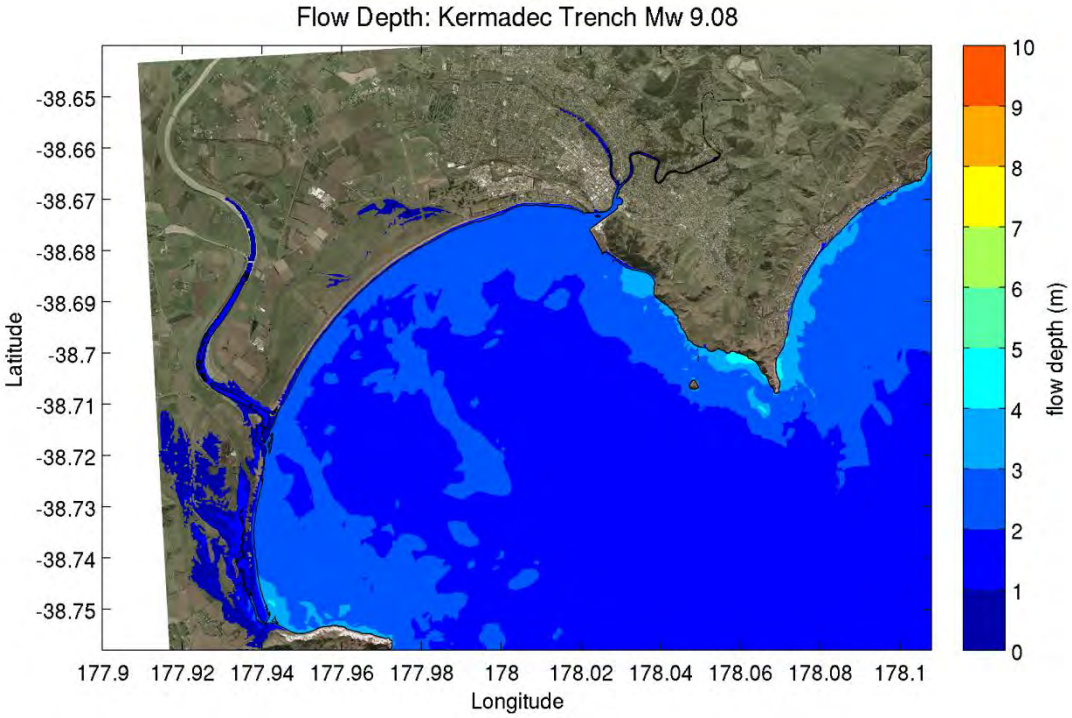

Figure 7.6 Maximum onshore flow depth in metres for the Kermadec Trench Mw 9.08 scenario (from the deaggregation of the 100 year tsunami). Offshore the colour scale shows the maximum water level.

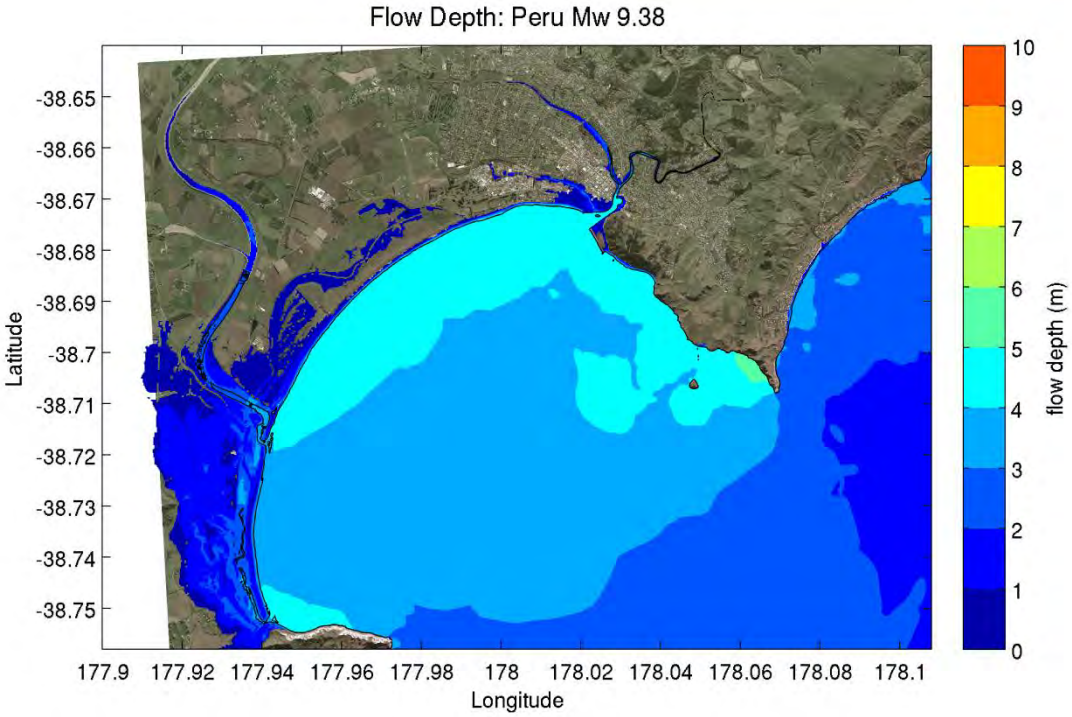

Figure 7.7 Maximum onshore flow depth in metres for the Peru Mw 9.38 scenario (from the deaggregation of the 500 year tsunami). Offshore the colour scale shows the maximum water level.

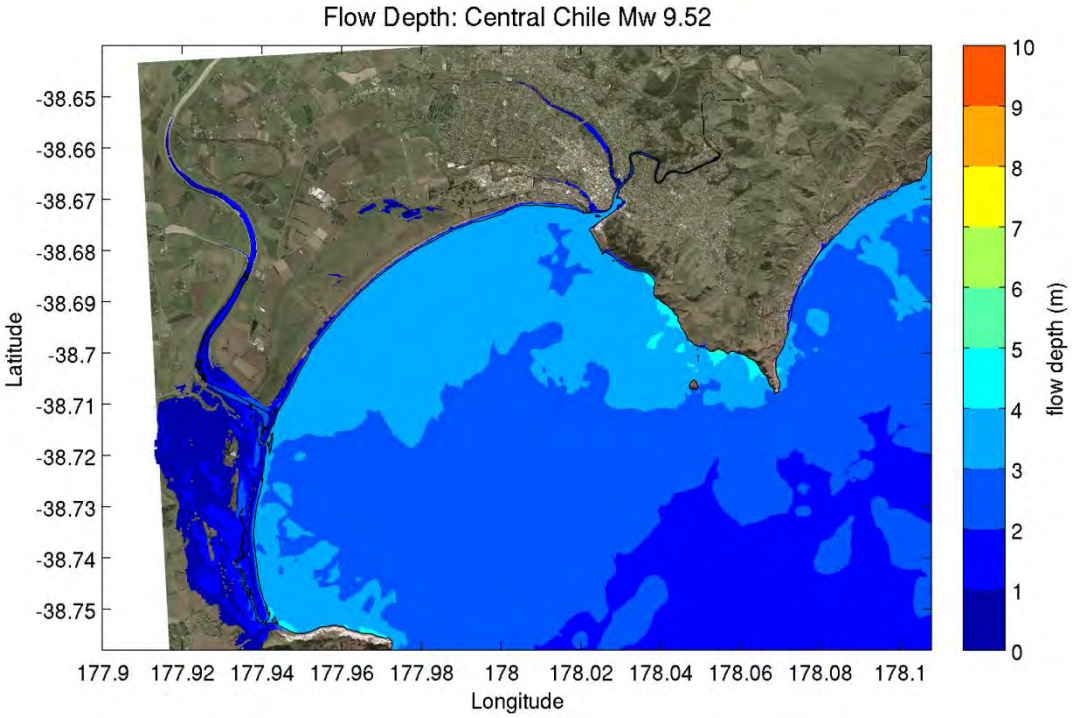

Figure 7.8 Maximum onshore flow depth in metres for the Central Chile Mw 9.52 scenario (from the deaggregation of the 500 year tsunami). Offshore the colour scale shows the maximum water level.

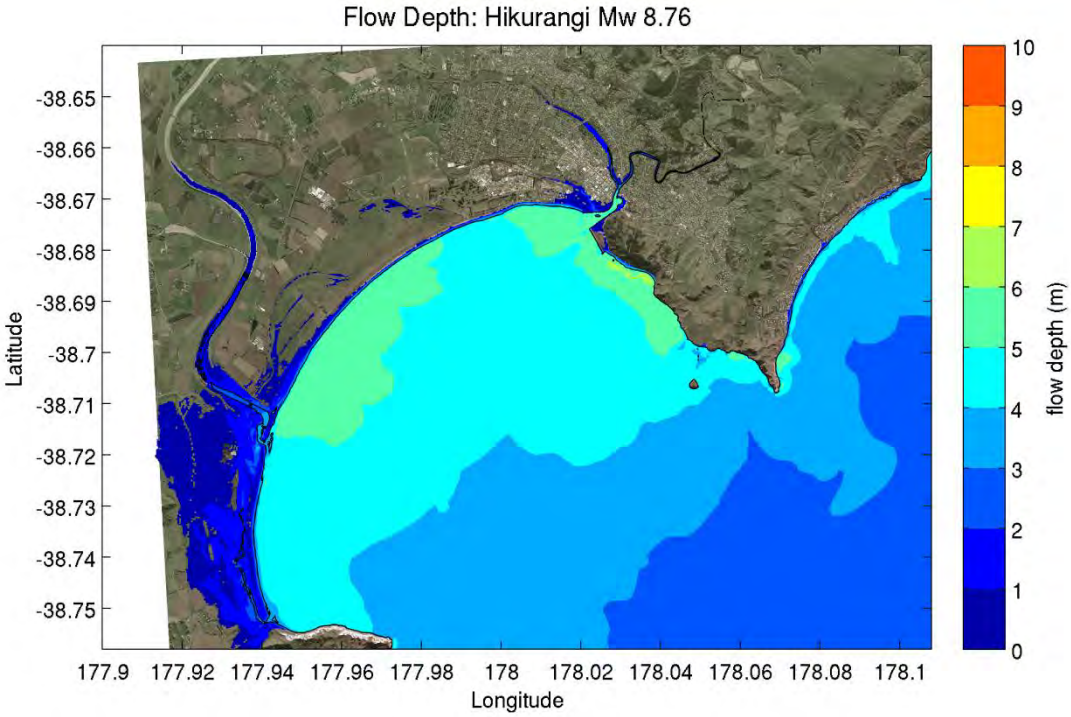

Figure 7.9 Maximum onshore flow depth in metres for the Hikurangi Mw 8.76 scenario (from the deaggregation of the 500 year tsunami). Offshore the colour scale shows the maximum water level.

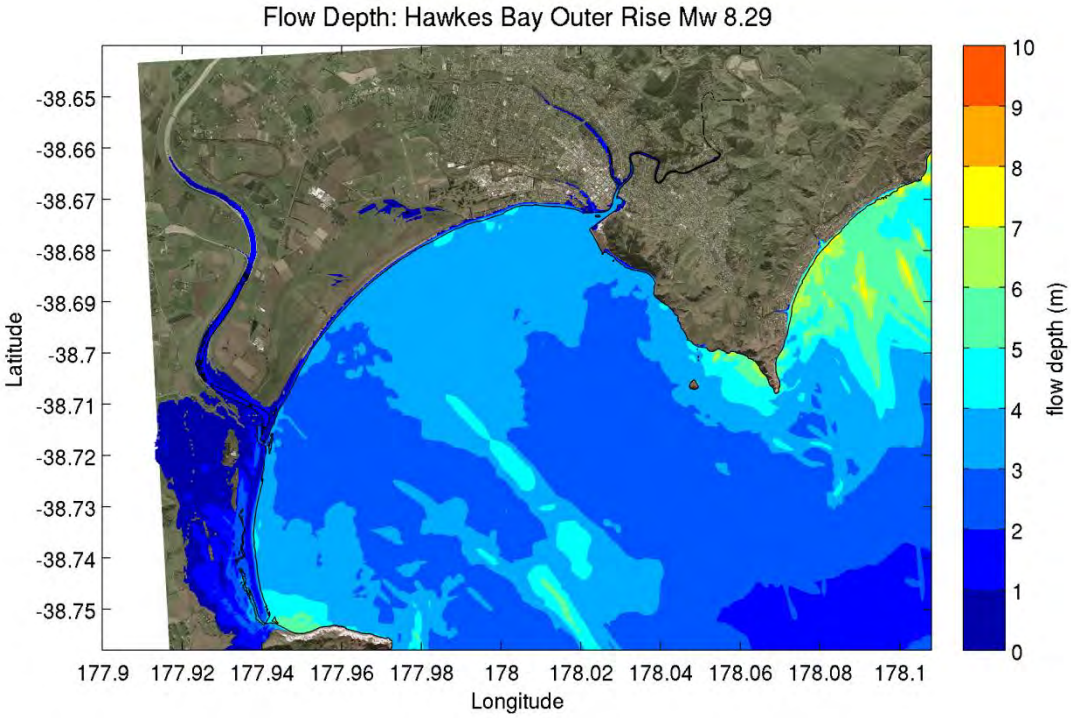

Figure 7.10 Maximum onshore flow depth in metres for the Hawkes Bay Outer Rise Mw 8.29 scenario (from the deaggregation of the 500 year tsunami). Offshore the colour scale shows the maximum water level.

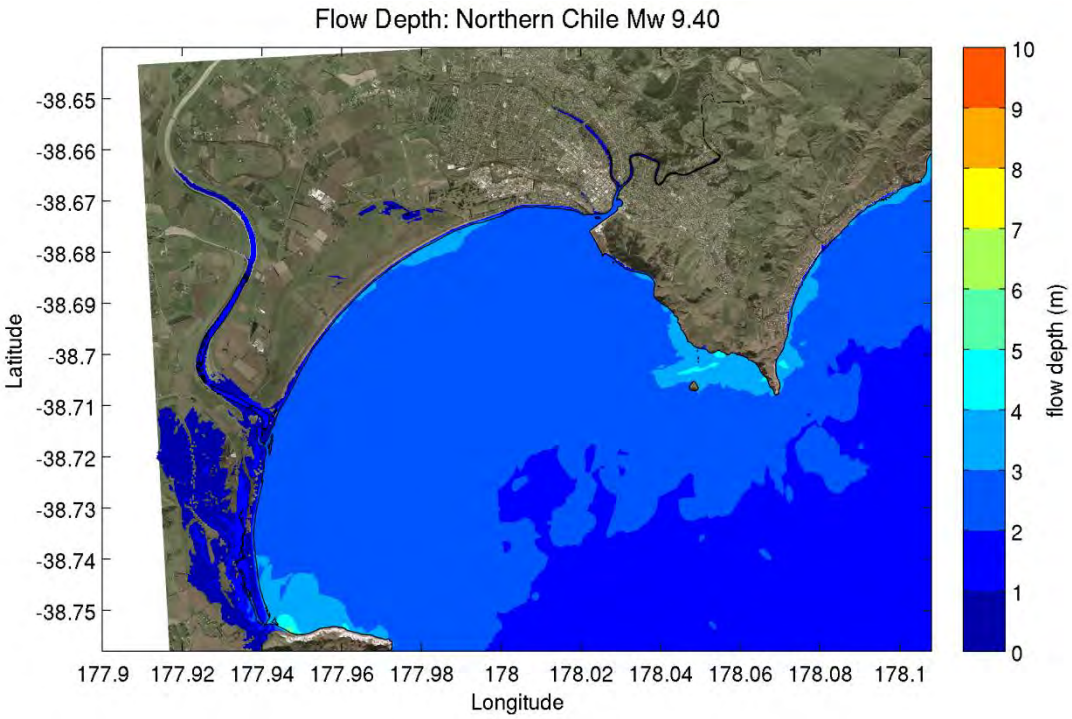

Figure 7.11 Maximum onshore flow depth in metres for the Northern Chile Mw 9.40 scenario (from the deaggregation of the 500 year tsunami). Offshore the colour scale shows the maximum water level.

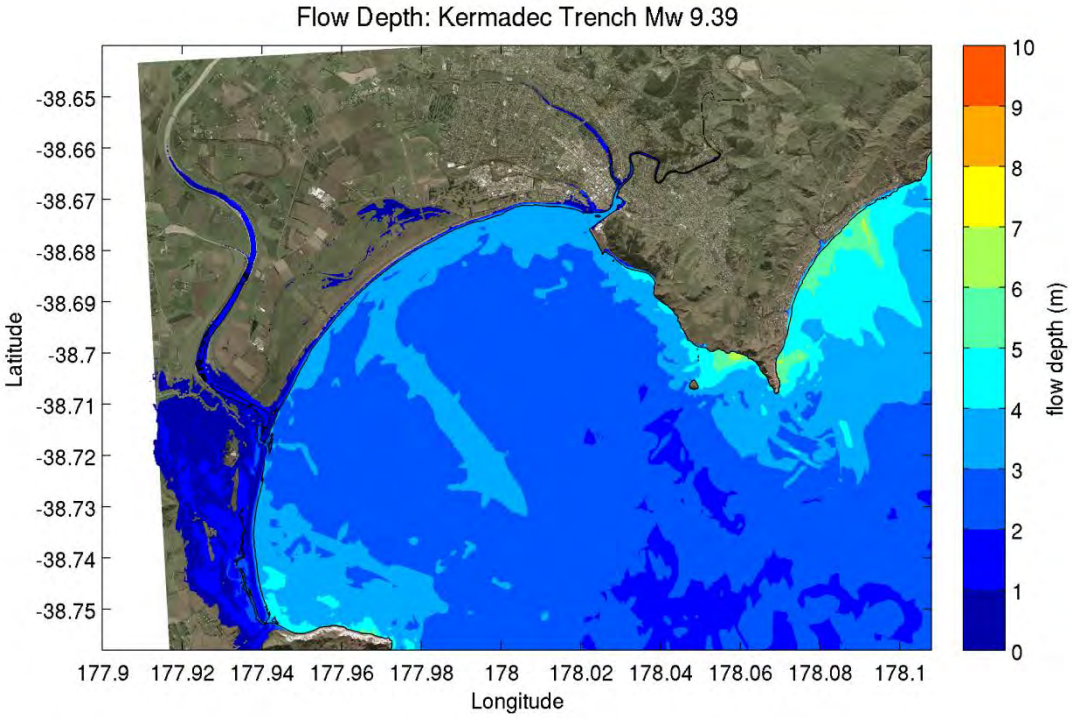

Figure 7.12 Maximum onshore flow depth in metres for the Kermadec Trench Mw 9.39 scenario (from the deaggregation of the 500 year tsunami). Offshore the colour scale shows the maximum water level.

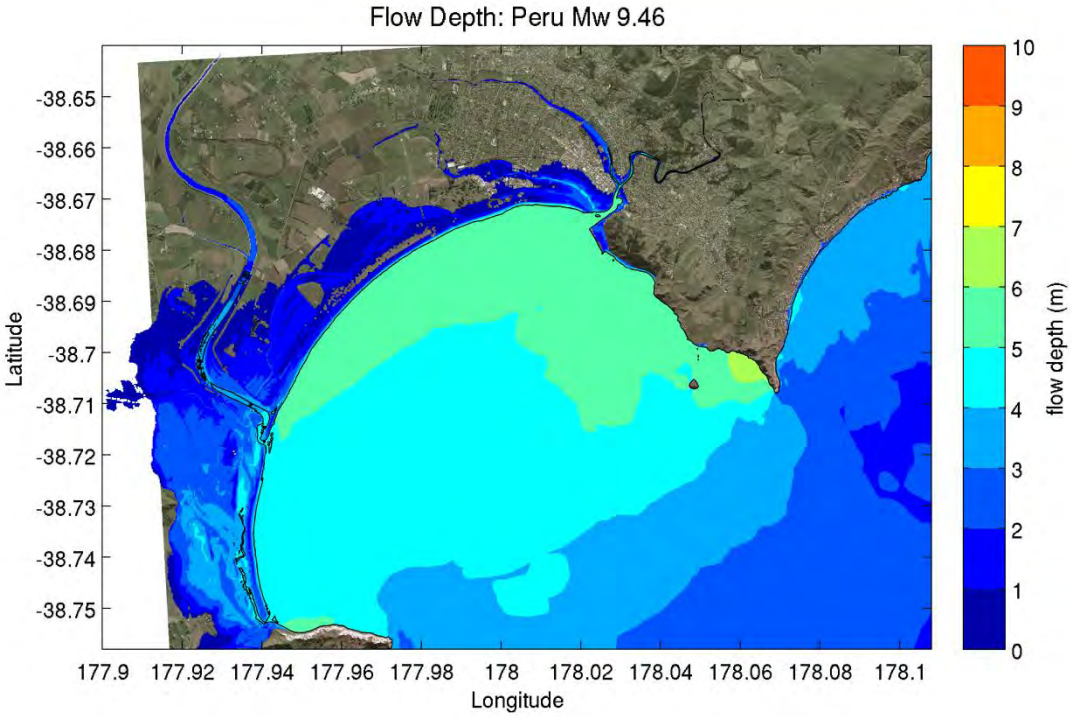

Figure 7.13 Maximum onshore flow depth in metres for the Peru Mw 9.46 scenario (from the deaggregation of the 1000 year tsunami). Offshore the colour scale shows the maximum water level.

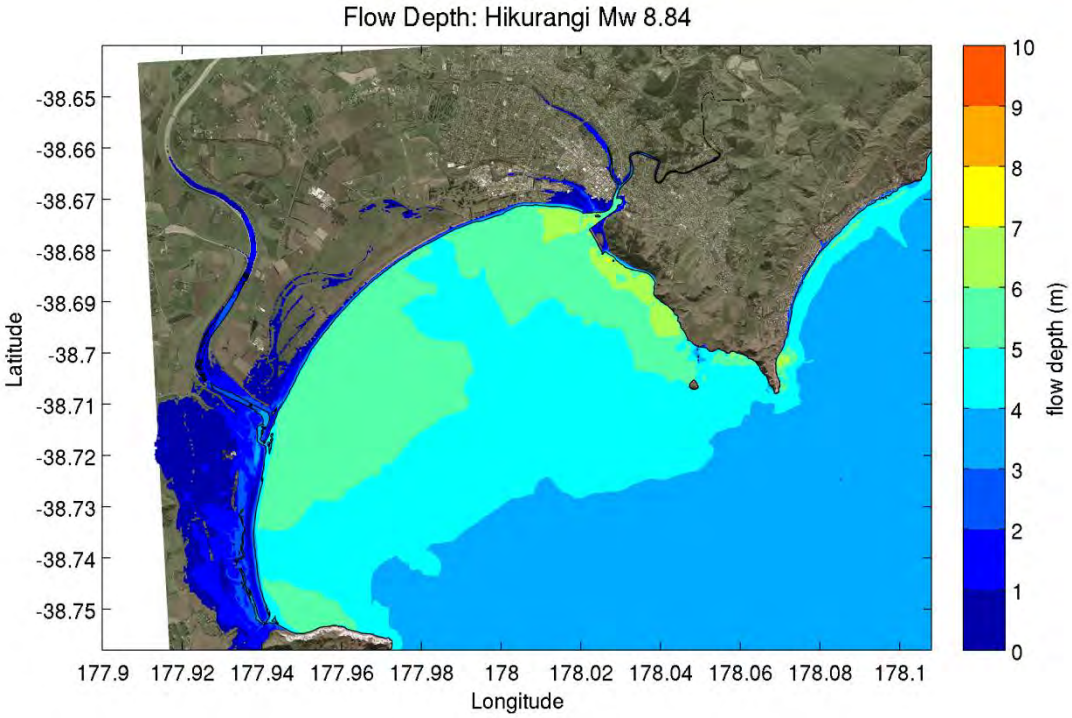

Figure 7.14 Maximum onshore flow depth in metres for the Hikurangi Mw 8.84 scenario (from the deaggregation of the 1000 year tsunami). Offshore the colour scale shows the maximum water level.

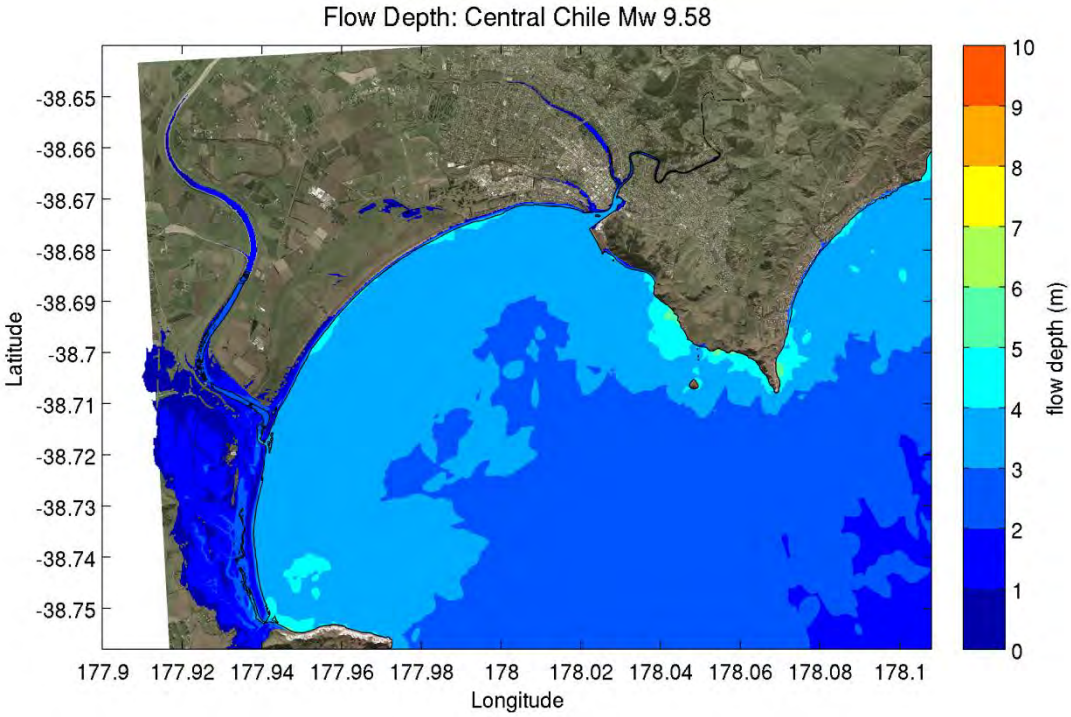

Figure 7.15 Maximum onshore flow depth in metres for the Central Chile Mw 9.58 scenario (from the deaggregation of the 1000 year tsunami). Offshore the colour scale shows the maximum water level.

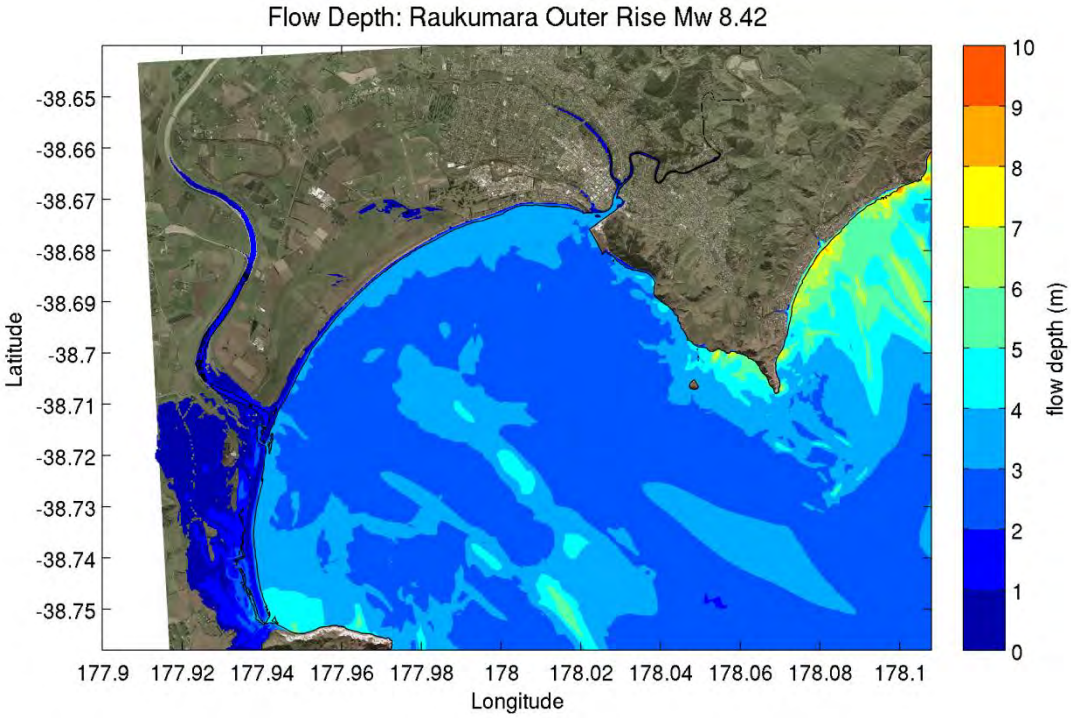

Figure 7.16 Maximum onshore flow depth in metres for the Raukumara Outer Rise Mw 8.42 scenario (from the deaggregation of the 1000 year tsunami). Offshore the colour scale shows the maximum water level.

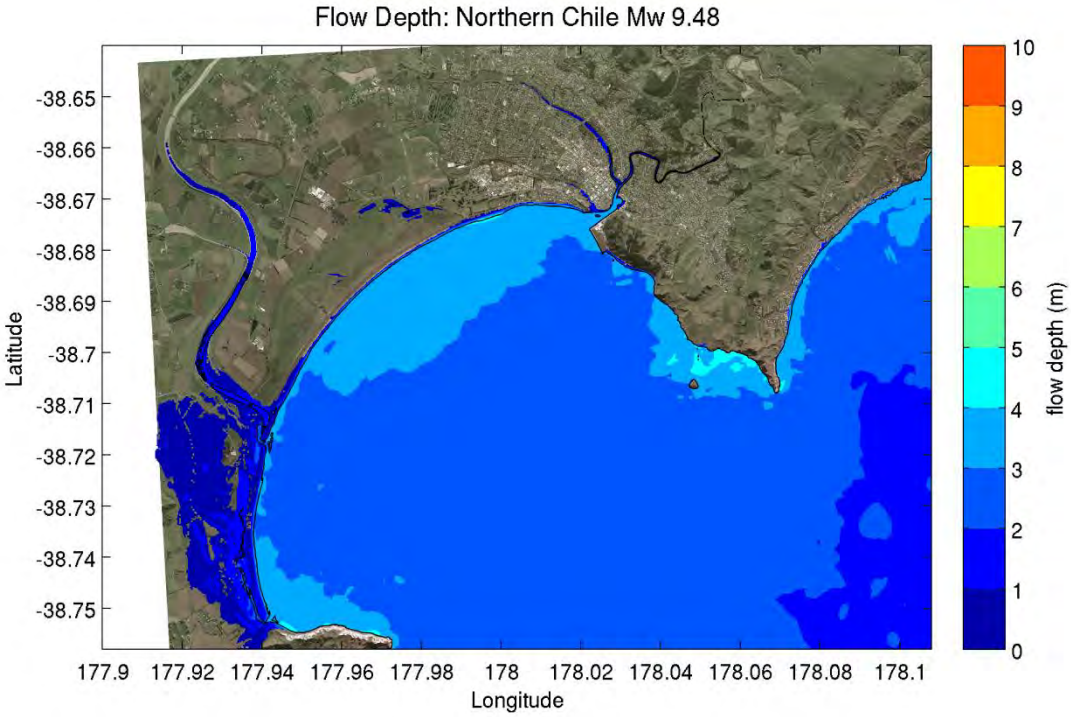

Figure 7.17 Maximum onshore flow depth in metres for the Northern Chile Mw 9.48 scenario (from the deaggregation of the 1000 year tsunami). Offshore the colour scale shows the maximum water level.

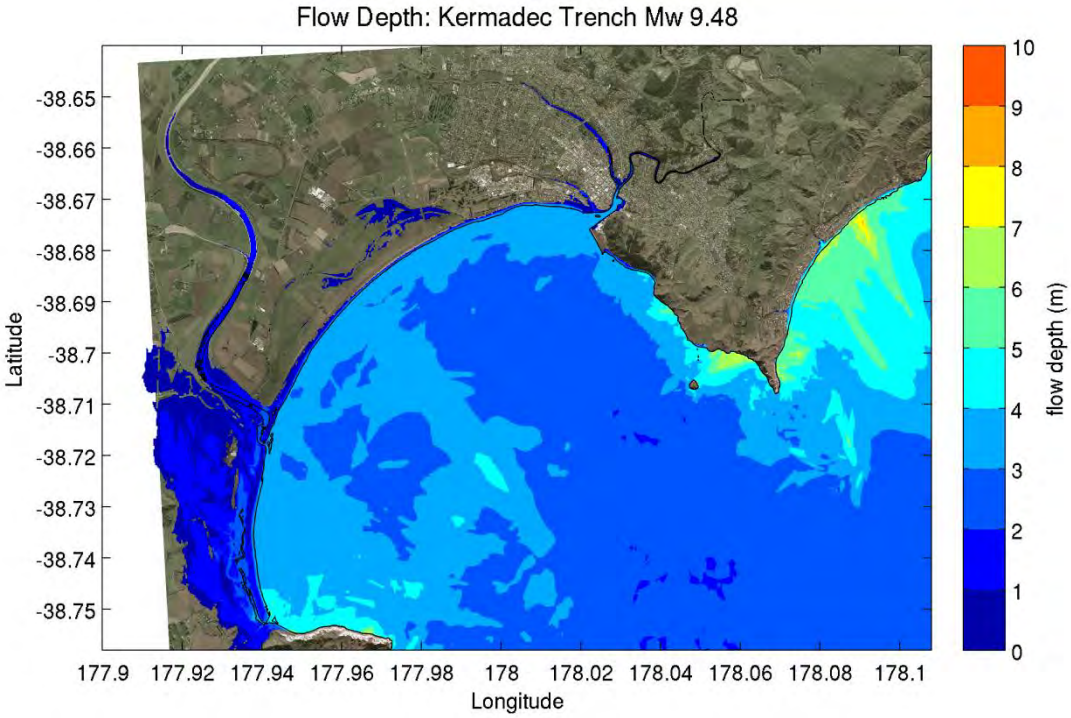

Figure 7.18 Maximum onshore flow depth in metres for the Kermadec Trench Mw 9.48 scenario (from the deaggregation of the 1000 year tsunami). Offshore the colour scale shows the maximum water level.

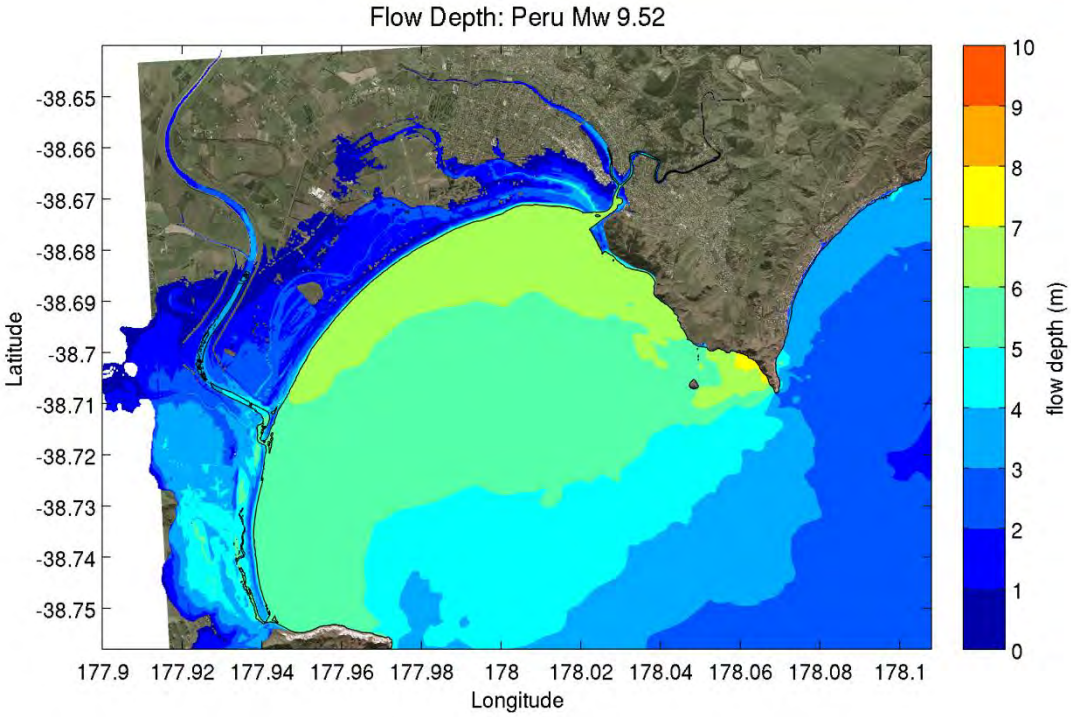

Figure 7.19 Maximum onshore flow depth in metres for the Peru Mw 9.52 scenario (from the deaggregation of the 2500 year tsunami). Offshore the colour scale shows the maximum water level.

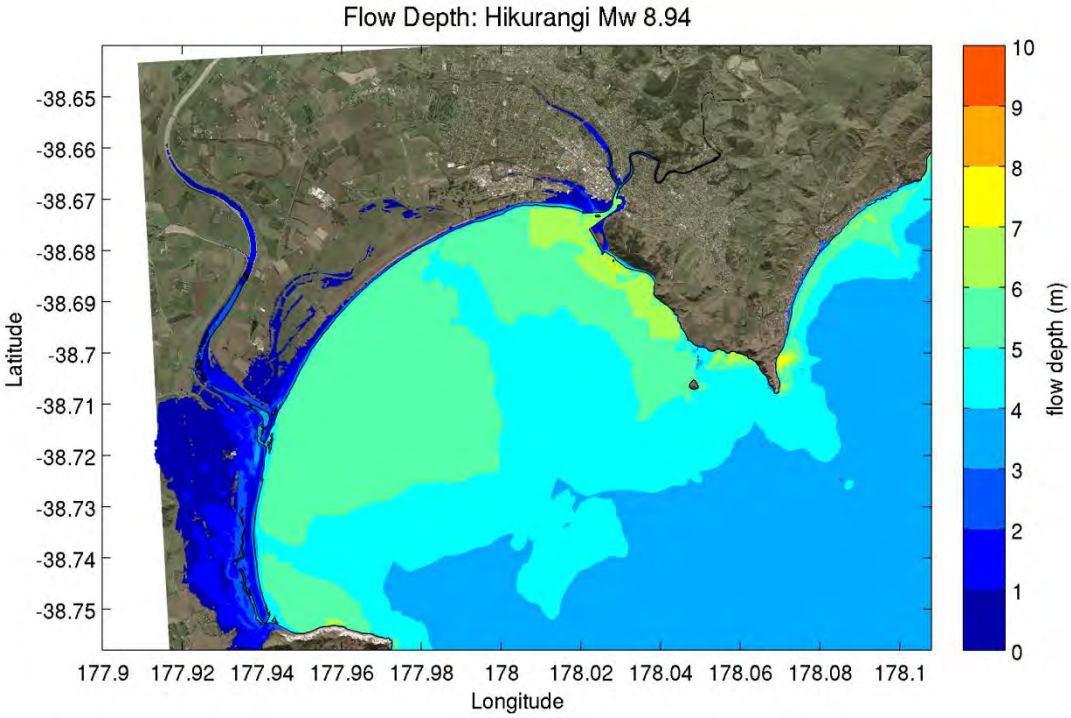

Figure 7.20 Maximum onshore flow depth in metres for the Hikurangi Mw 8.94 scenario (from the deaggregation of the 2500 year tsunami). Offshore the colour scale shows the maximum water level.

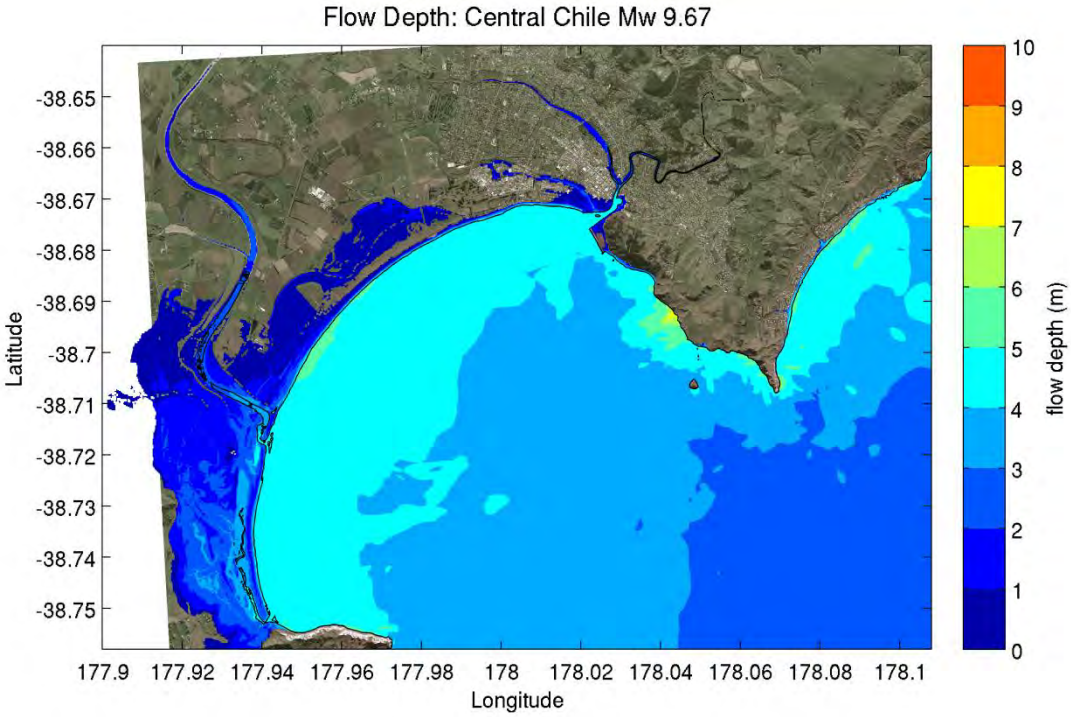

Figure 7.21 Maximum onshore flow depth in metres for the Central Chile Mw 9.67 scenario (from the deaggregation of the 2500 year tsunami). Offshore the colour scale shows the maximum water level.

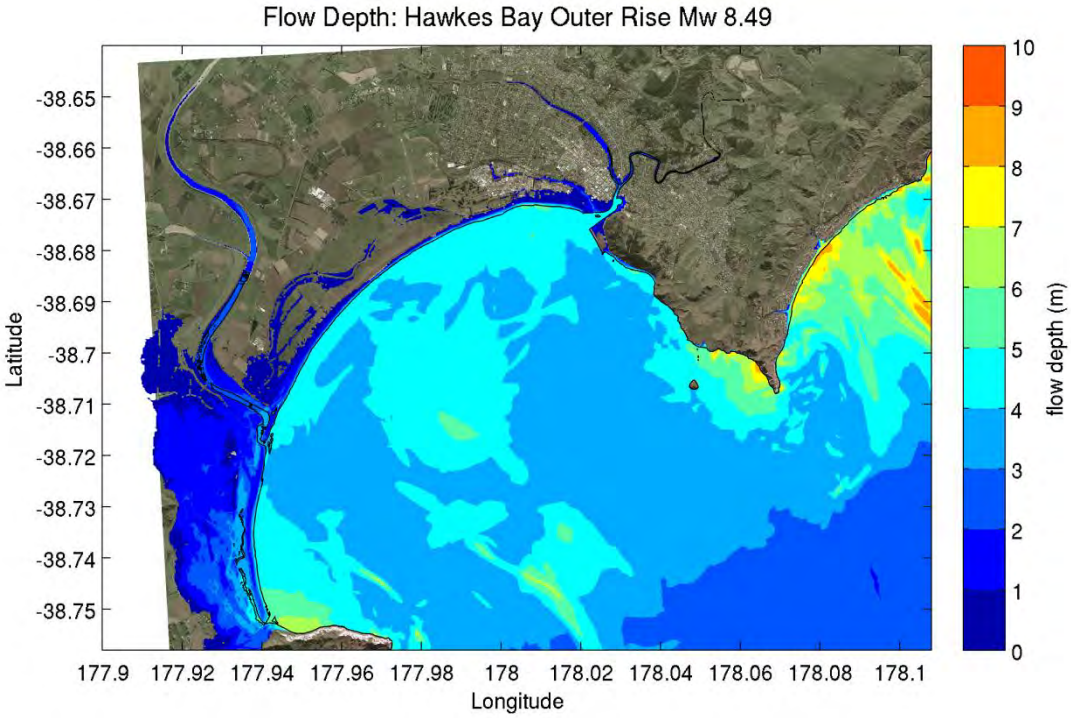

Figure 7.22 Maximum onshore flow depth in metres for the Hawkes Bay Outer Rise Mw 8.49 scenario (from the deaggregation of the 2500 year tsunami). Offshore the colour scale shows the maximum water level.

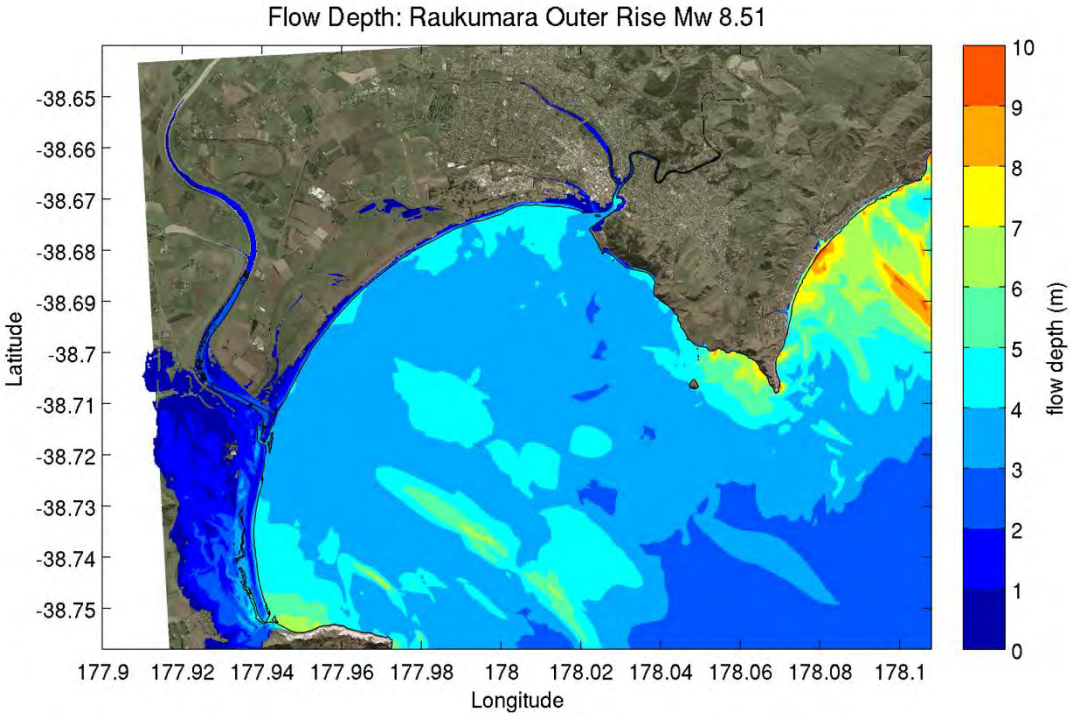

Figure 7.23 Maximum onshore flow depth in metres for the Raukumara Outer Rise Mw 8.51 scenario (from the deaggregation of the 2500 year tsunami). Offshore the colour scale shows the maximum water level.

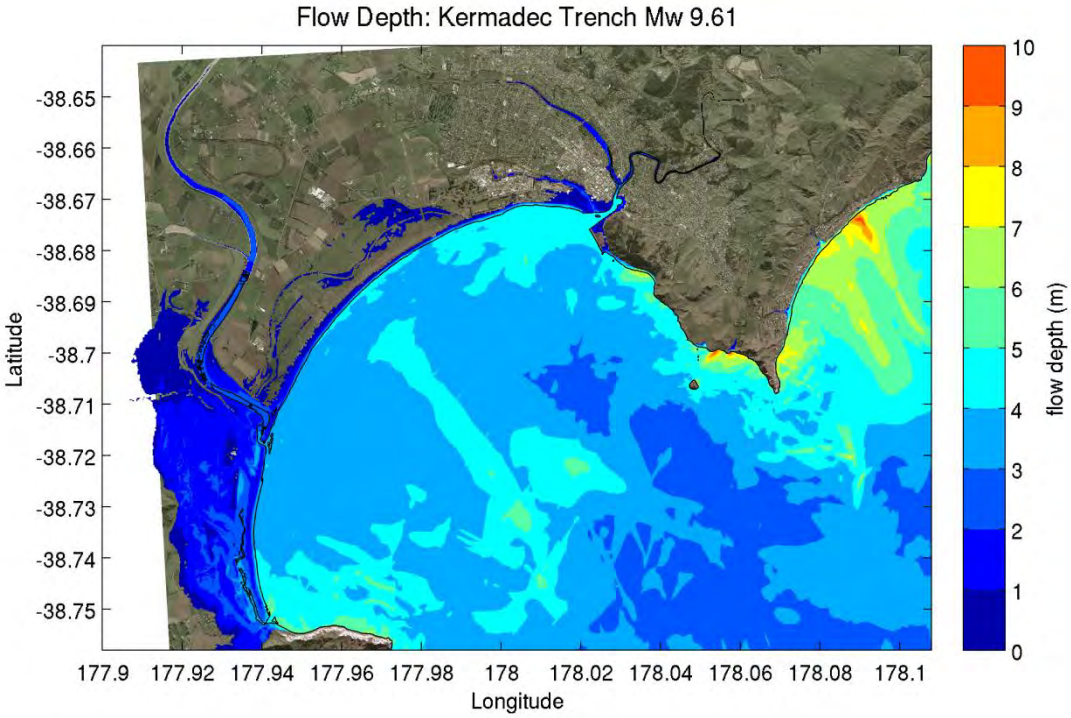

Figure 7.24 Maximum onshore flow depth in metres for the Kermadec Trench Mw 9.61 scenario (from the deaggregation of the 2500 year tsunami). Offshore the colour scale shows the maximum water level.

This page is intentionally left blank.

8.0 PROBABILISTIC TSUNAMI HAZARD ASSESSMENT (PTHA) RESULTS

The scenario flow depths at each return time were combined by estimating the weighted median of the flow depths at each point. The weightings were taken from the ‘Percentage of top six’ column of Table 6.1. The results are shown in Figure 8.1 - Figure 8.4.

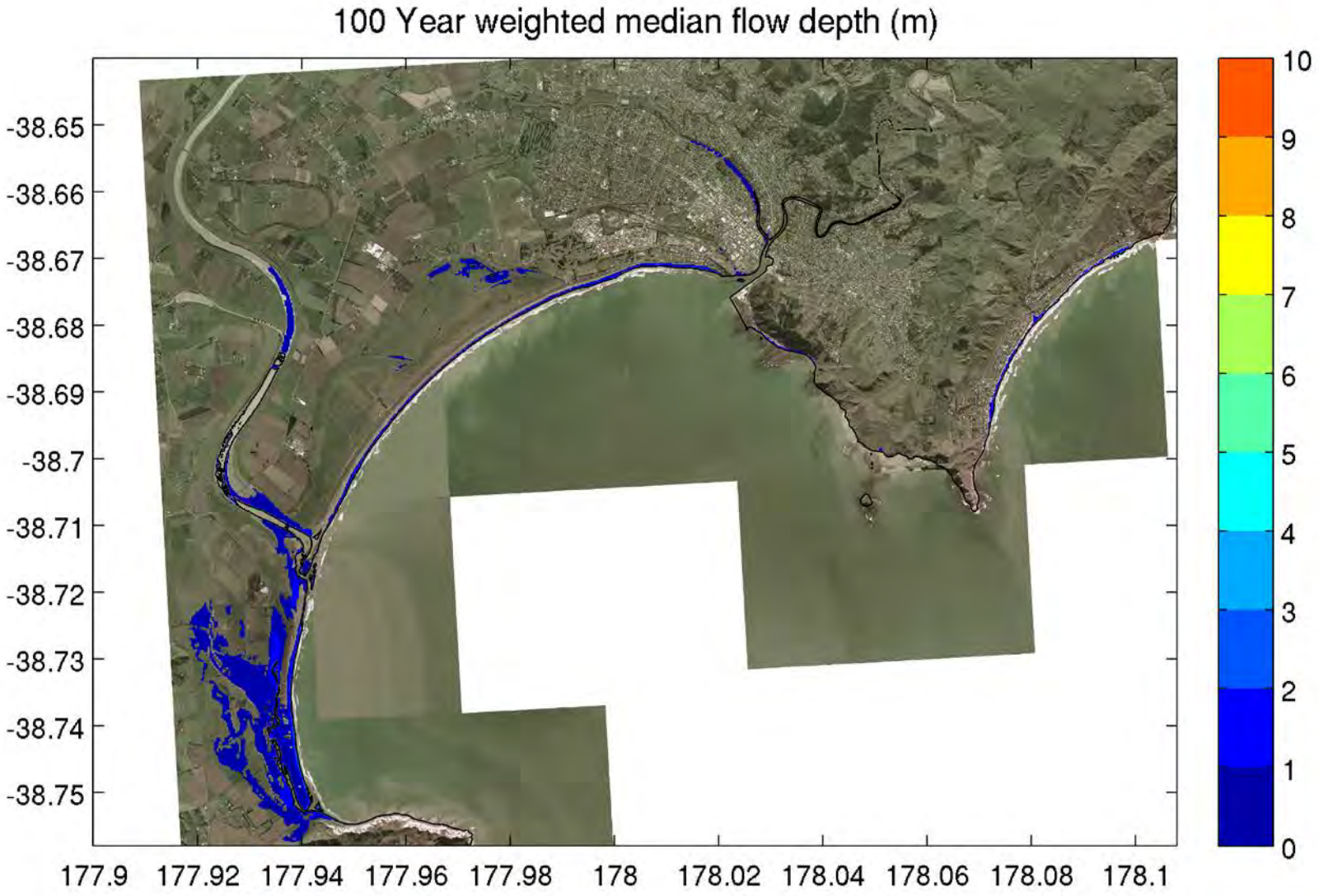

Figure 8.1 Weighted median of flow depths at 100 year Return Period for all sources. As estimated using the first six major contributors at this return period.

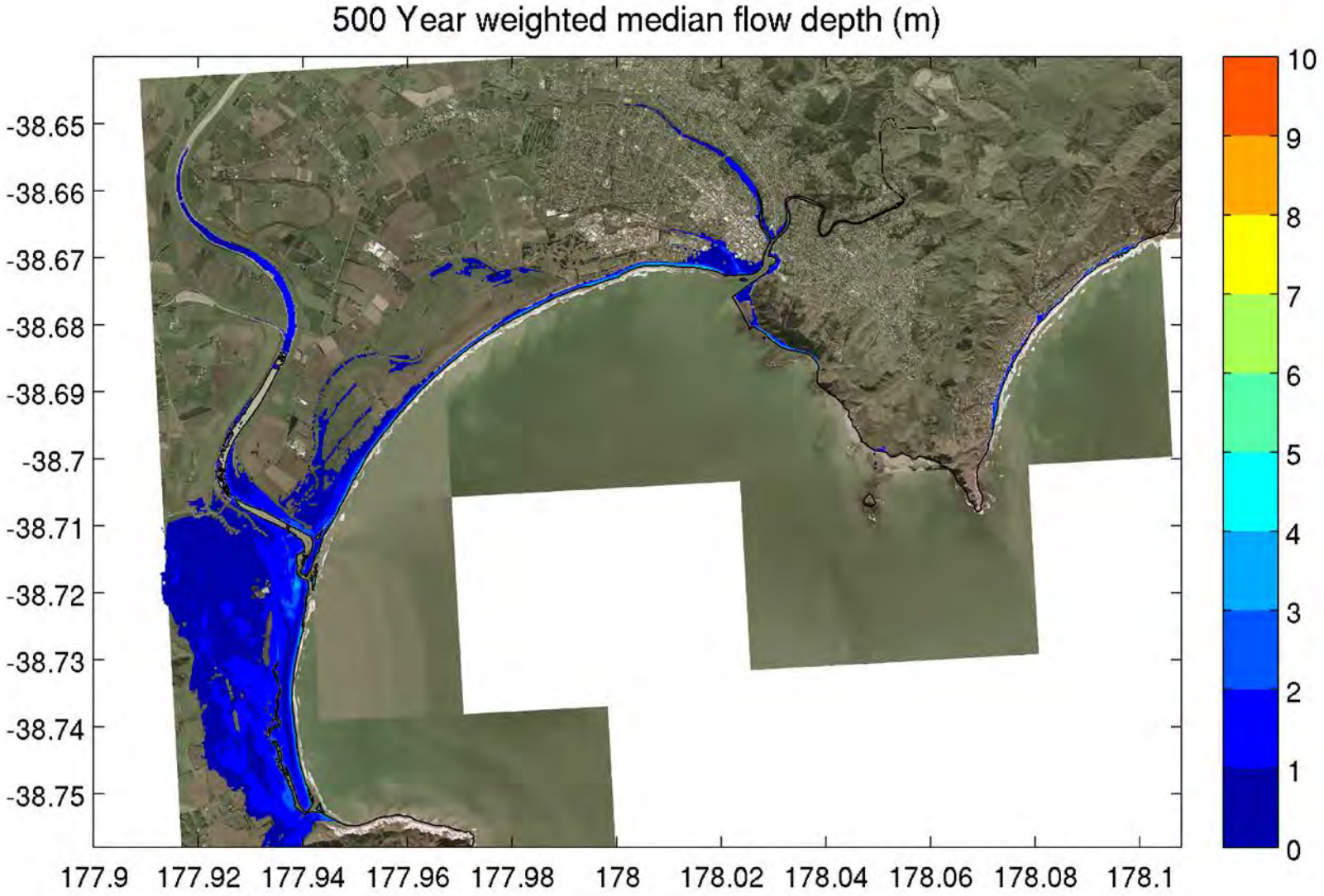

Figure 8.2 Weighted median of flow depths at 500 year Return Period for all sources. As estimated using the first six major contributors at this return period.

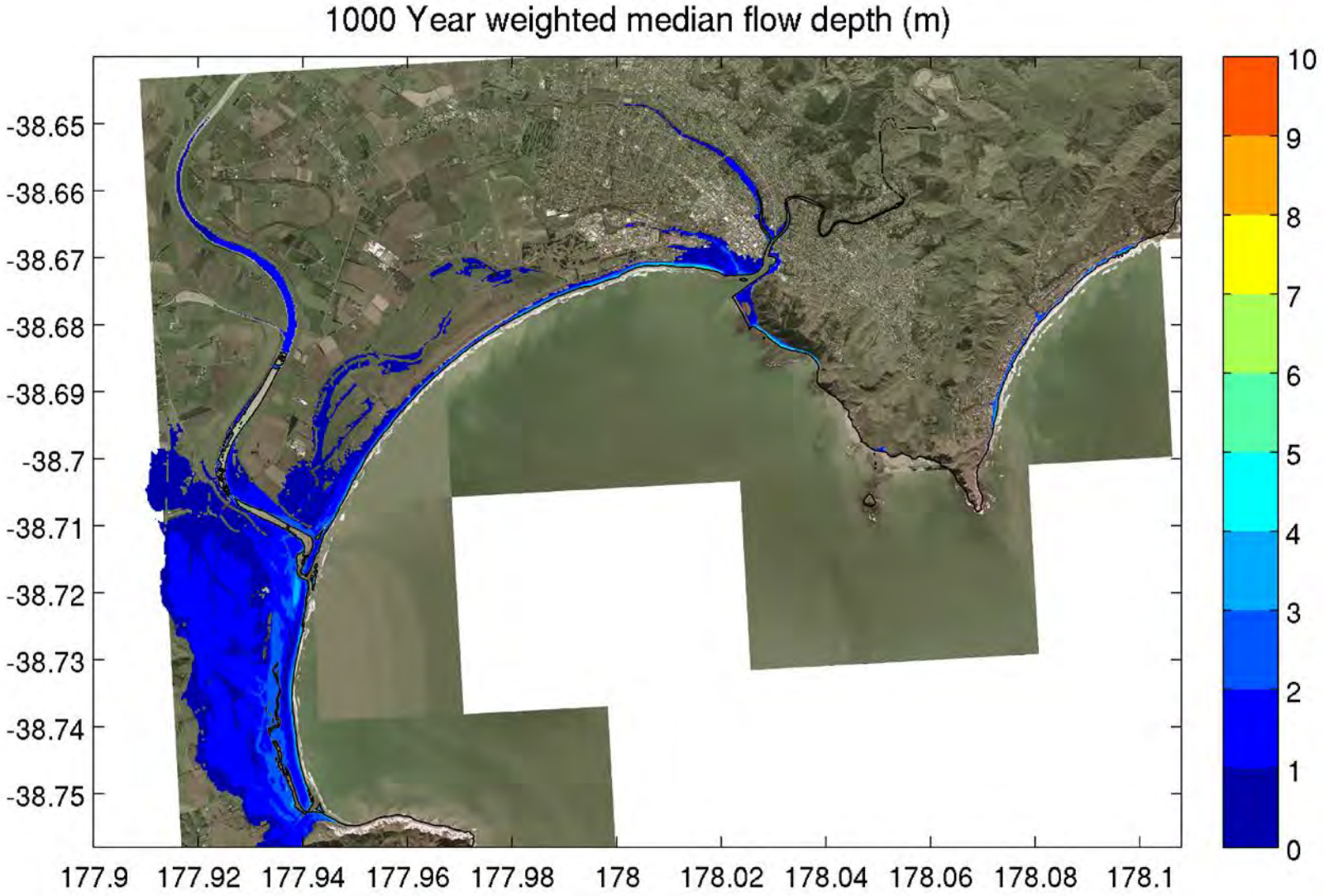

Figure 8.3 Weighted median of flow depths at 1000 year Return Period for all sources. As estimated using the first six major contributors at this return period.

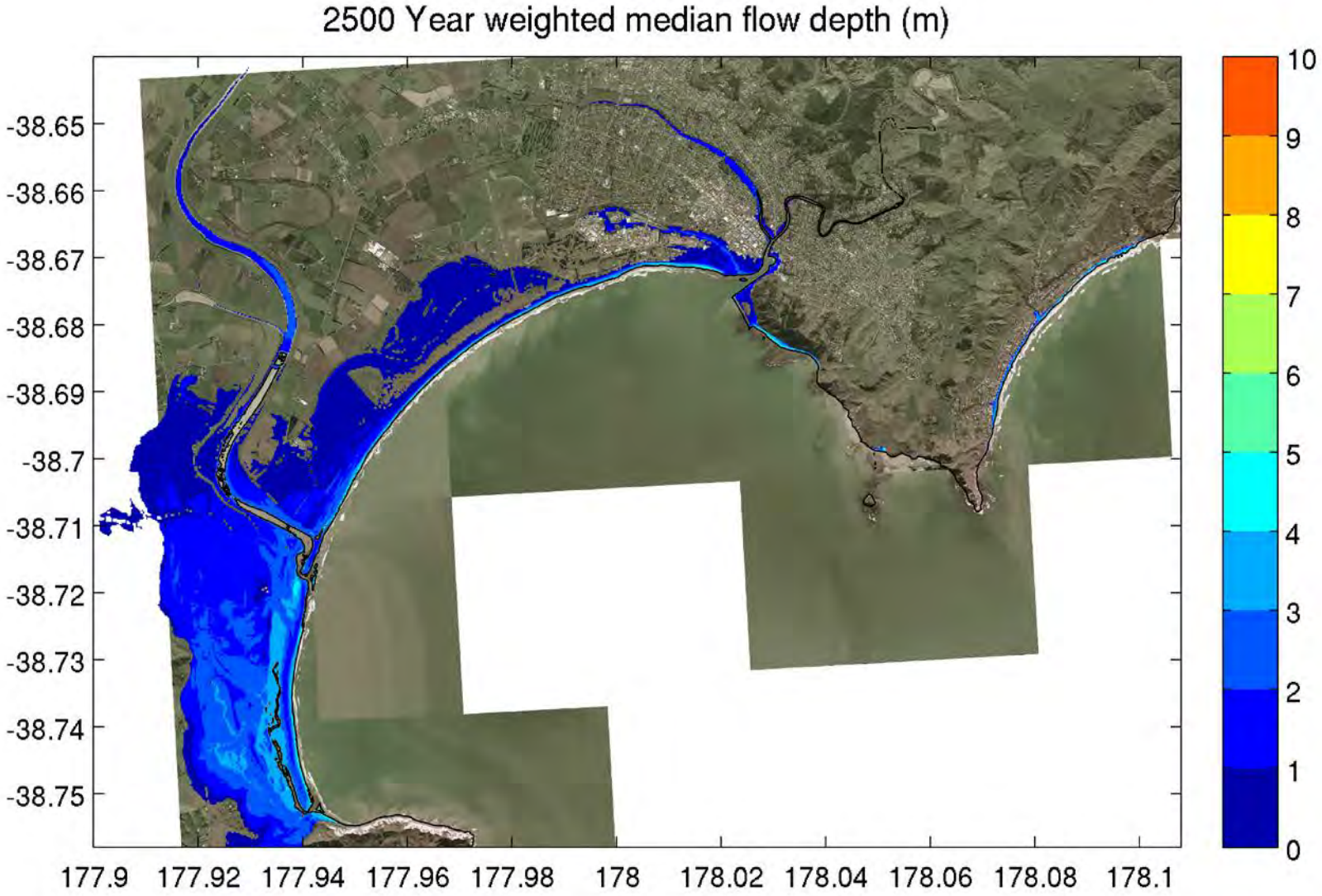

Figure 8.4 Weighted median of flow depths at 2500 year Return Period for all sources. As estimated using the first six major contributors at this return period.

This page is intentionally left blank.

9.0 RISK MODELLING RESULTS

9.1 RISK ASSESSMENT

The risk metric used in this study is the annual individual fatality risk (AIFR) and this is assessed for an individual living at the location of interest. AIFR represents the annualised probability that a person may be killed. For this study, the AIFR is calculated only for local earthquake-generated tsunami where an official warning is unlikely. It is assumed given the large travel times (20+ hours) for distant source tsunami (e.g. from South America) that an official tsunami warning will be issued, allowing for a complete evacuation. The quantitative risk assessment method is similar to that used by Massey et al (2014) for life safety risk and land use planning in the Port Hills of Christchurch following the 2010-2011 Canterbury Earthquake Sequence. It is also equivalent to the AIFR calculated for the recent Tsunami Risk Facing New Zealand report of Horspool et al. (2015) which estimated tsunami risk at a national scale. The current study aims to estimate the annual individual fatality risk at a local scale that is suitable for land use planning decision making. Taig et al. (2012) provide an overview of some of the issues in adopting a risk-based approach for disaster risk management. In this study, the annual individual fatality risk (annual probability of death) can be calculated from:

$$R(\text{Fatality}) = P(\text{Hazard Event}_i) \times P(\text{Death} \mid \text{Hazard Event}) \times P(\text{Present})$$

where

- R(Fatality) is the annual individual fatality risk (annual probability of death)
- $P(\text{Hazard Event}_i)$ is the probability of the tsunami event. This is sourced from the probabilistic tsunami inundation model (Section 8);
- $P(\text{Death} \mid \text{Hazard Event}_i)$ is the probability of death given the tsunami characteristics (e.g. inundation depth) for Hazard Event_i which is derived from the human vulnerability model (Section 9.2);
- P(Present) is the probability that an individual is present at the location (which is defined in Section 9.3).

9.2 FATALITY FUNCTION

To estimate the probability of a fatality given a certain tsunami characteristics (e.g. inundation depth) a human casualty model (Horspool, 2015) was adopted. This model expresses the probability of death as a linear function of the depth of water. The model of Horspool et al, (2015) was used in the recent Review of Tsunami Risk Facing NZ: A 2015 Update. These models were updated in 2015 utilising the latest data from recent tsunami events. The new models (Figure 9.1 and Figure 9.2) are as follows:

- Number of deaths = number of people exposed x 0.04 x water depth (m), and
- Number of injured people = number of survivors x 0.04 x water depth (m), where
- Number of survivors = number of people exposed – number of deaths

They provide better matches to the observed data than earlier models used in the 2005 Tsunami Risk Assessment for New Zealand (Berryman, 2005). The observed tsunami death rate data is from historical near-source tsunami events (less than 30 minutes between the

earthquake shaking and tsunami arrival) that had no official tsunami warning system. This would be considered equivalent to the current situation in New Zealand. However, variations between tsunami awareness, education of tsunami evacuation procedures and individual response in these countries contribute to the scatter in the data in Figure 9.1. The data used to develop these models are based on locations where limited evacuation occurred.

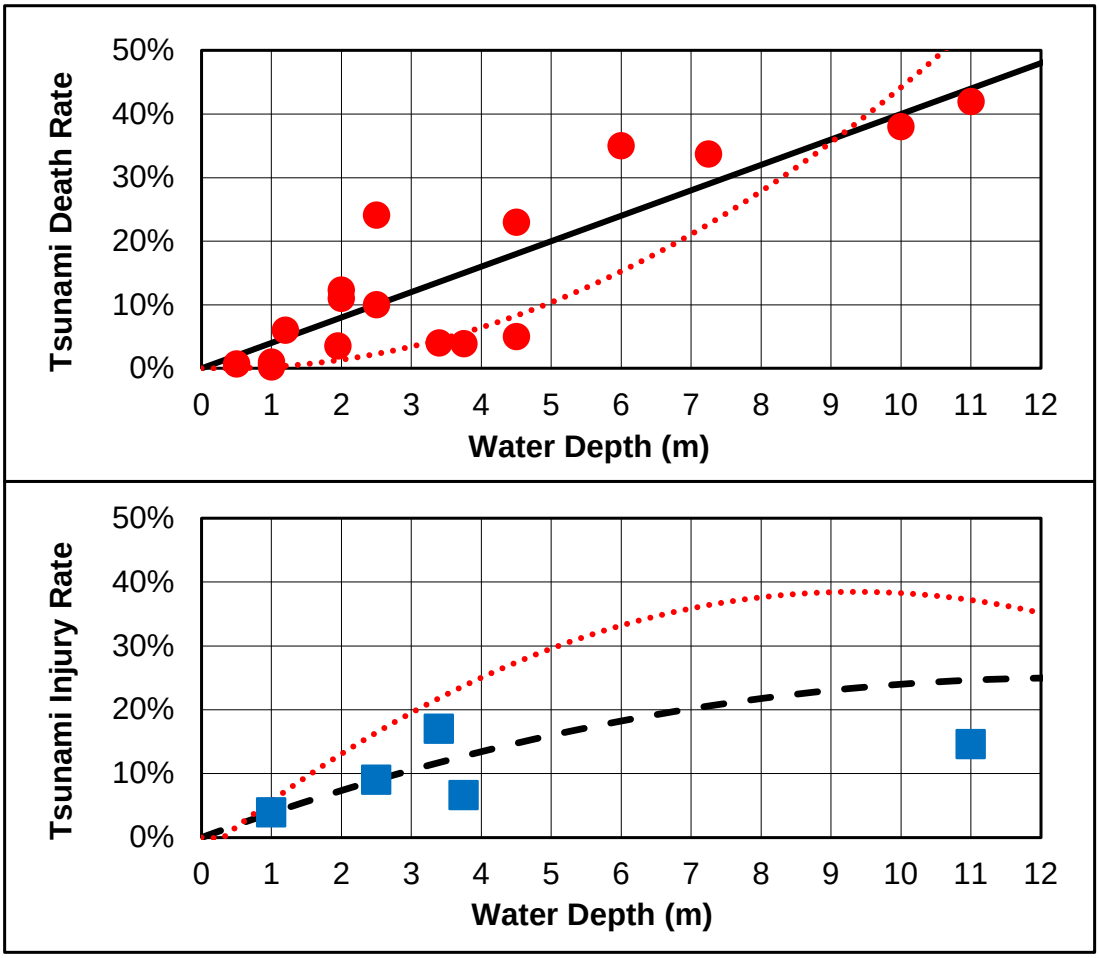

Figure 9.1 Data and models for death and injury rates as functions of flow depth of fast-flowing tsunami waves. In both cases the rates are percentages of the original population at risk. The black solid and dashed lines are the 2015 models, and the dotted red lines are the superseded 2005 models of Berryman (2005).

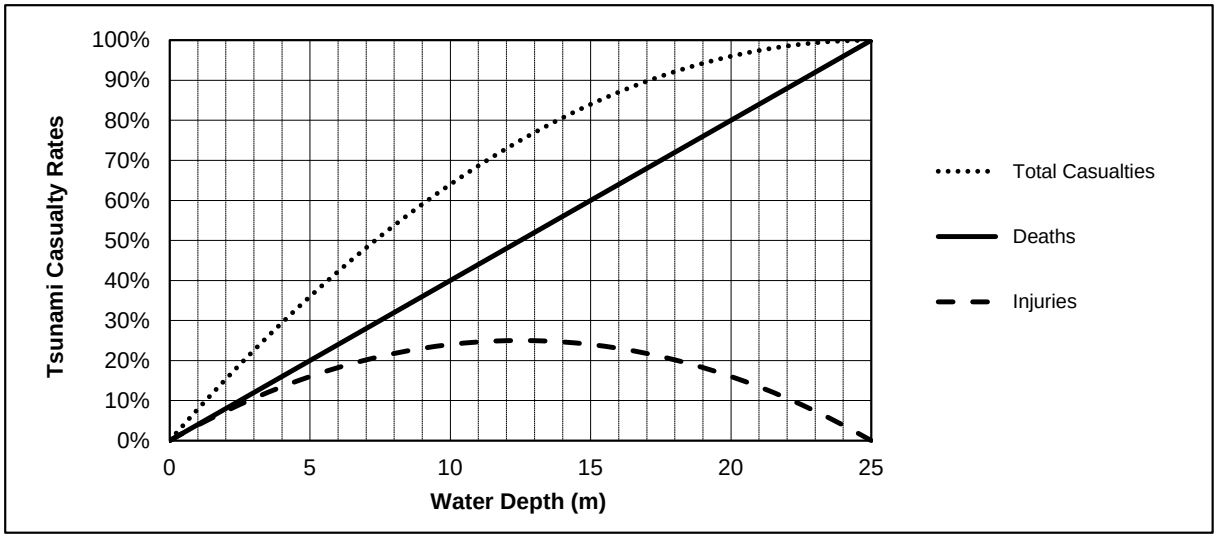

Figure 9.2 Extrapolation of the 2015 tsunami death and injury rate models to high water depths.

9.3 OCCUPATION RATES

The modelling assumes that there is a 100% occupancy at each location. This means that an individual would be present at the location 24 hours a day, 365 days a year. This is considered an end-member realisation of the risk (i.e. conservative), but doing so would capture people who may be confined to their residences due to illness or disabilities. An occupancy rate of 100% was also used in the Port Hills Rock Fall Risk Assessment (Massey, et al, 2014).

9.4 EVACUATION RATES

The risk modelling assumes that there is no evacuation prior to the tsunami. This was a parameter that was requested by the Gisborne District Council for the analysis.

9.5 CALCULATING ANNUAL INDIVIDUAL FATALITY RISK (AIFR)

To calculate AIFR, the following steps are undertaken:

1. The local source probabilistic tsunami hazard assessment (Section 8.0) results are used to develop a local source tsunami hazard curve for each 18 m grid cell across the area of interest (Figure 9.3). The curve is constructed by interpolating between the modelled tsunami inundation depths at each of the local source only return periods (Table 6.2). This curve represents the expected inundation depth as a function of return period for local source tsunami;
2. At each of the target return periods the fatality rate is calculated by using the fatality function described in section 9.2 to estimate the fatality rate as a function of return period. This is then multiplied by the occupancy rate, in this case 100% as described in section 9.3. This gives discrete values of the estimated fatality rate for each of the target return periods (Figure 9.4);
3. Finally, the area under the curve is integrated (Figure 9.5) to estimate the AIFR for that grid cell;
4. Steps 1 to 4 are then repeated for each 18m x 18m grid cell across the area of interest to create a spatial grid of AIFR.

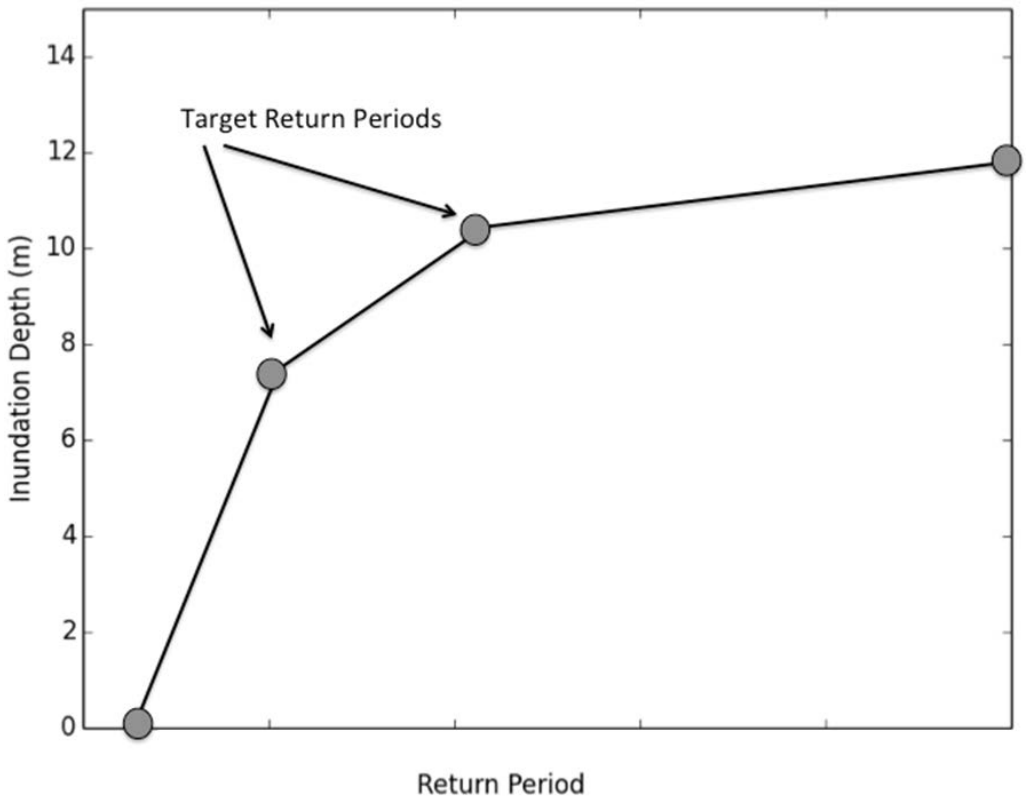

Figure 9.3 Example probabilistic tsunami hazard curve at an onshore location for local tsunami sources. The grey circles represent the weighted median inundation flow depth for the target return periods described in Section 8.0.

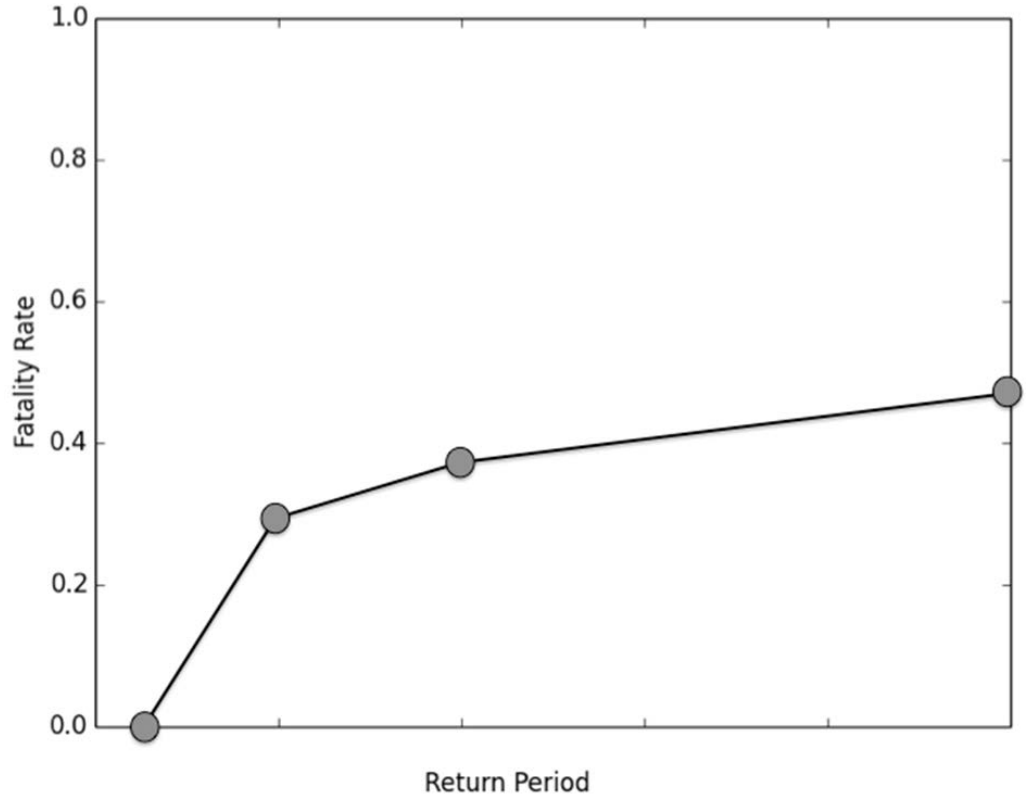

Figure 9.4 Example probabilistic tsunami risk curve at an onshore location for local tsunami sources. This curve has been derived from Figure 9.3 using a fatality function to convert inundation depths to fatality rates (probability of death). The grey circles represent the weighted median fatality rates for the target return periods.

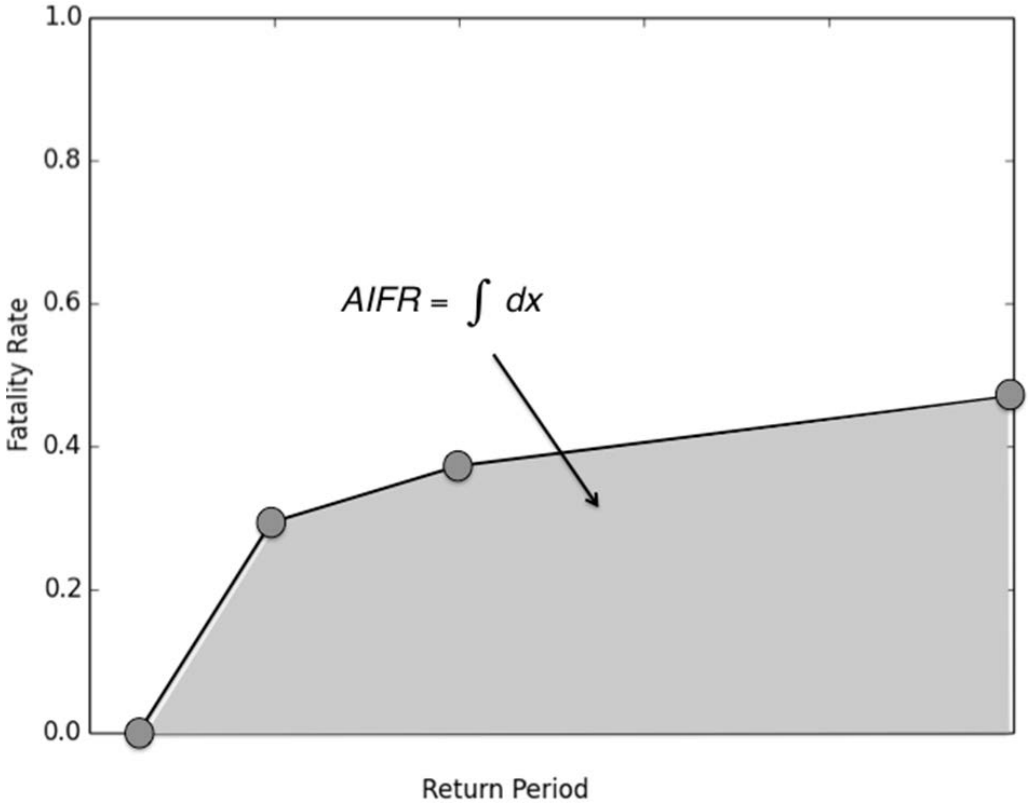

Figure 9.5 Using the curve shown in Figure 9.4 the area under the curve is integrated to estimate the Annual Individual Fatality Risk (AIFR) which is the annual individual probability of death.

Additional details of this calculation are presented in Appendix1.

9.6 ANNUAL INDIVIDUAL FATALITY RISK RESULTS

Annual Individual Fatality Risk (AIFR) from local source tsunami were calculated using the method described in Section 9.4 on an approximately 18 m x 18 m grid across the area of interest (see Section 12 for a description of how the data was converted into GIS layers). The AIFR was then grouped into logarithmic intervals (i.e. seperated by an order of magnitude) which is commonly used to differentiate between different levels of risk.

Figure 9.6 shows the estimated AIFR for the Gisborne Region. The results show AIFR values of 10^{-4} to 10^{-3} along the beach (sea side of the sand dunes) across the region, and in coastal estuaries near the Waipaoa River and the Taruheru and Waimata Rivers in Gisborne City (Figure 9.7).

AIFR levels of 10^{-5} to 10^{-4} are present in the western coast of Poverty Bay near Muriwai and in the Gisborne area around the south east corner of the CBD, the eastern end of Waikanae Beach near Salisbury Road and the Waiakane Beach Holiday Park. This level of risk also covers parts of SH35. There are also areas with this level of risk along the streams of Wainui Beach (Figure 9.8).

The lowest level of risk where AIFR is less than 10^{-5} are present along most of the area behind the sand dunes along Waikanae Beach, the south east Gisborne CBD, adjacent to streams along Wainui Beach, portions of SH2 near the Waipoa River and parts of Muirwai.

Areas that have no AIFR values were not inundated by any of the modelled local sources used in this analysis.

The level of uncertainty in the AIFR modelling is estimated to be around a factor of 10 (or one order of magnitude). This is similar to that estimated by Massey et al. (2012) and Taig et al. (2012) for the Port Hills Life Safety Risk Assessment.

If alternative values of occupancy rates or evacuation rates are desired, the AIFR results can be scaled by these rates. For example to estimate the AIFR for an occupancy rate of 67 %, where the occupant may be away from the area for 8 hours per day (e.g. at work), the estimated AIFR can be multiplied by 0.67 to get this desired result.

9.7 DISCUSSION

9.7.1 Expressing Risk Probabilities

Risk can be expressed in a number of ways. For this study the AIFR is defined as a logarithmic probability (e.g. 10^{-4}, which is said as 'ten to the power of minus four'). Table 9.1 shows different ways probabilities can be expressed for values similar to that observed in the present study.

Table 9.1 Different ways of expressing risk probabilities. The second column is how risk is represented in this study (adapted from Taig et al, 2012).

Probability 1 in… (per year)	Is the same as (per year)	Is the same as (per year)	Is the same as
100	10^{-2}	0.01 or 1%	80% per lifetime[†]
1,000	10^{-3}	0.001 or 0.1%	8% per lifetime
10,000	10^{-4}	0.0001 or 0.01%	0.8% per lifetime
100,000	10^{-5}	0.00001 or 0.001%	0.08% per lifetime
1,000,000	10^{-6}	0.000001 or 0.0001%	0.008% per lifetime

[†] Assuming a life expectancy of 80 years.

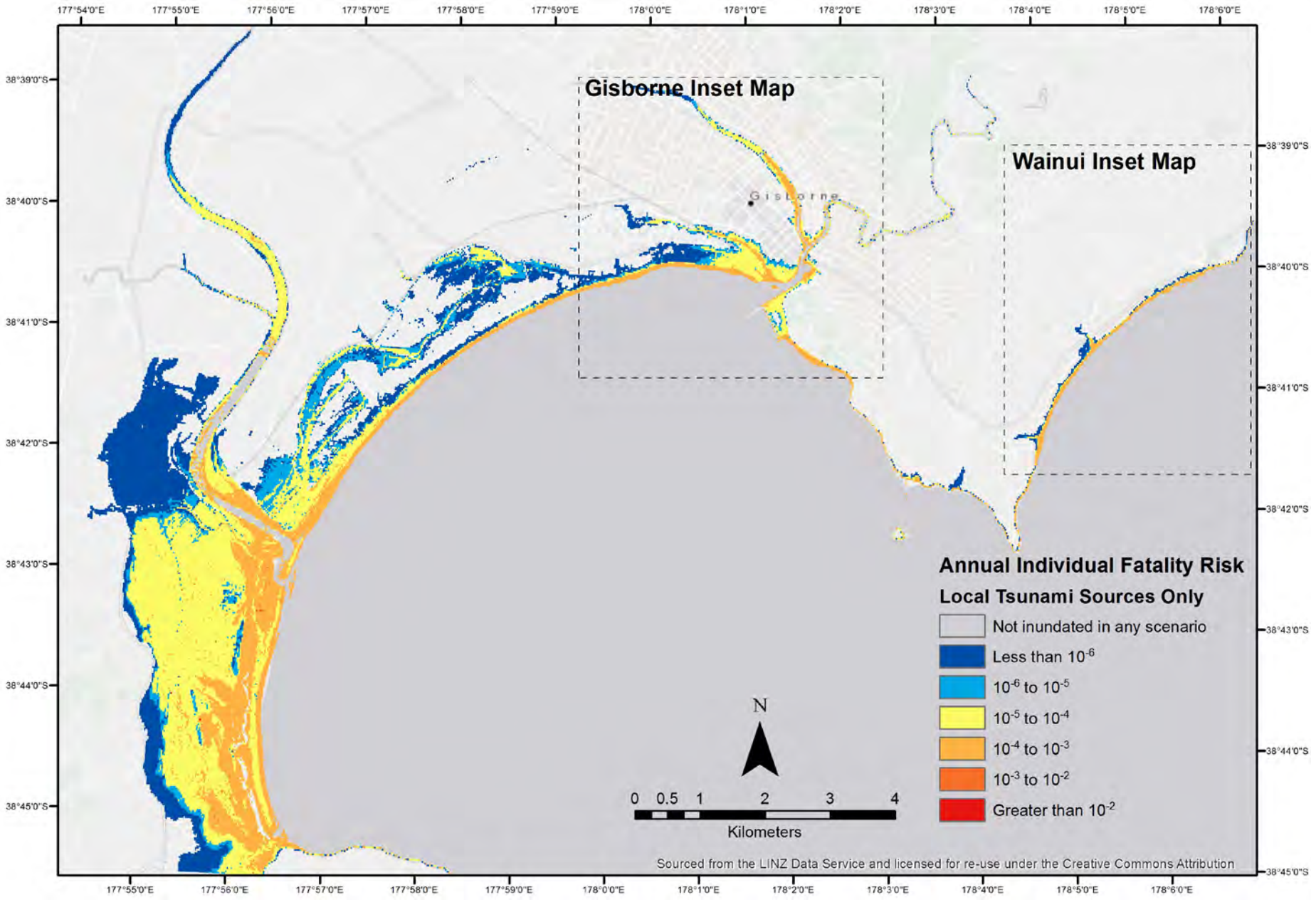

Figure 9.6 Map showing estimated Annual Individual Fatality Risk (AIFR) for Gisborne Region. The area showing AIFR less than 10^{-6} has been extended to cover all areas that were inundated in at least one local source scenario.

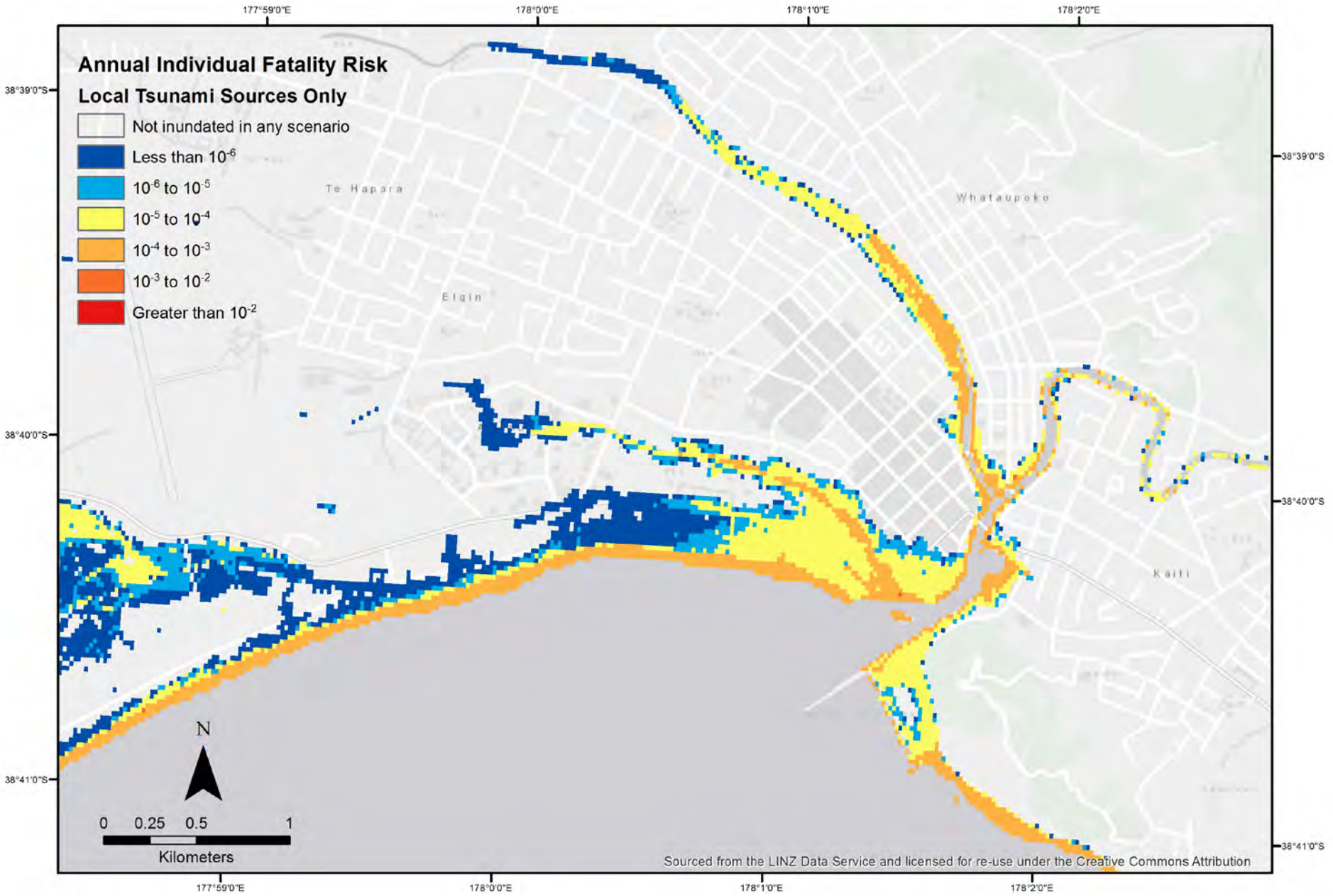

Figure 9.7 Map showing estimated Annual Individual Fatality Risk (AIFR) for Gisborne. The area showing AIFR less than 10^{-6} has been extended to cover all areas that were inundated in at least one local source scenario.

9.7.2 Comparison with Previous AIFR Estimates of Tsunami Risk in New Zealand

The AIFR values estimated for this study are compared with those from the Berryman et al, (2005) report, Review of Tsunami Hazard and Risk Facing New Zealand (Table 9.2). The 2005 estimates were calculated using a coastal estimate of the tsunami hazard from all sources, including local and distance sources. Furthermore, the occupancy rate assumed in the 2005 study was 50%, so someone would either be living or working at the location for 50% of the time. Whereas in the present study, and the recent work in the Port Hills in Christchurch, an occupancy rate of 100% was used. The 2005 AIFR estimates also have been calculated for two heights above mean sea level located at the coast, so they do not use detailed onshore hydrodynamic modelling (as is done in this study) to spatially map AIFR, that would consider the effect of the sand dunes along much of the Gisborne Coast that protect inland areas from inundation. The 2005 AIFR values have been recalculated to assume 100% occupancy and these are shown in brackets in Table 9.2. However, since the 2005 study used all sources the AIFR will be higher than the present study which only considers local sources for life safety risk.

Table 9.2 shows that for comparable locations in this study (e.g. Waikanae Beach front) the risk is within a factor of 10 (the level of uncertainty in the modelling) compared to the 2005 study at the 50th percentile level.

The recent update of the 2005 study by Horspool, et al., (2015) also estimated AIFR for select locations around New Zealand (Auckland, Tauranga, Napier, Wellington), but this did not include Gisborne so no comparison can be made. The 2015 update study included results from the recent 2013 National Tsunami Hazard Reivew (Power et al, 2013) which has also been used as the underpinning hazard model in this present study.

Table 9.2 Comparison of AIFR between the 2005 Reivew of Tsunami Hazard and Risk Facing New Zealand (Berryman et al, 2005) and this study. Note that the Berryman (2005) study assumed a person was at the location 50% of the time, whereas this study assumes 100% occupancy. For comparison purposes, the Berryman (2005) estimates were adjusted to assume 100% occupancy and these are shown in brackets. The two locations for this study are representative locations for Gisborne only.

Percentile	Berryman et al, 2005		This Study	
	2m Above Mean Sea Level	4m Above Mean Sea Level	Riverside Walkway/Waikanae Beach Front/Port	Waikanae Beach Properties/South East CBD
84th	1.7×10^{-3} (3.4×10^{-3})	9.7×10^{-4} (1.9×10^{-3})	-	-
50th	6.0×10^{-4} (1.2×10^{-3})	2.8×10^{-4} (5.6×10^{-4})	$1.0 – 7.0 \times 10^{-4}$	$1.1 – 8.0 \times 10^{-5}$
16th	2.0×10^{-4} (4.0×10^{-4})	6.4×10^{-5} (1.3×10^{-4})	-	-

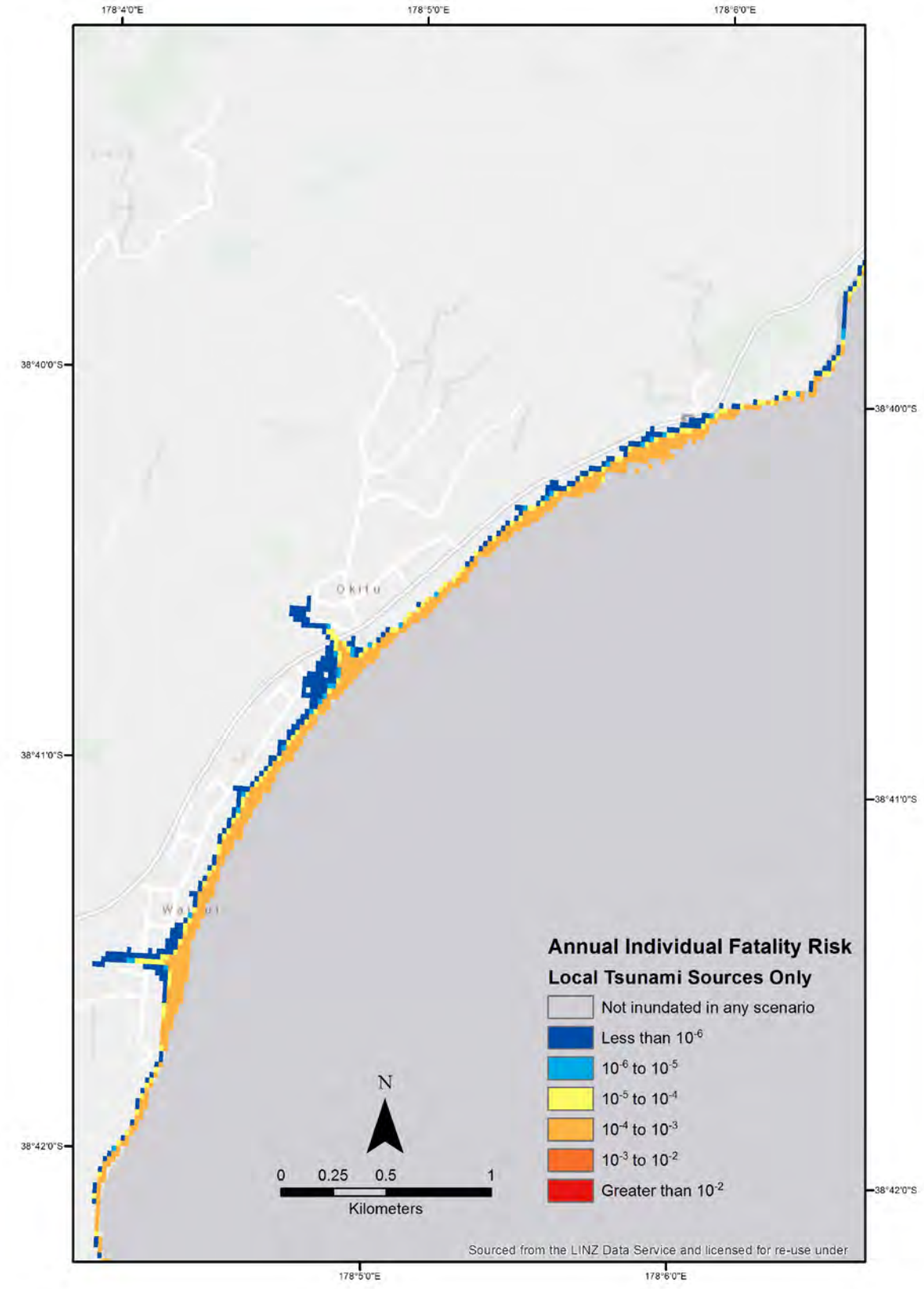

Figure 9.8 Map showing estimated Annual Individual Fatality Risk (AIFR) for Wainui. The area showing AIFR less than 10^{-6} has been extended to cover all areas that were inundated in at least one local source scenario.

9.7.3 Comparison with AIFR from the Port Hills Rock Fall and Landslide Risk Assessment

During the 2010-2011 Canterbury Earthquake Sequence, a number of hill slopes around the Port Hills in Christchurch experienced significant rock fall and landslide events. Some of the rock fall resulted in fatalities and also caused significant damage to buildings. Following the events the Christchurch City Council decided to use a risk-based approach to defining future land use in the Port Hills. Based on the risk assessment (Massey et al, 2014) a number of areas were "Red Zoned" where there was a high life safety risk beyond tolerable levels. The estimates of AIFR in the Port Hills ranged from 3×10^{-5} to 1×10^{-3}, with a value of 1×10^{-4} being adopted in the proposed Replacement District Plan (pRDP) by Christchurch City Council (Beaumont 2015, Carter 2015) as a level of risk which is intolerable. This is in comparison to 1×10^{-6} to 1×10^{-4} for habitated areas of Gisborne (exluding the beach areas which had AIFR levels between 1×10^{-4} and 1×10^{-3}).

Taig et al. (2012) provided recommendations to the Christchurch City Council on acceptable levels of life safety risk for properties that are at risk from rock falls. Taig et al. (2012) suggested that 10^{-4} be used to define the threshold for intolerable risk for existing properties and 10^{-5} for new development. It was suggested that for existing properties 10^{-4} would be a 'soft' limit, where householders had the option of staying, but if the level of risk exceeded 10^{-3} then relocation would be compulsory. It was also recommended that for new development a lower tolerance level (10x) should be used for general property uses which had significant occupancy (but what is defined as significant is not mentioned) and an even lower level (100x below the standard level of tolerance) for sensitive uses such as schools, hospitals and aged-care homes. These levels of risk tolerance were orginally based on that of the Australian Geomechanics Society (AGS) for landslide risk and the Australian National Committee on Large Dams (ANCOLD) that both recommend that levels of AIFR are intolerable above 10^{-4} for existing dams and 10^{-5} for new dams (or for sites near landslide prone areas) in the absence at the time of any New Zealand standards for levels of intolerable risk (Taig et al. 2012). These thresholds are compared in Figure 9.9 to other risks faced by New Zealanders.

Comparing the recommendations of Taig et al. (2012) with the modelled AIFR estimates for tsunami risk in Gisborne highlights that areas above 10^{-4} are mostly confined to beach areas. However there are large areas within the 10^{-4} to 10^{-5} band which Taig et al. (2012) recommend restrictions on further development. These areas are present in the western coast of Poverty Bay near Muriwai and in the Gisborne area around the south east corner of the CBD, the eastern end of Waikanae Beach near Salisbury Road and the Waiakane Beach Holiday Park. This level of risk also covers parts of SH35. There are also areas with this level of risk along the streams edges of Wainui Beach (Figure 9.8).

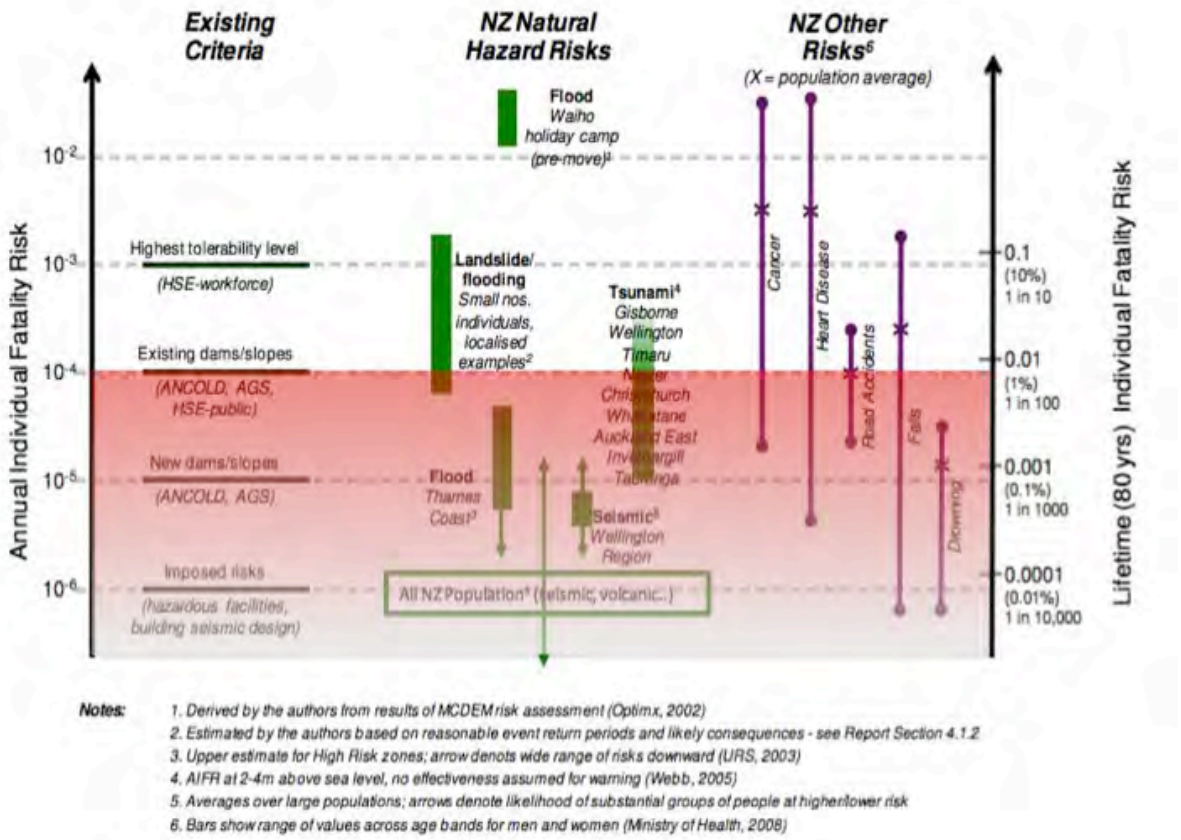

Figure 9.9 Comparison of existing risks to New Zealanders with the range of AIFR for Gisborne (excluding the beach areas) estimated in this study shown as a red shaded bar (Adapted from Taig et al, 2012).

9.7.4 Recommendations for Gisborne District Council

This study is to the authors knowledge, one of the first in New Zealand to quantify and spatially map life safety risk from local source tsunami. It builds on previous life safety risk assessments from tsunami (at the coast, e.g. Berryman et al., 2005, Horspool et al, 2015) and rock fall in the Port Hills in Christchurch (Massey et al, 2012, Taig et al, 2012).

This risk information can be used to inform risk based decision making for land use planning and other emergency management activities in Gisborne.

In doing so the Gisborne District Council will need to:

1. Define levels of tolerable and intolerable risk. This decision ultimately needs to be made at the community level involving community engagement. The recommendations by Taig et al. (2012) can be used as a reference point for framing this discussion.
2. The life safety risk from tsunami should be evaluated against risk from other natural hazards facing Gisborne as well as other risks as illustrated in Figure 9.9.

10.0 DISCUSSION AND LIMITATIONS OF THE HAZARD ANALYSIS

10.1 SAND DUNES

The coastal strip of sand dunes plays an important part in protecting Gisborne city and other areas of Poverty Bay from tsunamis. Even in the most severe events modelled in this study the sand dune ridge is only breached in areas where it is relatively lower or has gaps.

Tsunami modelling, as currently practised, does not have the capability to incorporate the erosion of sand dunes by tsunamis into the inundation modelling. Instead the sand dunes are assumed to remain intact and unaffected throughout. In reality once a sand dune has been overtopped, the high velocity associated with the running down of water on the inland side of the dune can cause erosion that may enlarge the channel available to the tsunami.

The model resolution of 18m limits the ability to resolve topographic features of smaller dimensions, and it is possible that very narrow cuts through the dune, if present, could be missed or poorly represented by the model.

Given the important role that the sand dune ridge plays, we recommend that maintaining the continuity and integrity of the coastal sand dune strip be treated as being a very important aspect of tsunami hazard and risk mitigation in Poverty Bay. To be more specific, we recommend against any future actions that would see the sand dune height lowered, even over only a small range (and also investigating the closing of any existing gaps in the dune belt); and we recommend investigating measures that would strengthen the resistance of the dune to erosion, which may include the planting of vegetation that helps to bind the dunes together.

10.2 TIDES

This study assumes that tsunamis occur at mid-tide. In reality tsunamis could occur at any point in the tidal cycle, and the sequence of tsunami waves may extend over several hours, particularly in the case of tsunamis from distant sources, so that the waves may arrive at different states of the tide during a single event.

The assumption of mid-tide was made to be as neutral as possible – neither optimistic or pessimistic – though in practise it is at least slightly optimistic due to the duration of tsunamis discussed in the previous paragraph.

Another important consideration is that in several of the scenarios the tsunami comes close to the point of a widespread overtopping of the sand dune, but in most places does not actually overtop. In this situation even a small increase in water level, such as resulting even from the small range of tides (about +/- 75cm) in Poverty Bay, can lead to a much greater extent of inundation.

To illustrate the effects of tides two additional scenarios were developed, describing the consequences of the tsunamis caused by the Peru Mw 9.52 and Hikurangi Mw 8.94 earthquake scenarios occurring at high tide – modelled as an additional 75cm increase in water level (the 50cm of sea level rise used in the original scenarios was also still assumed).

The results from these models are shown in Figure 10.1 and Figure 10.3, and may be compared with the corresponding mid-tide results in Figure 7.19 and Figure 7.20 (reproduced here as Figure 10.2 and Figure 10.4). The Peru Mw 9.52 scenario demonstrates the effect of

the tide in extending the extent of inundation and increasing the maximum flow-depth, while the Hikurangi Mw 8.94 scenario illustrates the way that a high tide enables the over-topping of sand dunes and the consequences of this.

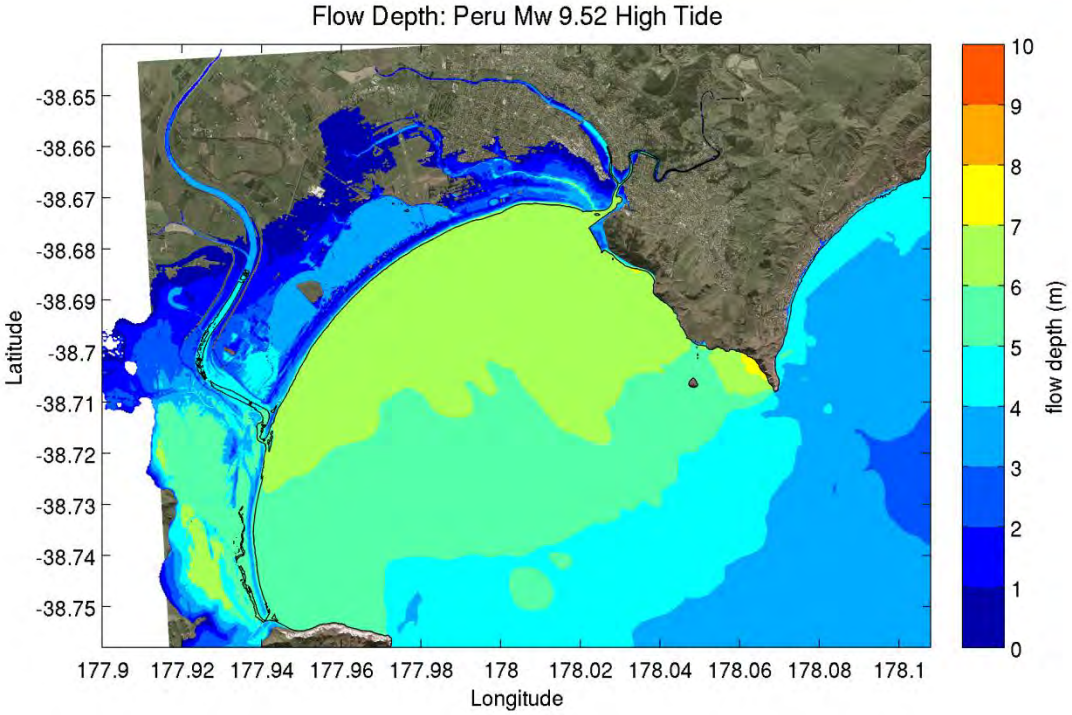

Figure 10.1 Maximum flow depth in metres for the Peru Mw 9.52 scenario at high-tide. Offshore the colour scale shows the maximum water level.

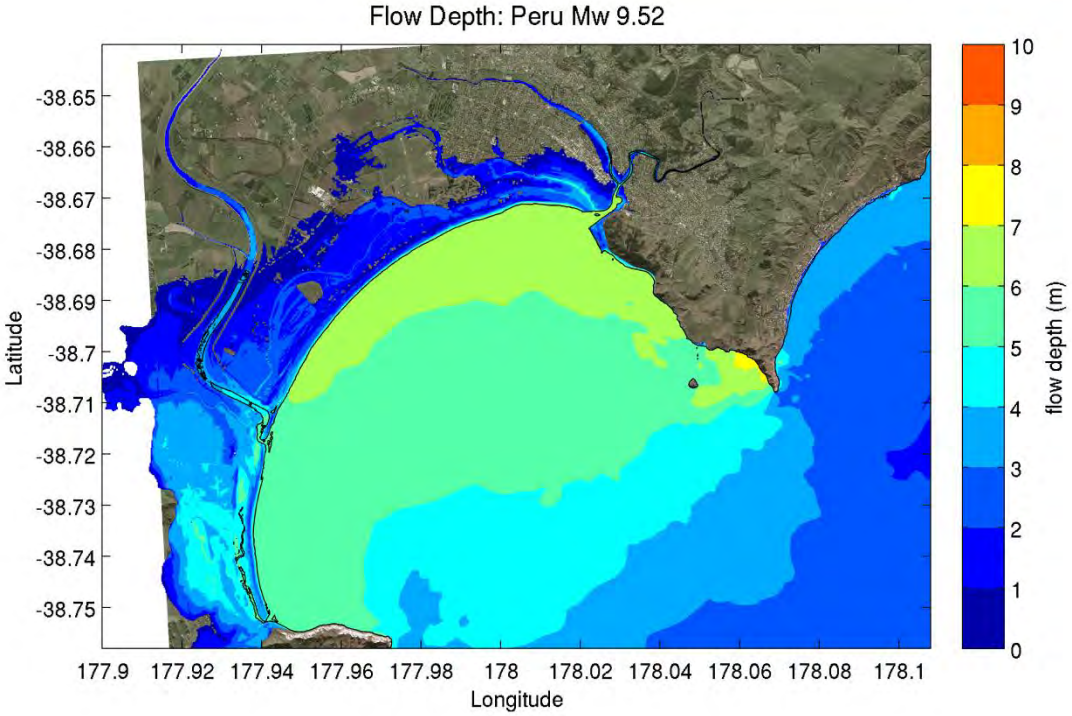

Figure 10.2 Maximum flow depth in metres for the Peru Mw 9.52 scenario at mid-tide. Offshore the colour scale shows the maximum water level.

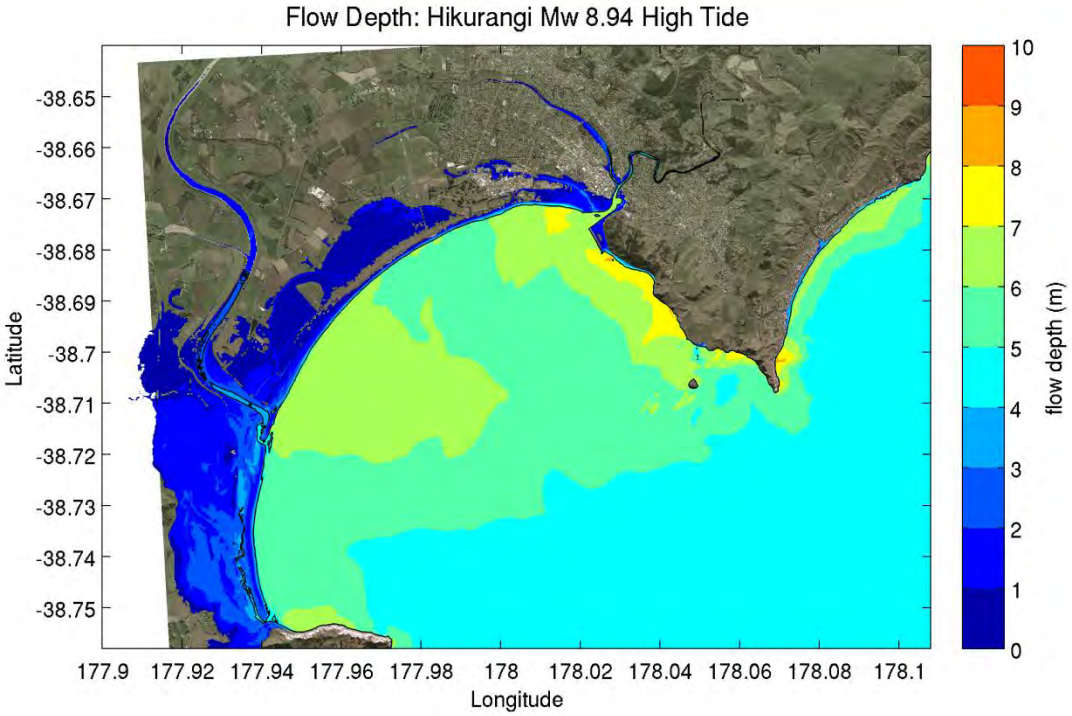

Figure 10.3 Maximum flow depth in metres for the Hikurangi Mw 8.94 scenario at high-tide. Offshore the colour scale shows the maximum water level.

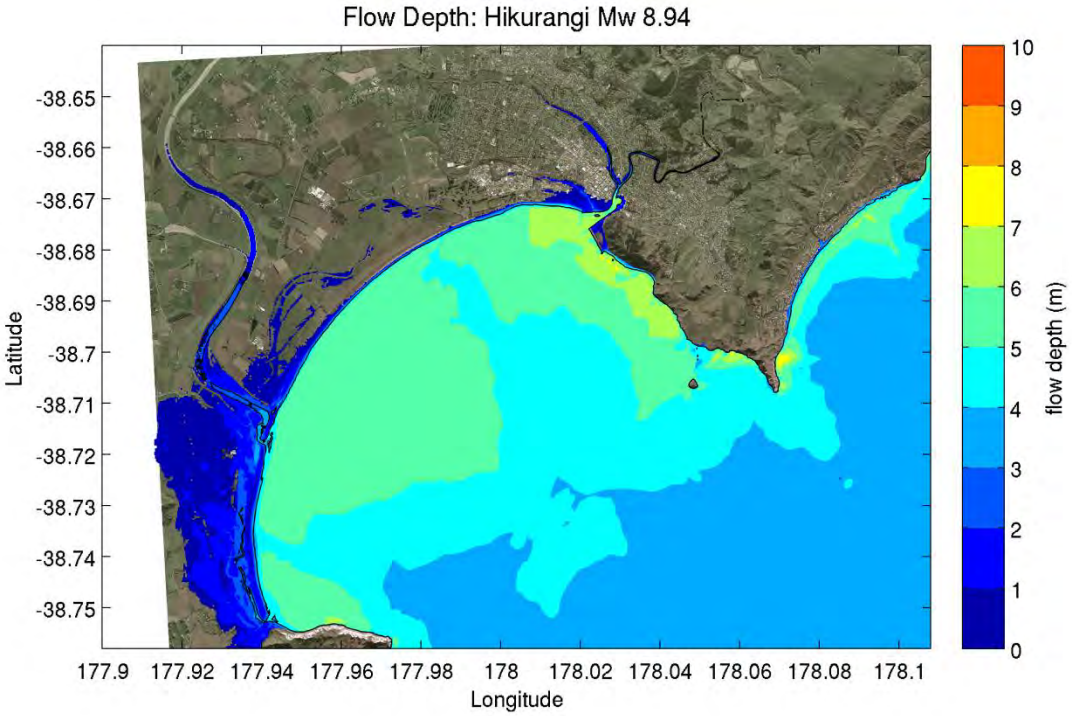

Figure 10.4 Maximum flow depth in metres for the Hikurangi Mw 8.94 scenario. Offshore the colour scale shows the maximum water level.

10.3 TSUNAMI EARTHQUAKES

The hazard and risk models used here are based on the national tsunami hazard model in Power (2013). One limitation of that study, which carries over to the present report, is the approximation of subduction zones as being uniform in their geophysical properties along their lengths.

One important variation is the historical occurrence of 'tsunami earthquakes' in the East Cape area. 'Tsunami earthquakes' are a special class of earthquakes characterised by low angle thrust faulting on the very shallowest part of the subduction interface, they produce large tsunamis relative to their magnitude and are often not strongly felt. A pair of earthquakes of this type occurred off the East Cape in March and May 1947. They were of magnitude Mw 7.1 and 6.9 respectively (Power et al, 2008; Bell et al, 2014), and caused tsunamis that affected the coast north of Gisborne.

The special properties of tsunami earthquakes are not included in the national tsunami hazard model (see p.169 of Power 2013), and there is no established process for estimating their magnitude-frequency. There is an indication that their might have been a tsunami earthquake in 1880, based on a brief newspaper report of a gentle earthquake at night and the finding of stranded fish the next morning. Consequently it is possible that these events might be relatively frequent on this coast.

Using the same setup used for the other simulations used in this report we have used the source model of the March 1947 tsunami developed in Bell et al (2014). For comparison with the other scenarios we have assumed 0.5m of sea level rise, though as the March 1947 tsunami occurred close to high tide this could instead be viewed as an approximation of the tide level.

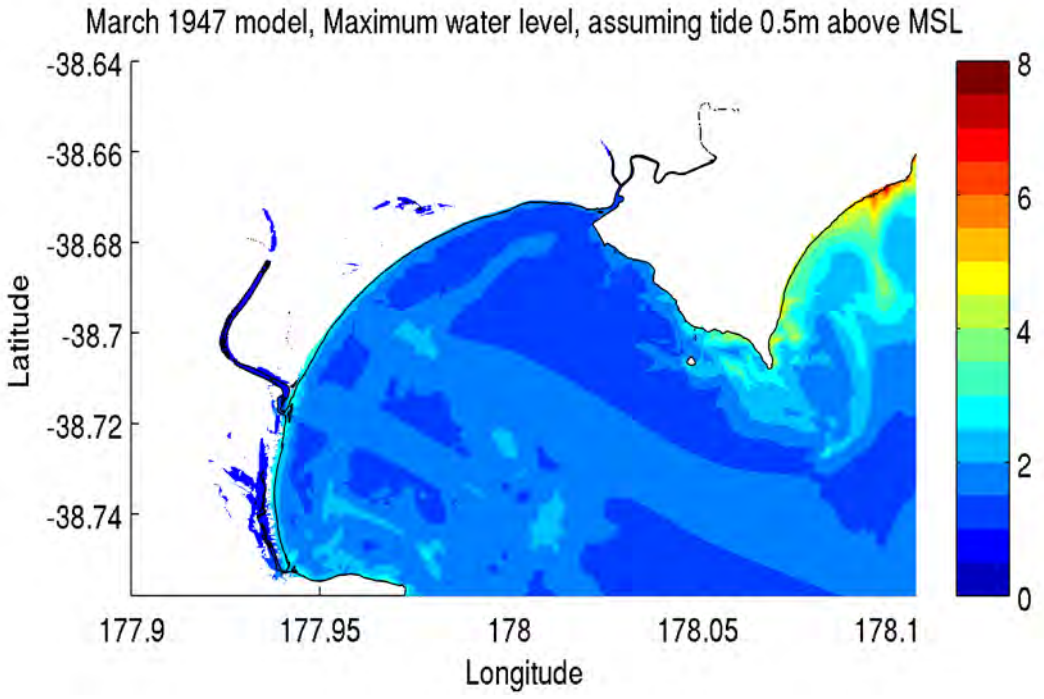

Figure 10.5 Maximum water surface level in meters for the model of the Mw7.1 March 1947 tsunami.

Figure 10.5 shows a maximum water surface level plot for the simulation of this event (note this is not a flow depth plot – the maximum water level plot is more helpful for comparing with historical water level measurements). The model shows tsunami run-up heights of 4-6m along Wainui Beach, consistent with historical measurements. Within Poverty Bay the modelled maximum tsunami heights are fairly low at 2-2.5m, consistent with historical observations of relatively little impact here.

Historically the March 1947 tsunami caused major damage to the surf club in Wainui. It also toppled a caravan and reached to the edge of houses around the creek mouths. Figure 10.6 shows modelled flow depths for this event around Wainui, which appear broadly consistent with the historical description.

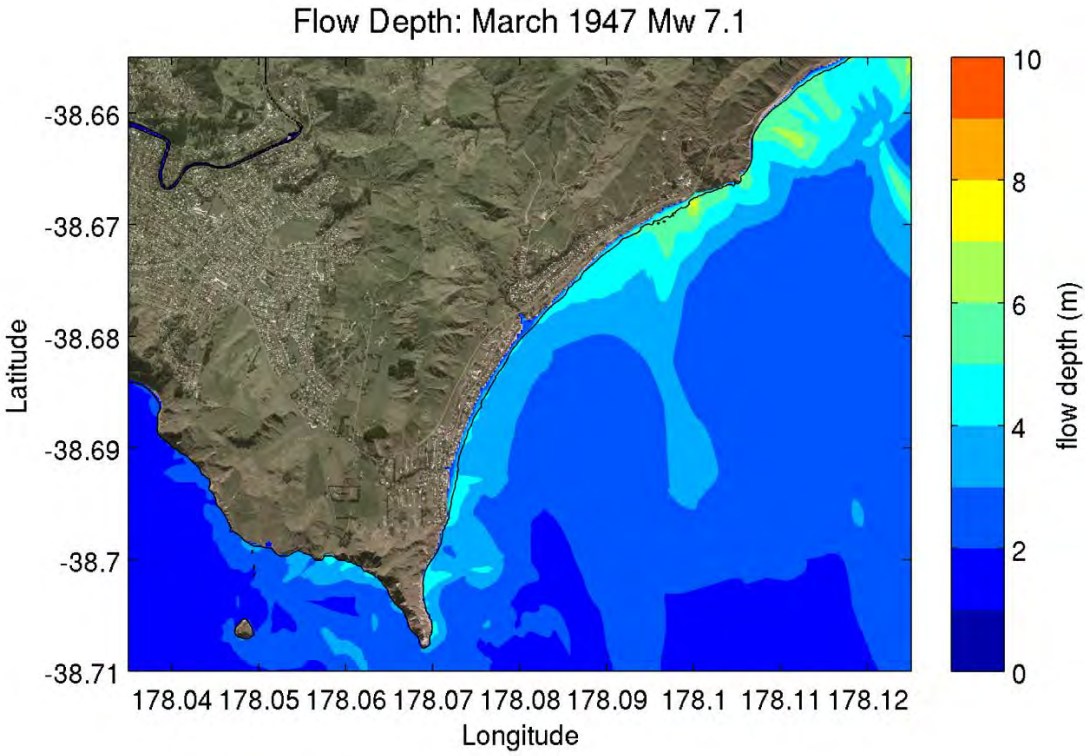

Figure 10.6 Maximum flow depth in metres for the model of the Mw7.1 March 1947 tsunami. Offshore the colour scale shows the maximum water level.

As events like the March 1947 tsunami could be relatively frequent on this coast we would recommend limiting development of those areas affected by the March 1947 tsunami on historical grounds.

10.4 OUTER RISE EARTHQUAKES

The Outer Rise fault models used in this study are speculative, and adapted from those used in Power (2013). Earthquakes with the expected 'normal fault' mechanism associated with Outer Rise faulting have been observed in this region, e.g. the 2007 Gisborne earthquake (Holden et al, 2008). However there is no direct geophysical evidence mapping faults at the assumed locations, and no indirect evidence for such faults has been identified in bathymetric data. Further research work to better constrain the parameters of Outer Rise faults is recommended as a priority at the national level.

The modelling of tsunami caused by the Outer Rise faults was challenging because of their large amplitudes and short wavelength. These properties lead to a strong interaction with the Penguin and Ariel Rocks that lie offshore of Poverty Bay and necessitated a non-standard modelling configuration that uses some of the less-used and less-tested features of the COMCOT model (see Section 5.1).

10.5 DISTANT SOURCE EARTHQUAKES

In the modelled scenarios for Distant source earthquakes it is notable that the maximum tsunami heights tend to underestimate the target heights from the Power (2013) report. The effect appears somewhat exaggerated in the figures in Section 7 because the figures show flow-depth onshore rather than tsunami height (which is often higher than the maximum offshore tsunami height), and in some cases the maximum tsunami heights for the Gisborne zone (top of Figure 6.1) occur outside of the study domain.

Nonetheless there remains a modest discrepancy which we attribute to the more accurate representation of the earthquake source geometry in the current study, and probably also to the tsunami scaling rules used in the Power (2013) study becoming increasingly inaccurate for very large earthquakes. Throughout this study we have chosen to prioritise accuracy of the tsunami source models over consistency with those used in the national model.

10.6 NON-EARTHQUAKE TSUNAMI SOURCES

This study and the Power (2013) hazard model it is based on, do not include tsunami caused by non-earthquake sources such as submarine landslides. Tsunami caused by very large landslides such as the Ruatoria debris avalanche are thought to have recurrence intervals measured in 100,000's of years, but the frequency of smaller events is not known. Some authors attribute the March and May 1947 tsunamis to submarine landslides, but this is not our interpretation.

10.7 DIFFERENCES WITH EVACUATION MAPS

It is very important to be clear that this study is focussed on land-use planning and not on tsunami evacuation zone development. The criteria used for these two processes are quite different. In particular the development of tsunami evacuation zones 'errs on the side of caution', while the assessment here is intended to be neutral.

Specific differences include:

	Land-use planning	**Evacuation zoning**
Confidence level	50th percentile (median)	84th percentile
Tide state	Mid-tide (MSL)	High-tide (MHWS)
Combining of scenarios	Weighted Median	Maximum
Return time	Various	At least 2500 years

The results presented here should not be used to argue against including any location in a tsunami evacuation zone.

10.8 SEA LEVEL RISE

As mentioned in Section 5, there are some areas south of the Airport that will become below Mean Sea Level after 0.5m of sea level rise. These are treated in the COMCOT model as being filled with water to the level of the new sea level, which may not be realistic if management of these areas enables them to drain. Consequently in the models they may appear to be inundated with water to a shallow depth even if not reached by the tsunami, and the hazard and risk may therefore be overestimated at these locations.

We do however recommend great caution in developing such areas in a situation of accelerating sea level rise, as they may become increasingly susceptible to several inundation hazards as well as tsunami. We therefore recommend a detailed site specific study before permitting any development of these areas.

This page is intentionally left blank.

11.0 LIMITATIONS OF THE RISK ANALYSIS

11.1 FATALITY FUNCTION

The fatality function used is based on empirical data from recent global tsunami events. The reliance on international data is due to New Zealand not experiencing tsunami that have caused fatalities in the past 100 years. There is a significant amount of spread in the data points (Figure 9.1) which is due to a number of factors specific to that location. These include the level of tsunami awareness of the community and their actions following the natural warning signs (e.g. strong, long ground shaking or sea withdrawl). The actual fatality rate is dependent also on the evacuation distance which varies between locations. To improve the fatality model, site specific information relevant to Gisborne could be included. This could include a better understanding of estimated evacuation rates for a local source tsunami given current community awareness through a survey to Gisborne residents, as has been done recently for the Hawkes Bay.

11.2 TREATMENT OF UNCERTAINTY

Adequate treatment of uncertainty is fundamental to any probabilistic analysis. While a number of sources of uncertainty have been included in the analysis, some sources have not been fully considered due to budget and time constraints. For the risk modelling, no uncertainty in the fatality function was considered. It is advised for future studies, including uncertainty in the fatality function should be included.

11.3 SENSITIVITY TESTING

It is recommended that future work should explore the sensitivity of the AIFR results to various components of the probabilistic model. This would be undertaken by varying one parameter at a time to understand how it changes the AIFR. This would include varying the number of sources selected for each target return period, the tide level, the fatality function, and the occupancy rate.

11.4 TARGET RETURN PERIODS

Due to constraints on budget for this project, a limited number of target return periods were selected. However, as described in Section 9.4, a tsunami risk curve was developed by interpolating between the target return periods. By increasing the number of target return periods, the shape of the curve, particularly the left hand side of the curve would be better defined and reduce any error by interpolating between points.

This page is intentionally left blank.

12.0 GIS DATA LAYERS

The tsunami hazard data from Section 8, and the annual individual fatality risk (AIFR) data from Section 9 were converted into GIS raster layers with a cell size of 0.00023 degrees (approximately 20m x 25m). At this cell size the majority of cells encompasss only a single datapoint from the modelling grid, but where there was more than one datapoint in a cell the average of the values was used (whether flow depth or AIFR). As a consequence of this resampling, caution should be used in situations where decisions depend on interpretation of the results at a very fine scale, i.e. at the level of individual raster cells.

Areas of low AIFR risk, where the AIFR was too low to be explicitly calculated, were assigned a nominal AIFR of 10^{-6} in the raster layer if they were inundated in at least one of the local source scenarios used in the analysis.

This page is intentionally left blank.

13.0 CONCLUSION

The purpose of this project has been to develop a set of probabilistic tsunami hazard maps for Gisborne City and Wainui Beach. This is intended to assist GDC in taking a risk-based approach to managing its tsunami risk.

A ‘level-3’ approach was adopted to achieve these goals. This type of analysis involves identifying and modelling tsunami events associated with particular return periods.

Two particular outputs were targeted:

1. Maps of expected tsunami inundation at 100, 500, 1000, 2500 year return periods.
2. Mapped estimates of the Annualised Individual Fatality Risk (AIFR) from local source tsunamis.

This report describes in detail the preparation of these outputs, and presents the results of this analysis.

This page is intentionally left blank.

14.0 REFERENCES

Abe, K. 1975. Reliable estimation of the seismic moment of large earthquakes, J. Phys. Earth. 23, 381–390.

Barberopoulou, A.; Wang, X.; Power, W.; Lukovic, B. 2014. Simulation of Tsunami Hazards Affecting the East Cape Region, New Zealand. *Pure and Applied Geophysics*, 1-21.

Beaumont, H. 2015. Statement of Evidence of Helen Beaumont on Behalf of the Christchurch City Council before the Christchurch Replacement District Plan Independent Hearings Panel.13 February 2015 http://www.chchplan.ihp.govt.nz/wp-content/uploads/2015/03/310-CCC-Ms-Helen-Beaumont-Natural-Hazards-13-2-15.pdf, last accessed 9 March 2016.

Carter, J. 2015. Statement of Evidence of Janice Carter on Behalf of the Christchurch City Council before the Christchurch Replacement District Plan Independent Hearings Panel.13 February 2015. http://www.chchplan.ihp.govt.nz/wp-content/uploads/2015/03/310-CCC-Ms-Janice-Carter-Natural-Hazards-13-2-15.pdf, last accessed 9 March 2016.

Cho, Y.-S. 1995 Numerical simulation of tsunami and runup. PhD thesis, Cornell University.

Eblé, M.; and NCTR Staff. 2014: A Tsunami Forecast Model for Newport, Oregon. NOAA OAR Special Report, PMEL Tsunami Forecast Series: Vol. 5, 2nd Ed., 146 pp, doi:10.7289/V5125QK9

François-Holden, C.; Bannister, S.; Beavan, J.; Cousins, J.; Field, B.; McCaffrey, R.' ... & Wallace, L. 2008. The Mw 6.6 Gisborne earthquake of 2007: Preliminary records and general source characterisation. *Bulletin of the New Zealand Society for Earthquake Engineering*, *41*(4).

Beavan, J.; Wang, X.; Holden, C.; Wilson, K.; Power, W.; Prasetya, G.; Bevis, M.; Kautoke, R. 2010. Near-simultaneous great earthquakes at Tongan megathrust and outer rise in September 2009. Nature, 466: 959–963

Bell, R.; Holden, C.; Power, W.; Wang, X.; Downes, G. 2014. Hikurangi margin tsunami earthquake generated by slow seismic rupture over a subducted seamount. *Earth and Planetary Science Letters*, *397*, 1-9.

Berryman, K. 2005. Review of tsunami hazard and risk in New Zealand: MCDEM Report No. 2005/104. Wellington. 139 pp.

Cho, Y.S. 1995. Numerical simulations of tsunami and runup, PhD thesis, Cornell University, Ithaka, New York, USA.

Eblé, M.; and NCTR Staff. 2014: A Tsunami Forecast Model for Newport, Oregon. NOAA OAR Special Report, PMEL Tsunami Forecast Series: Vol. 5, 2nd Ed., 146 pp, doi:10.7289/V5125QK9

Fraser, S.A.; Power, W.L.; Wang, X.; Wallace, L.M.; Mueller, C.; Johnston, D.M. 2014. Tsunami inundation in Napier, New Zealand, due to local earthquake sources. *Natural hazards*, *70*(1), 415-445.

Horspool, N.; Cousins, W.J.; Power, W.L. 2015. Review of Tsunami Risk Facing New Zealand: A 2015 Update. GNS Science Consultancy Report 2015/38. Lower Hutt, N.Z.: GNS Science.

Liu, P.L.-F., Cho, Y.-S. and Fujima, K. (1994a). Numerical solutions of three-dimensional run-up on a circular island, Proc. Of Int. Sym.: Waves – Physical and Numerical Modelling, pp. 1031-1040, Canada.

Liu, P.L.-F., Cho, Y.-S., Yoon, S.B. and Seo, S.N. (1994b). Numerical simulations of the 1960 Chilean tsunami propagation and inundation at Hilo, Hawaii. In Recent Development in Tsunami Research, pp99-115. Kluwer Academic Publishers, 1994.

Liu,P.L.-F.; Cho, Y-S.; Briggs, M.J.; Synolakis, C.E.; Kanoglu, U. 1995. Run-up of solitary waves on a circular island. Journal of Fluid Mechanics, 302: 259–285.

Liu, P.L.-F., Woo, S.-B. and Cho, Y.-S. (1998). Computer programs for tsunami propagation and inundation. Technical Report, Cornell University, 1998.

Massey, C.I.; McSaveney, M.J.; Taig, T.; Richards, L.; Litchfield, N.J.; Rhoades, D.A.; McVerry, G.H.; Lukovic, B.; Heron, D.W.; Ries, W.; Van Dissen, R.J. 2014 Determining rockfall risk in Christchurch using rockfalls triggered by the 2010-2011 Canterbury earthquake sequence, New Zealand. Earthquake Spectra, 30(1): 155-181; doi: 10.1193/021413EQS026M

Mueller, C.; Wang, X.; Power, W.L. 2014. Investigation of the effects of earthquake complexity on tsunami inundation hazard in Wellington Harbour. GNS Science Consultancy Report 2014/198. 43p.

Okada, Y. 1985. Surface deformation due to shear and tensile faults in a half-space. *Bulletin of the seismological society of America*, *75*(4), 1135-1154.

Power, W.; Downes, G.; Stirling, M. 2007. Estimation of tsunami hazard in New Zealand due to South American earthquakes. In *Tsunami and Its Hazards in the Indian and Pacific Oceans* (pp. 547-564). Birkhäuser Basel.

Power, W.L.; Wallace, L.; Reyners, M. 2008. Tsunami hazard posed by earthquakes on the Hikurangi subduction zone interface. GNS Science, Science Report 2008/40 Lower Hutt, New Zealand

Power, W.; Wallace, L.; Wang, X.; Reyners, M. 2012. Tsunami hazard posed to New Zealand by the Kermadec and southern New Hebrides subduction margins: an assessment based on plate boundary kinematics, interseismic coupling, and historical seismicity. *Pure and applied geophysics*, *169*(1-2), 1-36.

Power, W. 2013. Review of tsunami hazard in New Zealand (2013 update). *GNS Science Consultancy Report 2013*, *131*, 222.

Prasetya, G.; Wang, X. 2011 Tsunami inundation modelling for Tauranga and Mount Maunganui. GNS Science Consultancy Report 2011/193. 35 p.

Taig, T. 2012. A risk framework for earthquake prone building policy. *Wellington: TTAC Limited and GNS Science*.

Taig, T.; Massey, C.; Webb, T. 2012. Canterbury Earthquakes 2010/11 Port Hills Slope Stability: Principles and Criteria for the Assessment of Risk from Slope Instability in the Port Hills, Christchurch. GNS Science Consultancy Report 2011/319. Lower Hutt, N.Z.: GNS Science.

Wang, X; Power, W. 2011. COMCOT: a tsunami generation propagation and run-up model, GNS Science consultancy report 2011/43, GNS Science, Lower Hutt, New Zealand.

Wang, X. and Liu, P.L.-F. (2005). A numerical investigation of Boumerdes-Zemmouri (Algeria) earthquake and tsunami. Computer Modeling in Engineering and Science, Vol.10, No.2, pp.171-184.

Wang, X. and Liu, P. L.-F. (2006). An analysis of 2004 Sumatra earthquake fault plane mechanisms and Indian Ocean tsunami. Journal of Hydraulic Research, Vol. 44, No.2 (2006), pp.147-154.

Wang, X. and Liu, P. L.-F. (2007). Numerical simulation of the 2004 Indian Ocean tsunami – Coastal Effects. Journal of Earthquake and Tsunami. Vol.1, No.3 (2007). pp273-297.

Wang, X.; Liu, P.L.-F. 2007. Numerical simulation of the 2004 Indian Ocean tsunami – Coastal Effects. Journal of Earthquake and Tsunami, 1(3): 273-297.

Wang, X., Orfila, A. and Liu, P.L.-F. (2008). Numerical simulations of tsunami runup onto a three-dimensional beach with shallow water equations. Advances in Coastal and Ocean Engineering, Vol.10, pp.249-253, 2008. World Scientific Publishing Co.

Wang, X.; Prasetya, G.; Power, W.L.; Lukovic, B.; Brackley, H.; Berryman, K.R. 2009. Gisborne District council tsunami inundation study. *GNS Science consultancy report*, *233*, 130.

Williams, C.A.; Eberhart-Phillips, D.; Bannister, S.; Barker, D.H.; Henrys, S.; Reyners, M.; Sutherland, R. 2013. Revised interface geometry for the Hikurangi subduction zone, New Zealand. *Seismological Research Letters*, *84*(6), 1066-1073.

This page is intentionally left blank.

APPENDICES

This page is intentionally left blank.

A1.0 APPENDIX 1 – THE RELATIONSHIP BETWEEN THE HAZARD CURVE AND ANNUALISED PROBABILITY OF DEATH

Here we justify the estimation of the annual individual fatality risk (AIFR) by the area under the curve of fatality rate plotted against annual probability.

Consider a hazard curve with discrete hazard levels h_i at return periods γ_i:

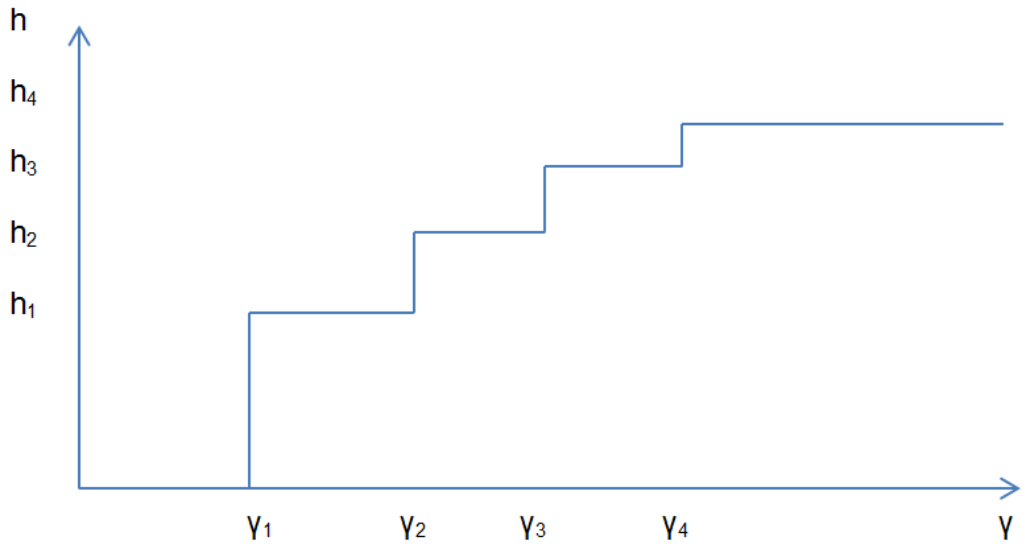

In the example 4 different types of events occur.

We can relate return period to frequency (annual probability) of exceedence:

$$v = \frac{1}{\gamma} \qquad (assuming\ \gamma \gg 1)$$

And with this look at the annual probability of individual types of events:

$$\Pr(h_1) = \frac{1}{\gamma_1} - \frac{1}{\gamma_2} = v_1 - v_2$$

$$\Pr(h_2) = \frac{1}{\gamma_2} - \frac{1}{\gamma_3} = v_2 - v_3$$

etc …and:

$$v_1 = \Pr(h_1) + \Pr(h_2) + \Pr(h_3) + \Pr(h_4)$$

$$v_2 = \Pr(h_2) + \Pr(h_3) + \Pr(h_4)$$

etc …

A given level of the hazard is associated with a probability of death (or damage state of a building, etc) through a hazard curve f(h):

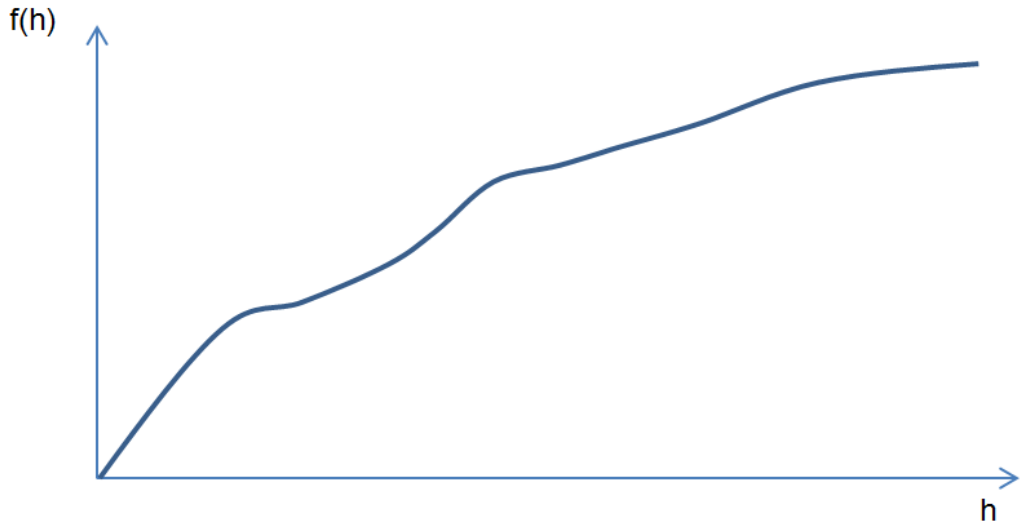

Applying f(h) to the original hazard curve:

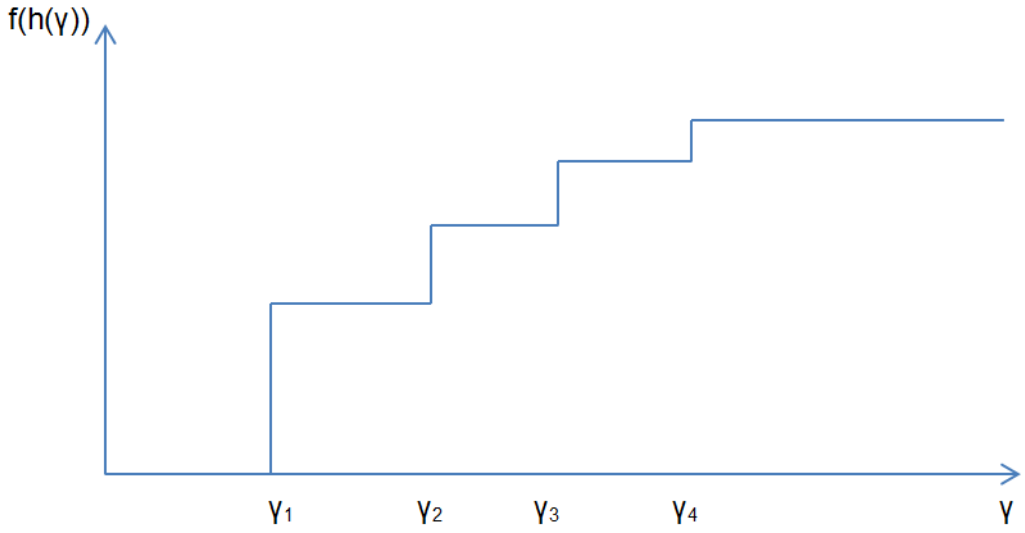

The annual probability of death from all 4 types of events:

$$\mathrm{Pd} = f(h_1)\,\mathrm{Pr}(h_1) + f(h_2)\,\mathrm{Pr}(h_2) + f(h_3)\,\mathrm{Pr}(h_3) + f(h_4)\,\mathrm{Pr}(h_4)$$

Drawing the above figure in terms of frequency, rather than return period:

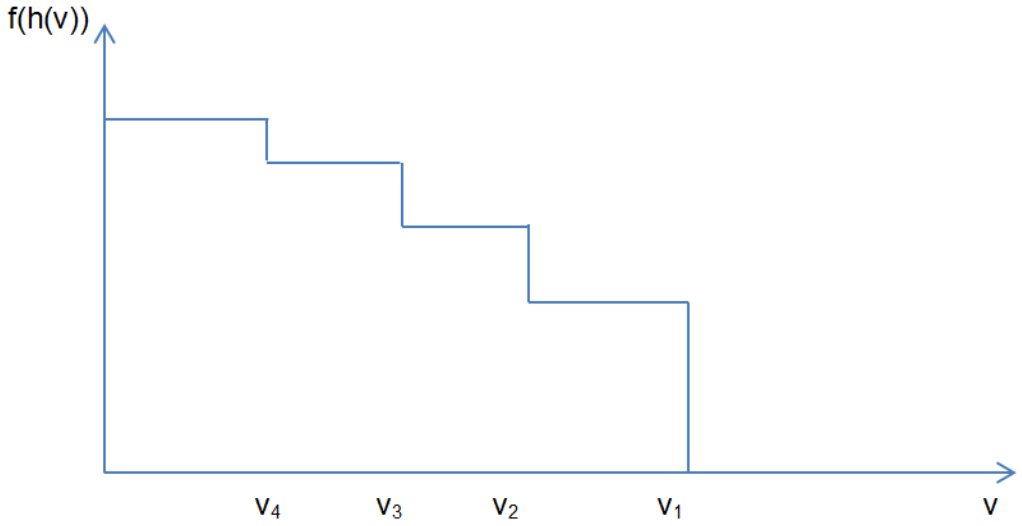

$$\text{Pd} = f(h_4)\,\text{Pr}(h_4) + f(h_3)\,\text{Pr}(h_3) + f(h_2)\,\text{Pr}(h_2) + f(h_1)\,\text{Pr}(h_1)$$

$$= f(h_4)(v_4 - 0) + f(h_3)(v_3 - v_4) + f(h_2)(v_2 - v_3) + f(h_1)(v_1 - v_2)$$

= area under the above curve

If the processes is repeated for curves with more and more discrete types of events the curve becomes smoother and smoother, but Pd remains the integral under the curve.

www.gns.cri.nz

Principal Location

1 Fairway Drive
Avalon
PO Box 30368
Lower Hutt
New Zealand
T +64-4-570 1444
F +64-4-570 4600

Other Locations

Dunedin Research Centre
764 Cumberland Street
Private Bag 1930
Dunedin
New Zealand
T +64-3-477 4050
F +64-3-477 5232

Wairakei Research Centre
114 Karetoto Road
Wairakei
Private Bag 2000, Taupo
New Zealand
T +64-7-374 8211
F +64-7-374 8199

National Isotope Centre
30 Gracefield Road
PO Box 31312
Lower Hutt
New Zealand
T +64-4-570 1444
F +64-4-570 4657